STABILITY OF SURFACTANT-LADEN LIQUID FILM FLOW DOWN A FLEXIBLE INCLINED PLANE

Ph.D. THESIS

by

DHARMENDRA SINGH TOMAR

DEPARTMENT OF CHEMICAL ENGINEERING
INDIAN INSTITUTE OF TECHNOLOGY ROORKEE
ROORKEE-247667 (INDIA)
APRIL, 2018

STABILITY OF SURFACTANT-LADEN LIQUID FILM FLOW DOWN A FLEXIBLE INCLINED PLANE

A THESIS

Submitted in partial fulfilment of the requirements for the award of the degree

of

DOCTOR OF PHILOSOPHY

in

CHEMICAL ENGINEERING

by

DHARMENDRA SINGH TOMAR

DEPARTMENT OF CHEMICAL ENGINEERING
INDIAN INSTITUTE OF TECHNOLOGY ROORKEE
ROORKEE-247667 (INDIA)
APRIL, 2018

INDIAN INSTITUTE OF TECHNOLOGY ROORKEE
ROORKEE

CANDIDATE'S DECLARATION

I hereby certify that, the work which is being presented in the thesis entitled **"STABILITY OF SURFACTANT-LADEN LIQUID FILM FLOW DOWN A FLEXIBLE INCLINED PLANE**" in partial fulfilment of the requirements for the award of the Degree of Doctor of Philosophy and submitted in the Department of Chemical Engineering, Indian Institute of Technology Roorkee, Roorkee is an authentic record of my own work carried out during a period from August, 2012 to April, 2018 under the supervision of Dr. Gaurav, Assistant Professor, Department of Chemical Engineering, Indian Institute of Technology Roorkee, Roorkee.

The matter presented in this thesis has not been submitted by me for the award of any other degree of this or any other institution.

(DHARMENDRA SINGH TOMAR)

This is to certify that, the above statement made by the candidate is correct to the best of my knowledge.

(Gaurav)
Supervisor

Date:

Acknowledgements

Firstly, I would like to express my sincere gratitude to my thesis supervisor Dr. Gaurav, Department of Chemical Engineering, Indian Institute of Technology Roorkee for the continuous support of my Ph.D. research work, for his patience, motivation, and immense knowledge. His guidance helped me in all the time of research and writing of this thesis.

Besides my thesis supervisor, I would like to thank the rest of my students research committee members: Dr. Shishir Sinha, Head of Chemical Engineering, Dr. B. Prasad (DRC Chairman), Dr. P. Bera, and Dr. R. P. Bharti for their insightful comments, encouragement, but also for the research concerned basic questions which incented me to widen my research knowledge. I would also like to thank the Prof. I. M. Mishra (Ex. DRC Chairmain) and Prof. I. D. Mall who supported and motivated me for doing quality research.

I would like to thank my present and past fellow labmates: Supriya, Sheeba, Hemant, Manne Sai Teja, Vidit, Ashwin, Hariom, Akanksha, Rishab and Mahendra Baingne for the stimulating discussions and enjoying the Doctral research with fun. Also thank to my friend-Dr. Ravi and Prof. Surendra Singh Tanwar for motivating me to work with patience by sending motivational quotes through Whatsapp. Specially, I would like to thank to Mahendra Baingne for discussing various codes, finding the errors in code and in Mathematical equations by rechecking.

Words cannot express the feelings that I have for my parents and in-laws, uncles-Shri Suresh and Shri Shyambeer, brother in law-Deepak. They were supported me both emotionally and financially and were standing with me at the critical time. I would like to thank my younger brother-Yogendra, and sisters-Rani, Sangeeta and my daughter Aaradhya for their constant unconditional support and love.

Finally, I would like to acknowledge the important person in my life-my wife Jyoti. She has been a constant source of strength and inspiration. There were many times during Ph.D. research work when everything seemed difficult. I can honestly say that it was only her determination and constant encouragement that ultimately made it possible for me to see this research work through to the end. Last but not least, thanks to almighty god for giving me everything essential for life.

Dharmendra Singh Tomar

Publications From Dissertations

- **Refereed Journals**

1. Tomar, D.S., Baingne, M., and Sharma, G., "Stability of gravity-driven free surface flow of surfactant-laden liquid film flowing down a flexible inclined plane''. Chemical Engineering Science 165, 216-228, (2017).
2. Tomar, D.S., and Sharma, G. "Manipulation and control of instabilities for surfactant-laden liquid film flowing down an inclined plane using a deformable solid layer''. Physics of fluids 30, 014104 (2018).

Abstract

Liquid film flows with free-surface occurs in a wide variety of technological applications such as coating flows, falling film reactors, absorption column etc. These film flows fall prey to free-surface instability due to jump in fluid properties (like viscosity, elasticity etc.) across the gas-liquid interface. Such interfacial instabilities are desirable in some applications while undesirable in others. For example, instabilities are detrimental to product quality in coating flows as they result in non-uniform film thickness. On the other hand these instabilities are useful for heat and mass transfer applications, or for patterning applications (Bandyopadhyay *et al.* 2008; Mukherjee & Sharma 2015). Thus, it is frequently required to control and manipulate instabilities observed in liquid film flows with free surface. In the present thesis, we explore ways to manipulate and control the interfacial instabilities observed for the single liquid film with free surface flowing down an inclined plane. For single liquid film flow down an inclined plane, only a gas-liquid interface is present. Further, these film flows are often accompanied by surface active agents or surfactants in several technological and physiological flow systems. It is well known that the presence of surfactant have significant effect on the stability of different interfaces present in a particular flow configuration. Thus, we also consider the presence of surfactant at gas-liquid interface in the present thesis. In view of the above discussion, we explore the use of a passive deformable solid coating as a means to manipulate and control the interfacial instabilities for single liquid film flow down an inclined plane when the gas-liquid interface is contaminated with a mono-layer of insoluble surfactant.

We investigate the linear stability of a surfactant-laden single liquid film with free surface flowing down an inclined plane under the action of gravity when the inclined plane is coated with a deformable solid layer. We first examine the stability of flow configuration in creeping flow (or $Re = 0$) limit. In this zero Reynolds number limit, the surfactant covered liquid film flowing down a rigid inclined wall admits two normal eigenmodes: (i) a gas-liquid (GL) interfacial or free surface mode, and (ii) a surfactant-induced Marangoni mode. The GL free surface mode

is the usual Yih (1963, 1967) type mode which is present because of jump in viscosity across the gas-liquid interface. This GL interfacial mode remains stable in creeping flow limit. The Marangoni mode arise because of the convective motion of surfactant along the gas-liquid interface and this mode also remains stable for liquid film flow down a rigid inclined wall. We examine how the stability characteristics change when the surfactant-laden liquid film flow occurs down a flexible inclined wall instead of a rigid inclined wall. The effect of presence of deformable wall or soft solid coating on GL mode has already been discussed by Shankar and coworkers (Gaurav & Shankar 2007; Sahu & Shankar 2016; Shankar & Sahu 2006). The primary aim of this study is to explore the role of wall deformability on the stability characteristics of Marangoni mode. Two parameters, namely, shear modulus and thickness of deformable solid layer appear in presence of a deformable solid coating in addition to the parameters which were present for flow down a rigid inclined wall. We performed a long-wave asymptotic analysis and observed that the Marangoni mode becomes unstable in presence of deformable solid coating. This long wave instability was further continued to finite wavelength perturbations using a numerical shooting procedure. Specifically, we have shown that for a given solid thickness, the Marangoni mode becomes unstable when the shear modulus of solid layer decreases below a critical value (i.e. the solid layer becomes sufficiently soft). The effect of increasing solid thickness is found to be destabilizing. The liquid-solid (LS) interfacial mode also becomes unstable at high wave numbers below a threshold value of shear modulus, however, this value is much smaller than that required to trigger Marangoni mode instability. This implies that as the solid coating becomes more and more deformable, the Marangoni mode becomes unstable first followed by the LS interfacial mode. The GL mode was always found to be stable in creeping flow limit. Further, our long-wave analysis shows that the solid deformability has an additional stabilizing effect on GL mode. We defined a non-dimensional solid deformability parameter as $G = \mu V / E_s R$, where μ is the viscosity of the liquid, V is the characteristic velocity, R is the liquid layer thickness, and E_s is the shear modulus of solid layer. Note that higher value of G implies lower E_s value, and hence, more soft (deformable) solid layer. We plotted neutral stability diagram in terms of this non-dimensional parameter G (or equivalently shear modulus) vs. wavenumber for all the unstable modes, and these diagrams clearly show

that the Marangoni mode is the dominant mode of instability in creeping flow limit. This observation related to destabilization of Marangoni mode due to the presence of deformable wall for free surface liquid film flow is important because we believe that this is the first example of the case where the instability of the Marangoni mode is observed when the fluid-fluid interface (here, GL interface) remains stress-free in the basic state.

We further investigated the linear stability of the surfactant-loaded liquid film flowing down a flexible inclined plane in presence of inertia ($Re \neq 0$). For non-zero Reynolds number, it is well known that the GL interfacial mode becomes unstable for a clean liquid film flowing down a rigid inclined plane when Re increases above a critical value. The presence of surfactant at GL interface is known to suppress this GL mode instability when the Marangoni number (Ma) increases above a threshold value (Blyth & Pozrikidis 2004*a*). The Marangoni number is defined as $Ma = E\Gamma_0/\sigma_0$, where E refers to surface elasticity, Γ_0 denotes the surfactant concentration at GL interface in steady base state configuration, and σ_0 represents the corresponding unperturbed GL interfacial tension. Recall that we have shown that when the rigid wall is replaced by a deformable wall, the Marangoni mode becomes unstable in creeping flow limit. We first continue this Marangoni mode instability to finite Reynolds number, and observed that this Marangoni instability persists at non-zero values of Reynolds number. The GL interfacial mode can also become unstable as Reynolds number increases above the critical value for (clean or surfactant-covered) film flow down an inclined (flexible or rigid) plane. We observed that as Reynolds number is increased above zero, the Marangoni mode remains the dominant mode of instability for small Reynolds number until the GL mode also becomes unstable with increase in Reynolds number. Once, the GL mode becomes unstable, it dominates the stability of falling film configuration. Thus, there is an exchange in the dominant mode of instability with the increase in Reynolds number. Previous works have also demonstrated the potential of using a deformable solid coating in suppressing the interfacial instabilities for a wide variety of configurations (Gaurav & Shankar 2015; Shankar 2015). The presence of surfactant also suppresses GL interfacial instability when the Ma increases above the critical value. We explore whether it is possible to use a deformable solid coating to achieve stable flow configuration for surfactant-loaded film when the stabilizing contribution from sur-

factant is not sufficient to suppress the GL instability (i.e. when Ma remains below the threshold value to stabilize the GL mode for a given Reynolds number). This question becomes important in view of the recently observed Marangoni mode instability solely induced due to the presence of the deformable wall (Tomar *et al*. 2017). We show in the present thesis that for such cases as well, a deformable solid coating could be employed to suppress free surface instability without triggering Marangoni or liquid-solid interfacial modes. Specifically, we have shown that for a given solid thickness, as the shear modulus of the solid layer decreases (i.e. the solid becomes more deformable) the GL mode instability is suppressed. With further decrease in shear modulus, the Marangoni and liquid-solid interfacial modes become unstable. Thus, there exists a stability window in terms of shear modulus where the surfactant-laden film flow remains stable even when the Marangoni number is below the critical value required for free surface instability suppression. Based on our numerical results (primarily G vs. wavenumber neutral stability curves), we estimated that typical values of shear modulus of elasticity for the deformable solid layer is of the order of 10^4 Pa to obtain stable flow of surfactant-laden liquid film down a flexible inclined plane. Further, when the Marangoni number is greater than the critical value so that the GL mode remains stable in the rigid limit or with the deformable wall, the increase in wall deformability or solid thickness triggers Marangoni mode instability and thus, renders a stable flow configuration into an unstable one. Thus, we show that the soft solid layer can be used to manipulate and control the stability of surfactant-laden film flows.

Contents

List of Tables

List of Figures

Chapter 1

Introduction

1.1 Motivation

Flows which involve more than one immiscible liquid layers (or phases) with one or more fluid-fluid interfaces are known as multilayer/interfacial flow. The fluid-fluid interface could be either a liquid-liquid interface or a gas-liquid interface. Examples include gravity-driven free surface flow of one or more liquid layers (present in coating applications), flow in channel or tube involving more than one liquid layers (core-annular flow in lubricated pipe lining, liquid-liquid extraction, co-extrusion of polymers etc.). Multilayer flows are presents in many technological applications like coating, co-extrusion, and lubricated pipelining etc. These flows are susceptible to interfacial instabilities at the distinct interfaces due to jump in fluid properties like viscosity, density, and elasticity (in case of polymeric liquids) across the interface. Such interfacial instabilities could be desirable or undesirable depending on the objectives or final product requirements. For example, instabilities are desirable when the objective is to achieve high heat and mass transfer rates in heat exchangers, distillation units (Craster & Matar 2009), and falling film evaporator/reactor. Instabilities, if present, in such cases could lead to secondary flows or turbulence which in turn enhances heat and mass transfer rates. The examples where interfacial instabilities are undesirable include manufacturing of photographic film and coating processes (Wenstein & Ruschak 2004), and biological flows (Grotberg & Jensen 2004; Halpern & Grotberg 1993, 1992).

A process by which a thin liquid-layer is made and applied to a surface of a solid

is called a coating process. Coating flows are the flows employed in coating technique and also include the secondary flows that occur after coating of a solid surface and before immobilization of the same solid surface. The applications of the coating flows are in manufacturing of photographic film, wire coating etc. In manufacturing of photographic films, flow of multiple liquid layers down an inclined plane is a basic configuration. The liquid layers flow through an inclined surface of coating die distributor and stacked on the top of each other in development for simultaneous coating film on a moving solid surface. A major requirement in coating applications is that the final product must be superior quality and free from all the defects. In such type of flows, the fluid-fluid interface becomes unstable (Chen 1993; Yih 1963) above a critical value of Reynolds number or equivalently by variation in fluid properties, fluid thickness and fluid velocity. These instabilities are detrimental to the required product quality as they result in discontinuous film thickness. Control and suppression of these instabilities remains a crucial aspect to ensure smooth process and to maintain the higher-grade quality of product. We explore ways to control such interfacial instabilities. Specifically, we consider gravity-driven free surface flow of a single liquid film flowing down an inclined plane. A soft solid coating is attached on to the inclined plane and the gas-liquid interface is loaded with a monolayer of surfactant. We examine the effect of simultaneous presence of deformable solid layer and surfactant layer on the stability of gas-liquid interface.

The surfactant is present in several coating applications and is known to have a stabilizing effect on the gas-liquid interfacial instability. Recently, the use of a soft solid coating is proposed as a means to suppress fluid-fluid interfacial instabilities for variety of fluid rheology and for a wide class of flow settings (e.g. see review by Gaurav & Shankar (2015)). Moreover, for multiple liquid layers flowing down an inclined plane during coating process, there is a possibility that one of the (bottom) layer solidifies before the other layer. In such cases as well, a deformable liquid-solid interface will be present in addition to the presence of other fluid-fluid interfaces and surfactant layer at different fluid-fluid interfaces. Thus, it is of interest to know the effect of presence of a soft solid layer on fluid-fluid interfacial instabilities when the fluid-fluid interface is contaminated with surfactant monolayer.

Another interesting area is biological flows where liquid soft solid interaction

occurs. For example, in blood vessels where blood flows through an arteries and veins whose walls are made of soft tissues, and air flow in lung-airways where air flows through a small flexible capillaries. In lung airways, the cell walls are coated with a liquid lining and air flows in the lumen as core fluid. A monolayer of surfactant is also present at air-liquid interface. The interaction between the air-liquid interface, flexible wall and surfactant forms an important aspect of pulmonary fluid mechanics. The presence of capillary instability at air-liquid interface is considered to be the primary mechanism for several respiratory distress syndrome. The liquid film forms the plug and blocks the airway as a result of the capillary instability. Presence of natural surfactant is known to delay or avoid the closure. However, a dificiency in surfactant may lead to early closure of pulmonary airways and hence, a clear understanding of the role of surfactant on the film dynamics and in presence compliant surface will help in better design of treatment of various respiratory diseases. The work presented in this thesis deals with such kind of interaction between surfactant, air-liquid interface and flexible wall. We show that the wall flexibility significantly change the stability characteristics of the system.

In this thesis, at the beginning, we studied the stability analysis of surfactant-laden Newtonian liquid layer flowing down an inclined rigid surface which generate two stable mode, namely GL and Marangoni (Blyth & Pozrikidis 2004*a*).The gas-liquid interfacial mode destabilizes above a critical Reynolds number and Marangoni mode remains stable for all Reynolds number. If rigid surface of this configuration is coated with deformable solid in presence of insoluble surfactant then Marangoni mode destabilizes for low and finite wavenumbers at any Re. The destabilization of Marangoni mode in presence of deformable solid for creeping and inertial flows is a new finding or which was not discussed in previous studies. This instability has a wide applications where high heat and mass transfer rates are required. We discussed extensively these problems in chapter 2 for creeping flow and in chapter 3 for inertial flow.

1.2 Literature review

The stability of gravity-driven fluid flow down a rigid vertical/inclined plane has wide variety of applications in engineering such as distillation columns, condensers, heat exchangers (Craster & Matar 2009), coating processes (Wenstein & Ruschak

2004) and biological applications in pulmonary fluid flows in lung airways (Grotberg & Jensen 2004; Halpern & Grotberg 1993, 1992). In all of these technological and natural settings, the film flow of a liquid layer with free surface is encountered. It is well known that these liquid film flows are prone to a free surface gas-liquid interfacial instability which leads to undulations in free surface, and hence, the film thickness becomes non-uniform. While these instabilities are undesirable in applications like coating process, they are advantageous for achieving high heat & mass transfer rates. The interfacial instabilities are widely useful in patterning applications as well (Bandyopadhyay *et al.* 2008; Mukherjee & Sharma 2015). The early studies related to stability of liquid film flow past rigid incline surface was conducted by Benjamin (1957), and Yih (1963) for a Newtonian liquid film flow down a rigid incline. Benjamin (1957) detected a category of undamped surface waves which exists for all finite values of Reynolds number for which flow remains always unstable. However, the rate of amplification of unstable surface waves becomes very small for low wavenumber (or long wavelenghts) when Reynolds number is fairly small. Yih (1963) demonstrated that the liquid film becomes unstable for long-wave perturbations when the Reynolds number increases above a critical value. This long wavelength (or low wavenumber) instability is referred as Yih mode or GL mode or free surface mode instability in literature. Yih (1963) observed that his results for small wave number and low Reynolds number matched with Benjamin's results. However, Yih's results for high wavenumbers and vertical configuration were found to contradict with the results predicted by Benjamin (1957). The Benjamin's work was extended by Whitaker (1964) for studying the effect of surface active agents (surface tension, surface viscosity, and surface elasticity) on the vertical film flows for low Reynolds number. Whitaker (1964) observed that the surfactant has low stabilizing effect on the free-surface instability of vertical falling film. The effect of surface active agents (soluble and insoluble) was re-examined by Lin (1970) and observed that the effect of both soluble and insoluble surfactants is stabilizing on the flow. It was found that the stabilizing effect of soluble surfactant is comparatively strong than the insoluble one. The stability of inclined falling film was also investigated in several previous studies (Anshus & Acrivos 1967; Lin 1967; Whitaker & Jones 1966). Whitaker & Jones (1966) predicted, when the interfacial mass transfer and the elasticity of interface is considered as compositional, the existence of

critical Reynolds number is prohibited. The results show that both the magnitude and mechanism of mass transfer affect the stability of the liquid film. Anshus & Acrivos (1967) used the asymptotic analysis which depends on the assumption of a large elasticity parameter. They found enormous increase in the wave length and enormous decrease in the growth rate of the most quickly amplified perturbations. Lin (1967) studied the mechanism of the instability of a single liquid layer flowing down an inclined plane. In his study, Lin (1967) found the existence of critical wavelength of the surface wave formation for a given angle of inclination of a plane. It was also found that the film can become unstable due to shear waves before it becomes unstable with respect to surface waves when the wavelengths of a free surface disturbance is smaller than the critical wavelength. Furthermore, the film always becomes unstable due to free-surface disturbance when the wavelength of free-surface disturbance higher than its critical value. Ji & Setterwall (1994) studied the configuration of vertical falling film with soluble and volatile interfacial surfactant. They studied the desorption and adsorption of solute at gas-liquid interface for both surface wave mode and a new wave mode, and finally predicted that the desorption is responsible for Marangoni instability of the new mode. There are several more recent studies related to the stability of surfactant loaded liquid film flowing down an inclined plane (Anjalaiah *et al.* 2013; Blyth & Pozrikidis 2004*a*,*b*; Samanta 2014; Wei 2005*a*), however, we discuss them a little later. The central conclusions from the above cited studies were: (i) the insoluble surfactant layer has a stabilizing effect on the gas-liquid interfacial (or surface) mode, and (ii) there exists an additional mode purely due to disturbances in surfactant concentration which remains stable for surfactant-laden falling film down an inclined plane. This mode is referred to as Marangoni mode and this mode remains stable as long as the gas-liquid interface remains stress free in basic state (Wei 2005*a*).

The stability and dynamics of cylindrical viscous film has also been extensively investigated by several researchers. Goren (1961) theoretically analyzed the stability of a Newtonian liquid film inside and outside of a circular tube and observed that the free surface is susceptible to a Yih type gas-liquid interfacial instability at any non-zero Reynolds number. This cylindrical liquid film configuration also exhibits a capillary instability due to the presence of cylindrical fluid-fluid interface for any non-zero value of gas-liquid interfacial tension. Goren (1961) also performed exper-

iments for annular liquid film lining a tube for a range of film thickness and demonstrated that plug formation occurs at multiple spatial locations in a periodic manner (which is related to a critical wavenumber) and this plug formation was shown to weakly depend on the film thickness. Cassidy *et al.* (1999) examined the effect of surfactant on the growth rates of capillary instability and plug formation, both by experiments and theory, for a liquid film lining the interior of a tube. The liquid film was static and the linear stability results demonstrated that the presence of surfactant enhances stability. The linear stability results demonstrated that the presence of surfactant decreases the growth rates by a factor of four compared to its surfactant free value. The experiments were performed by infusing water into an initially oil filled tube. The experiments suggested a decrease in initial growth rate by 20% and a decrease in time of formation of plug by a factor of about 3.8. Hammond (1983) and Gauglitz & Radke (1988) derived the non-linear evolution equation for surfactant free film using lubrication approximation and when Reynolds number remains $O(1)$. These one-dimensional film evolution equations were derived using lubrication approximation and were used to predict the conditions for the formation of collars, or plugs or liquid bridges. Halpern & Grotberg (1992) analyzed the liquid film flow inside of a flexible tube with the motivation to understand lung airway closure phenomena. They proposed that the airway closure occurs either by formation of liquid plug, collapse of compliant airway wall, or a combination of both the mechanisms. The liquid plug formation occurs due to capillary destabilization of liquid film, and there exists a critical film thickness beyond which the unstable waves grow to form liquid bridges. The critical film thickness is strongly dependent on fluid and wall properties. Halpern & Grotberg (1992) have particularly demonstrated that the wall flexibility significantly effects the value of critical film thickness. Halpern & Grotberg (1993) examined the same problem as analyzed by Halpern & Grotberg (1992) in presence of an insoluble surfactant adsorbed at air-liquid interface. They demonstrated that the presence of surfactant delayed the instability process and the time required for airway closure could be four to five times longer than the case of surfactant free film. They also showed that the value critical film thickness was not affected by the presence of monolayer of surfactant at air-liquid interface. Similar conclusions were made by Kwak & Pozrikidis (2001) for the rod-annular type of configuration. By taking appropriate limits, they were able to obtain either an an-

nular layer coated on the interior or exterior of a rigid tube, or an infinite thread suspended in an infinite ambient fluid. Their linear stability analysis showed that the growth rate of interfacial instabilities decreases in presence of insoluble surfactant layer at fluid-fluid interface. Their non-linear results demonstrated that while the presence of surfactant do not alter the final shapes taken by interface, surfactant does delay the process by decreasing the growth of interfacial waves. In a slightly different context, Quere *et al.* (1997) studied the effect of surfactant on the formation of liquid layer on the solid surface. They first drawn the solid from pure wetting liquid and found a coated solid surface with layer of liquid, and the thickness of this liquid layer is given by the Landau eqation for small coating liquid velocities. In another case they drawn the solid from a solution containing surfactant. They found that the thickness of the coated liquid layer is higher when the solid is withdrawn from a surfactant solution as compared to the case when the solid was withdrawn from a liquid which do not contain surfactant. This observation again shows that the presence of surfactant causes significant changes in final coating properties.

All the studies mentioned above related to the stability of surfactant-laden liquid film flow down a rigid inclined plane or film flow on the inside/outside of a tube demonstrated that while the effect of presence of surfactant monolayer is stabilizing on the interfacial mode, the presence of surfactant do not introduce any additional unstable mode. Frenkel & Halpern (2002) first discovered the presence of a surfactant-induced unstable mode for the case of two-layer channel flow when the fluid-fluid interface is covered with a monolayer of surfactant. They examined the linear stability of combined Couette-Poiseuille flow of two immiscible fluid layers in a channel when the fluid-fluid interface was loaded with a monolayer of surfactant. They considered creeping flow and examined the problem in the limit of long-wave disturbances. They observed that there are two eigen modes: the usual Yih type mode which exist due to jump in viscosity across the fluid-fluid interface, and a surfactant mode which exists solely due to presence perturbation in concentration of surfactant. They observed that while the fluid-fluid Yih type interfacial mode remains stable for long wave perturbations, the surfactant mode could become unstable for certain values of viscosity ratio and fluid thickness ratio of two fluids even in Stoke's flow limit. They concluded that this mode becomes unstable even in absence of any interfacial deflection and becomes unstable due to fluctuations

in surfactant concentration. The fluctuations in surfactant concentration results in surface tension gradients which generates Marangoni stresses and these Marangoni stresses in turn introduces Marangoni flow which induces an instability. This surfactant induced instability is termed as Marangoni instability in literature. Halpern & Frenkel (2003) examined the same problem as studied by Frenkel & Halpern (2002) by including arbitrary wavelength perturbations, entire range of Marangoni number, viscosity ratio, interfacial shear, and fluid-thickness ratio. They observed that the Marangoni instability is not necessarily a long-wave instability in the sense that the unstable waves may not be much longer than the depth of thinner fluid layer. Further, for several parametric regimes, this surfactant-induced instability has a mid-wave character while the long-wave and short wave perturbations remain stable.

The linear stability of surfactant-laden Newtonian liquid film flowing down an inclined plane was examined by Pozrikidis (2003) in the limit of vanishing Reynolds number. Pozrikidis (2003) observed the occurrence of two normal modes. The first one is the classical free-surface Yih's mode and the second is the surfactant induced Marangoni mode. The solutions reveal that while both the modes remain stable in this vanishing Reynolds number limit, the decay rate of Marangoni mode is lower than that of free-surface gas-liquid interfacial mode. The effect of surfactant was also examined for liquid film flow down a wavy inclined wall in the same study (Pozrikidis 2003). Blyth & Pozrikidis (2004*a*) analyzed the effect of surfactant on the stability of liquid film flow down an inclined plane in presence of inertia using the Orr-Sommerfeld formulation. For non-zero Reynolds number, they observed that the Yih's mode and the Marangoni mode remain the two most (least) unstable (stable) mode. In creeping flow limit, the decay rate of Marangoni mode remains lower than that of gas-liquid interfacial mode. As Reynolds number increases above zero, while the decay rate of Marangoni mode remains almost unaffected, the decay rate of gas-liquid interfacial mode decreases and it eventually becomes unstable showing positive growth rates above a critical Reynolds number. Thus, it is concluded that for zero and low Reynolds numbers, the Marangoni mode remains the least stable mode (or dominant mode) and for sufficiently large Reynolds number, the gas-liquid interfacial mode becomes the dominant mode of instability. They also showed that the presence of surfactant have a stabilizing effect on interfacial mode

and the critical Reynolds number is higher for film contaminated with surfactant as compared to the case of clean film. Blyth & Pozrikidis (2004*b*) investigated the influence of surfactant on the stability of two fluid flow in an inclined channel to include the effect of gravity, and surfactant diffusivity (both of which were excluded by Frenkel & Halpern (2002) and Halpern & Frenkel (2003)). They confirmed the findings of Frenkel & Halpern (2002) and Halpern & Frenkel (2003) that the presence of an insoluble surfactant at fluid-fluid interface introduces a Marangoni instability depending on the values of viscosity and thickness ratios of two fluid layers.

The dynamics of liquid film in presence of an insoluble interfacial surfactant flowing down a rigid inclined plane was also investigated by Pereira & Kalliadasis (2008). Their linear stability results reveal a similar stabilizing effect on free-surface interfacial mode as observed in previous studies (for example, Blyth & Pozrikidis (2004*a*)). However, they remarked that (stable) Marangoni mode as observed in previous study by Blyth & Pozrikidis (2004*a*) is, to be precise, a diffusional mode which would be present even if the species present at the gas-liquid interface is not a surfactant species. They argued that the decay rate of this mode is proportional to Peclet number (which is related to diffusional properties of any species) and not to Marangoni number which captures the effect of surface tension changes with respect to variations in concentration. Off course, the stabilizing effect on gas-liquid interfacial mode is due to the presence of surfactant species. They also examined the evolution of free surface height and surfactant concentration. In the non-linear regime, they observed that solitary wave pulses for both clean and contaminated film. The presence of surfactant reduces the amplitude and velocity of these pulses. All these studies which examined the stability of surfactant loaded liquid film concluded that the surfactant or Marangoni mode do not become unstable in contrast to finding of Halpern & Frenkel (2003) or Blyth & Pozrikidis (2004*b*). It is important to point out here that Halpern & Frenkel (2003) and Frenkel & Halpern (2002) demonstrated that both the presence of surfactant and a basic interfacial shear is required in order to cause destabilization of Marangoni mode. Since, the basic shear stress at gas-liquid interface for the liquid film flowing down an inclined plane in above mentioned studies was absent, this was suggested as the reason for Marangoni mode remaining stable for liquid film flows (planar and cylindrical). In order to in-

vestigate this aspect, Wei (2005*a*) performed a long wave asymptotic analysis to examine the stability of surfactant covered liquid film flow down an inclined plane in presence of an imposed shear stress on the air-liquid interface. It was clearly shown that the Marangoni mode becomes unstable depending on the direction and magnitude of the applied shear stress. Similar conclusion was also made for a viscoelastic liquid film flowing down a rigid inclined plane (Wei 2005*b*), and for a viscoelastic liquid film coating the inside of a tube (Zhou *et al.* 2014). Wei (2007) investigated the role of basic flow on such surfactant-induced instabilities for a variety of configurations and demonstrated that the base flow plays a dual role in modifying the stability characteristics. These studies reconsolidated the idea that base state interfacial shear is always required to cause the destabilization of Marangoni mode. In the present work, we analyzed the stability of surfactant-laden liquid film flowing down an inclined plane when the plane is coated with a deformable solid layer. We explore the effect of adding a flexible or compliant wall on the stability of both interfacial and Marangoni modes. We show that the presence of deformable wall dramatically changes the stability characteristics of the surfactant-covered film flow down an inclined plane. When the fluid flows past a soft, deformable wall, the moderate fluid stresses are sufficient to cause deformations in the solid layer and these deformations in turn can alter the fluid flow. The velocity field in fluid layer and the displacement field in solid layer are related via boundary conditions at fluid-solid interface. Thus, mathematically speaking, the presence of a deformable wall amounts to change in boundary conditions at fluid-solid interface from no-slip to continuity of velocities and stresses in solid and fluid layers. There are few studies which analyzed the effect of change of type of substrate/wall (or equivalently changing the fluid-solid conditions) on the stability of surfactant-laden liquid film flow down an inclined plane. For example, Anjalaiah *et al.* (2013) analyzed the stability of a liquid film flow down a porous inclined wall in presence of an insoluble surfactant at gas-liquid interface. For the case of porous wall as well, they observed the presence of two dominant modes: gas-liquid interfacial (or Yih's) mode, and the Marangoni mode. The effect of surfactant on interfacial mode was found to be stabilizing while porosity has a destabilizing effect on the overall stability of the system. The Marangoni mode was always found to be stable and dominates the Yih's mode at smaller Reynolds number. However, with increase in Reynolds number,

an exchange of dominant mode of instability occurs and interfacial (Yih's) mode becomes the critical mode of instability. This interfacial mode becomes unstable above a critical Reynolds number and the presence of surfactant increases this critical Reynolds number as compared to the clean film case. It was demonstrated that it is possible to modify the stability characteristics of the system by changing the properties (like porosity, permeability, and thickness) of wall. A similar conclusion was made in Chattopadhyay & Usha (2016) for pressure driven flow two fluid layers in presence of an interfacial surfactant. The effect of having hydrophobic channel walls was investigated and it was demonstrated that it is possible to manipulate Yih-Marangoni type instabilities in by making walls rough/hydrophobic/porous.

The effect of adding interfacial surfactant at fluid-fluid interface has also been investigated for the case of two liquid layers falling down an inclined wall (Anjalaiah & Usha 2015; Chattopadhyay & Usha 2016; Gao & Lu 2007; Samanta 2014). The linear stability analysis of two liquid layers flowing down an inclined plane in Stoke's flow limit and in presence of an insoluble interfacial and surface surfactant is carried out by Gao & Lu (2007). In this inertialess limit, they observed occurrence of four normal modes and found that only one of them exhibits instability. When the upper layer is more viscous than the lower layer, this two-layered configuration remains unstable due to inertialess instability of liquid-liquid interface in absence of surfactant. The effect of adding a surface surfactant is found to be stabilizing as it decreases the growth rate of this inertialess instability. For highly viscous upper layer in comparison to the lower layer, the growth rate of inertialess unstable mode increases due to the presence of surface surfactant. The effect of interfacial surfactant was observed to be destabilizing in the sense that it enhances the growth rate of inertialess instability for more viscous upper layer. For less viscous upper layer, the interfacial surfactant induces a new mode of instability. We believe that this mode is the (interfacial) surfactant induced Marangoni mode similar to the unstable mode observed by Halpern & Frenkel (2003). The effect of surface surfactant was found to be stabilizing for this mode. Samanta (2014) extended the work by Gao & Lu (2007) by including the effect of inertia. It was observed that the maximum growth rate decreases for both interface and surface modes due to the presence of surface surfactant when the less viscous layer is adjacent to the inclined plane. When the more viscous liquid is adjacent to the inclined plane, inertial effects induces a new

instability. The presence of interfacial surfactant have a stabilizing effect on this inertial instability. In this study (Samanta 2014), only interface and surface modes out of the four dominant normal modes were analyzed in detail. Thus, no information is clearly available regarding the stability of characteristics of Marangoni modes for free surface and liquid-liquid interface. In the present work, we examine the effect of surface surfactant on the stability of free-surface mode and the Marangoni mode when the lower liquid layer is replaced by a soft, deformable elastic solid layer. We show that the Marangoni mode can also become unstable due to presence of a deformable liquid-solid interface. The effect of change of substrate or wall properties for the case of two layer surfactant-laden film flow on interface and surface modes instabilities has been addressed by Anjalaiah & Usha (2015). They examined the linear stability of two liquid film flow in presence of either an interfacial surfactant or surface surfactant or both when the film flow occurs past a slippery inclined wall. The presence of velocity slip at fluid-solid boundary resulted in decrease of growth rates for the parameter regimes where instabilities occur. The range of unstable wavenumbers also shrinks showing the stabilizing effect of slip for this flow configuration. It was suggested that slip could be used to control instabilities for such two-layer flows.

Thus far, we have discussed studies related to single or two liquid film flow down a rigid inclined plane when the fluid-fluid interface remains populated with a monolayer of insoluble surfactant. In the present work, we analyze the stability of a surfactant-laden liquid film flowing down a inclined plane when the plane is coated with a soft, deformable solid layer. When a fluid flows past a soft solid with relatively smaller shear modulus, the moderate fluid stresses at fluid-solid interface are sufficient to cause deformations in solid layer. These deformations in turn can alter the fluid flow. Thus, a flow configuration with deformable fluid-solid interface is expected to be qualitatively very different than the same flow configuration with rigid fluid-solid interface. Indeed the early theoretical works by Kumaran and coworkers suggested the same (see for example, Kumaran (2000)). Thus, we may expect that the presence of deformable liquid-solid interface could effect the stability characteristics of both Yih's type of free-surface gas-liquid mode and the surfactant induced Marangoni mode. In the following, we review the studies which focuses on the effect of compliant/deformable wall on the stability of fluid flow.

Kumaran *et al.* (1994) analyzed the stability of Couette flow of a Newtonian fluid past a flexible gel surface. The Couette flow configuration with rigid walls remains linearly stable at any Reynolds number, while experimentally, it is known to exhibit a transition from laminar flow profile above Reynolds number of $O(1000)$. Kumaran *et al.* (1994) analyzed the linear stability of a fluid flowing between two plates where top plate was moving with a specified speed and the bottom stationary plate was coated with a deformable solid layer. They analyzed the stability of the system in creeping flow limit and observed that the flow is linearly unstable even in the absence of inertia when the soft solid layer becomes sufficiently deformable. They introduced a dimensionless deformability parameter $G = \mu V/ER$, where μ is viscosity of fluid, V is the characteristic velocity, R is the thickness of fluid layer, and E is the shear modulus of deformable solid layer. This parameter G can be interpreted as ratio of viscous shear stresses in fluid layer to the elastic stresses in solid layer. As $G \to 0$, one obtains the rigid solid limit. The other important non-dimensional parameter was solid to fluid thickness ratio H or non-dimensional solid thickness. It was demonstrated that for a given solid thickness, the flow becomes unstable when the wall deformability parameter increases above a critical value and this critical value of G was shown to decrease with increase in solid thickness. They used a linear elastic solid model to represent the dynamics of soft solid layer. The stability of Hagen-Poiseuille flow in a flexible tube in creeping flow limit was examined by Kumaran (1995) using a linear elastic solid model for the flexible wall. The pressure-driven flow in a flexible tube was also found to become unstable in creeping flow limit when the tube becomes sufficiently soft, or equivalently, the dimensionless wall deformability parameter increases above a critical value. However, unlike the case of Couette flow, it was observed that the critical value of wall deformability parameter G asymptotes to a constant value as the solid layer thickness is increased. The instability observed in these two cases exists purely due to the presence of a deformable fluid-solid interface. There are several other studies by Kumaran and coworkers (Shankar & Kumaran 1999, 2000, 2001*a*,*b*, 2002) which analyzed the linear and non-linear stability of flow in flexible tube examining the entire range of Reynolds number from zero to infinity. All of these studies employed a linear viscoelastic solid model to represent the deformable wall. An excellent summary of findings in the above mentioned papers are given in a review

by Kumaran (2003). Broadly, there are multiple modes which exist due to the presence of a deformable solid coating and these modes could become unstable as wall deformability is increased. These modes are classified into two types: viscous wall modes and inviscid modes. The instability mode observed in creeping flow limit for flow in a flexible tube when continued to finite and high Reynolds number, forms the most dominant viscous wall mode. Other modes emerge for non-zero values of Reynolds number. The central conclusion from these studies is that the transition in flexible tubes or channels can occur at Reynolds number much lower than the corresponding transition Reynolds number in rigid configuration and that this transition occurs due to the deformability of the wall. In the present work, since we focus on small Reynolds number, the continuation of creeping flow viscous mode to small and finite Reynolds number is expected to be important in context of the work presented in this thesis.

Kumaran & Muralikrishnan (2000) and Eggert & Kumar (2004) performed experiments in parallel plate geometry when the bottom plate was coated with a deformable solid layer and the top plate was set in motion. These experiments were performed at slow plate speeds such that low Reynolds number prevails during experiments. These experiments confirmed the findings related to creeping flow instability induced due to flexible wall as predicted in Kumaran *et al.* (1994). Experiments performed by Verma & Kumaran (2012*b*, 2013*a*) examined the transition Reynolds number as a function of shear modulus for flow of water type fluid in flexible tubes and channels. Verma & Kumaran (2012*b*) fabricated tubes in poly-dimethyl siloxane (PDMS) blocks using the technique described in Verma & Ghatak (2006) and Majumder & Ghatak (2010). It was observed that the laminar flow undergoes a transition to a more complex flow profile for Reynolds number as low as 500 for the softest gels used in this study. Similarly, Verma & Kumaran (2013*a*) demonstrated transition Reynolds number to be as low as 200 for the softest micro-channel fabricated in their work. These flow instabilities arising due to fluid-structure interactions have been a subject of numerous studies and are reviewed in Gad-el hak (2003); Kumaran (2015); Shankar (2015). The central conclusions from these investigations were that the stability characteristics get significantly affected by the presence of a deformable wall, and new unstable modes proliferate for flow past deformable solid surface. While all of these studies focused on new instabilities

that arise due to the presence of compliant/soft wall, Shankar and coworkers (see for example, a recent review by Gaurav & Shankar (2015) investigated the effect of including a soft solid coating on flow configurations which involves one or more fluid-fluid interfaces. The work presented in this thesis also involves presence of a deformable fluid-solid interface and a fluid-fluid interface. Thus, in the following, we review the studies which explored the effect of deformable wall on fluid-fluid interfacial instabilities which are known to exist in the rigid configuration.

Shankar & Kumar (2004) analyzed the linear stability of two-layer Couette flow past a deformable solid surface using an Orr-Sommerfeld type analysis, and solved the resulting linear stability problem by using an asymptotic long wave technique for low wavenumbers and a shooting method for arbitrary wavenumbers. This problem configuration involved a fluid-fluid interface and a deformable fluid-solid interface. The fluid-fluid interface becomes unstable when the more viscous layer occupies the lesser space for non-zero Reynolds number, however small it may be Yih (1967). This fluid-fluid instability occurs due to a viscosity jump across the fluid-fluid interface. The configuration also admits a fluid-solid mode similar to that observed by Kumaran *et al.* (1994). The long wave asymptotic analysis demonstrated that when the more viscous fluid layer is thinner than the less viscous layer (a configuration which remains unstable in rigid limit for any non-zero Reynolds number), the soft solid layer could completely suppress the fluid-fluid interfacial instability when the dimensionless wall deformability parameter increases beyond a critical value. For the other case i.e. when the more viscous layer occupies more space, the solid layer effect could be stabilizing or destabilizing depending on the solid thickness. Whenever the effect of solid layer is stabilizing, the continuation of long wave results for arbitrary wavelength disturbances show that the suppression continues to finite and high wavenumbers as well. As the wall deformability parameter is increased to sufficiently high values, the fluid-solid interfacial mode becomes unstable. It was further demonstrated that it is possible to obtain a completely stable flow configuration using a deformable solid layer for those sets of parameters where the flow otherwise remains unstable in the rigid limit. A similar manipulation and control of instabilities for two-layer viscoelastic plane Couette flow using deformable solid coating was demonstrated by Adepu & Shankar (2007); Shankar (2004, 2005).

The stability of gravity driven free surface flow of a Newtonian liquid film falling down an inclined plane coated with a deformable solid layer was analyzed by Shankar & Sahu (2006). They used a linear viscoelastic model for soft solid layer. As mentioned earlier, the Newtonian liquid film flowing down an inclined plane falls prey to a free surface instability for a given angle of inclination, when the Reynolds number number increases above a critical value. Shankar & Sahu (2006) analyzed the effect of presence of a deformable solid coating by carrying out a low wavenumber analysis and demonstrated that the long wavelength perturbations can be completely suppressed by using a deformable solid layer. Their numerical results demonstrated that the suppression continues to finite and high wavenumbers as well. Neutral stability curves constructed in wall deformability parameter G vs. wavenumber plane demonstrated that the film remains unstable because of free-surface instability in rigid limit ($G \to 0$) and as G increases, the free-surface instability is suppressed. As wall becomes more and more softer (i.e. higher G values), the gas-liquid free-surface and the deformable gas-liquid interface becomes unstable due to wall deformability. Thus, there exist a window in terms of wall deformability parameter (or equivalently, in terms of shear modulus of solid) where the falling film can be made stable where it otherwise remains unstable in the rigid limit.

While the above mentioned studies by Shankar and coworkers (Adepu & Shankar 2007; Shankar 2004, 2005; Shankar & Kumar 2004; Shankar & Sahu 2006), used a linear elastic solid model to represent the deformations in soft solid layer, Gkanis & Kumar (2003, 2005, 2006) highlighted the importance of using a nonlinear solid model even for linear stability analysis to accurately capture the stability behavior of the composite fluid-solid configurations.For example, Gkanis & Kumar (2003) analyzed the linear stability of Couette flow of a single Newtonian fluid past a deformable solid surface when the soft solid layer is modeled using a simple non-linear neo-Hookean solid model. They examined this problem in creeping flow limit and the stability was governed by three dimensionless parameters namely: imposed strain (which is nothing but the wall deformability parameter defined above), solid to fluid thickness ratio or dimensionless solid thickness, and a dimensionless fluid-solid interfacial tension parameter. The neo-Hookean solid exhibits a non-zero first normal stress difference which is zero for a linear elastic solid model.

This non-zero first normal stress difference in base state causes significant changes in stability characteristics for Couette flow past a flexible surface when a non-linear neo-Hookean solid model is used instead of a linear elastic constitutive relation. A short wave instability was observed for flow past neo-Hookean solid which remains absent for flow past linear elastic solid. Also, finite wavelength perturbations become unstable in a similar fashion as observed for linear elastic solid (Kumaran *et al.* 1994). Thus, with neo-Hookean solid model, both finite wavenumber and high wavenumber perturbations can become unstable with increase in deformability parameter while only finite wavenumber instability is observed for Couette flow past linear elastic solid model. It was shown that for sufficiently thin solid layer, the short wave mode becomes unstable first as G is increased, and thus, dominates the stability behavior. However, for thick solid, the finite wavenumber perturbations remain the most dominant mode of instability. The presence of interfacial tension have a strong stabilizing effect on the short wave mode instability. Similar conclusion were made for pressure-driven flow in a neo-Hookean deformable channel (Gkanis & Kumar 2006) and for gravity driven flow of a Newtonian liquid film flowing past a neo-Hookean solid (Gkanis & Kumar 2006). Motivated by these observations, Gaurav & Shankar (2007) re-examined the stability of a Newtonian liquid film falling down an inclined plane when the inclined plane is coated with a neo-Hookean deformable solid layer. They re-examined this problem in order to find out whether the stabilization predicted by Shankar & Sahu (2006) using a linear elastic solid layer holds with a neo-Hookean solid as well. They first carried out a low wavenumber analysis and observed that in this long wave perturbation limit, the governing equations for a neo-Hookean solid model reduces to that of linear elastic model, and hence, the suppression predicted using linear elastic solid holds well in this low wavenumber limit. The low wavenumber results with neo-Hookean solid were found to be exactly identical to results obtained using linear elastic solid. Their results at finite and high wavenumbers show that while the neutral curves corresponding to suppression of free-surface instability remains unaffected, the neutral curves corresponding to destabilization of gas-liquid free-surface and liquid-solid interface get modified on using a neo-Hookean solid model. They observed the existence of short wave mode instability as predicted by Gkanis & Kumar (2003, 2005, 2006) and this becomes important in determining the width of stability win-

dow (predicted by Shankar & Sahu (2006)) for thinner solid layers. The critical value of G required for destabilization of gas-liquid interface do not change much, however, the band of unstable wavenumbers increases. Thus, in this sense, the effect of neo-Hookean solid was observed to be more destabilizing. However, the width of stability window remains almost same for both solid models. Shankar and coworkers (Gaurav & Shankar 2013; Jain & Shankar 2007, 2008) further analyzed the stability of different flow configurations with the motivation of manipulation and control of fluid-fluid interfacial velocities using a deformable solid layer. For example, Jain & Shankar (2007) analyzed the stability of a viscoelastic liquid film flowing down an inclined plane coated with a neo-Hookean deformable solid layer. They observed that the stability suppression holds well with neo-Hookean solid. More importantly, in this study, they demonstrated that it is possible to use a deformable solid layer to suppress free-surface instabilities for a viscoelastic liquid film as well. Jain & Shankar (2008) analyzed the stability of cylindrical Newtonian liquid film flowing inside/outside of tube which is coated with a neo-Hookean deformable solid layer and Gaurav & Shankar (2013) analyzed the stability of core-annular flow in a flexible tube. For both of these configurations, the fluid-fluid interface was cylindrical and hence can also become unstable due to capillary instability in additional to interfacial instability caused due to jump in viscosity across the fluid-fluid interface. It was again demonstrated that it is possible to obtain stable configuration for those parameter sets for which the flow remains unstable in rigid limit. The stability of two liquid layers flowing down an inclined plane was also analyzed (Gaurav & Shankar 2010*a*). This flow configuration involves the presence of three interfacial modes: a gas-liquid mode, a liquid-liquid mode, and a deformable liquid solid mode. The effect of soft solid layer was found to be stabilizing for gas-liquid mode while the effect of solid layer on liquid-liquid mode depends on whether the more viscous or less viscous liquid is adjacent to the soft solid surface. When more viscous liquid is adjacent to the deformable wall, the wall deformability has a stabilizing effect on liquid-liquid (and gas-liquid) interface. In this case, it is possible to obtain stable flow configurations for those cases where the two interfaces otherwise remain unstable for flow past a rigid incline surface. On the other hand, when less viscous liquid is near the wall, the wall deformability has a destabilizing effect on liquid-liquid interface and stabilizing effect on gas-liquid

interface. As a result, it is not possible to stabilize both the interfaces simultaneously. It was also shown that it is possible to select wall properties (solid thickness and shear modulus) to selectively destabilize one of the interfaces while keeping the other two as stable. In a related fashion, it was shown to selectively destabilize a finite band of wavenumbers for core-annular flow in a flexible tube by appropriately choosing the soft solid parameters. Thus, these studies demonstrates that the presence of deformable solid surface could significantly affect the stability behavior of fluid-fluid interface. In the present work, we focus on whether the presence of deformable solid layer could affect the stability of surfactant-induced Marangoni mode for liquid film flow down a flexible inclined plane.

1.3 Structure of the thesis

Above, we have discussed the literature based on our objective and the scope of the work, the research work presented in this thesis are categorized into two parts, one is based on the stability analysis of gravity-driven surfactant-laden liquid film flowing down an inclined plane for creeping flow limit and another is based on the manipulation and control of instabilities for surfactant-laden liquid film flowing down an inclined plane using a deformable solid layer for finite Reynolds number. The above discussed first part is presented in chapter 2 and second in chapter 3. In chapter 2, we explore the effect of various parameters (importantly soft solid) on the unstable Marangoni mode which was absent in single contaminated liquid layer flowing down an inclined plane studied by Blyth & Pozrikidis (2004*a*). In chapter 3, we focus the effect of various parameters mainly on the stability window where flow remains completely stable. In both the parts (or problems), we also focus on the dynamics of deformable solid layer as well as insoluble surfactant.

All the chapter contains abstract, introduction (consist of motivation and literature review which presents the insight of previous works concerning to our research studies), problem formulation (consists of governing equations, linearised govering equations and boundary conditions), results and discussion and conclusion of the chapter. We presented abstract of thesis at the beginning of thesis, list of tables, list of figures. Finally, we presnted conclusion of thesis separately in chapter 4.

Chapter 2

Stability of gravity-driven free surface flow of surfactant-laden liquid film flowing down a flexible inclined plane

Abstract

We examined the linear stability of gravity-driven creeping flow of a liquid film flowing down an inclined plane when the inclined plane is coated with a deformable solid layer and the gas-liquid interface is contaminated with a monolayer of insoluble surfactant. The contaminated liquid film flowing down a rigid incline admits gas-liquid (GL) interfacial mode and surfactant-induced Marangoni mode, both of which remain stable in the creeping flow limit. The primary aim of this study is to explore the effect of the presence of a deformable wall, in place of a rigid inclined wall, on the stability behavior of Marangoni mode which originates because of the transport of surfactant at the GL interface. In presence of a deformable solid layer, two additional parameters namely, shear modulus and thickness of deformable solid layer also affects the stability behavior of falling film configuration. Our long-wave asymptotic analysis and results at finite and arbitrary wavenumbers demonstrated the destabilization of Marangoni mode solely due to the presence of deformable solid layer. Specifically, we have shown that for a given solid

thickness, the Marangoni mode becomes unstable when the shear modulus of solid layer decreases below a critical value (i.e. the solid layer becomes sufficiently soft). The effect of increasing solid thickness is found to be destabilizing. The LS interfacial mode also becomes unstable at high wavenumbers below a threshold value of shear modulus, however, this value is much smaller than that required to trigger Marangoni mode instability. This implies that as the solid coating becomes more and more deformable, the Marangoni mode becomes unstable first followed by the LS interfacial mode. The GL mode was always found to be stable in creeping flow limit. Further, our long-wave analysis shows that the solid deformability has an additional stabilizing effect on GL mode. The neutral stability curves in nondimensional solid deformability parameter (or equivalently shear modulus) vs. wavenumber plane clearly depicts that the Marangoni mode is the dominant unstable mode in the creeping flow limit. Thus, the present study shows the destabilization of Marangoni mode solely due to presence of deformable solid layer and this we believe is the first example of the case where the instability of the Marangoni mode is observed when the fluid-fluid interface (here, GL interface) remains stress-free in the basic state.

2.1 Introduction

The stability of gravity-driven liquid film flow with free surface is an extensively studied problem because of its relevance in many engineering applications such as coating processes (Wenstein & Ruschak 2004), distillation units, condensers, heat exchangers (Craster & Matar 2009), as well as in biological systems such as pulmonary fluid mechanics (Grotberg & Jensen 2004; Halpern & Grotberg 1993). Beginning from the pioneering investigations by Benjamin (1957) and Yih (1963), there have been a large number of studies exploring the onset of instability of a falling liquid film and subsequent non-linear evolution of surface waves at gas-liquid interface. A comprehensive summary of the work done in the field is given in Chang & Demekhin (2002) and Craster & Matar (2009). Further, many interfacial flow systems, including the falling film configuration, contain surface active agents or surfactants which play a critical role in different applications (Goerke 1998; Morrow & Mason 2001; Quere *et al.* 1997). The surfactant present at the fluid-fluid interface not only significantly affects the stability behavior of the existing fluid-fluid

interfacial mode (Blyth & Pozrikidis 2004*a*; Samanta 2014) but also introduces a new additional normal mode originating from the transport of surfactant at the interface (Frenkel & Halpern 2002). A large number of papers concerning the effect of insoluble or soluble surfactant on the stability of different interfacial flow systems have appeared in the last decade (Bassom *et al.* 2012; Blyth & Bassom 2013; Blyth & Pozrikidis 2004*a*; Gao & Lu 2007; Halpern & Frenkel 2003; Karapetsas & Bontozoglou 2013; Peng & Zhu 2010; Picardo *et al.* 2016; Pozrikidis 2003; Samanta 2014). However, a majority of the studies considered interfacial flows over a rigid wall. Flow past soft, deformable solid surface occurs in a wide variety of settings; for example, in microfluidic devices made of soft elastomers, flow in lung airways (Halpern & Grotberg 1992), use of rubber-covered rolls to reduce defects in coating processes Carvalho & Scriven (1997), potential use of soft walls in instability suppression (Shankar & Sahu 2006), inducing ultra-fast mixing and enhancement of mass transfer in microfluidic channels Bandaru & Kumaran (2016); Shrivastava *et al.* (2008). There are several studies which examined the stability and evolution of (clean) liquid film flow down a flexible inclined wall. However, very few studies investigated the stability of surfactant-laden film flow down a flexible incline Matar & Kumar (2004); Peng *et al.* (2016). In this paper, we attempt to fill this gap and examine the linear stability of liquid film falling down an inclined plane when the plane is coated with a soft, deformable solid layer and the free surface is contaminated with a monolayer of insoluble surfactant. In the following, we briefly review the literature and motivate the context of the present study.

Yih (1963) analyzed the linear stability of liquid film flow down an inclined plane for long-wave perturbations and Lin (1967) extended this analysis to finite and arbitrary wavenumbers. It was demonstrated that the liquid film becomes unstable in presence of inertia when the Reynolds number increases above a critical value. This long-wave instability is referred as Yih mode or GL mode or free surface mode in the present work. The dynamics of the falling film is affected by the presence of surface active agents or surfactants. The surface tension depends on the concentration of surfactants and any gradient in surfactant concentration causes a gradient in surface tension which results in the generation of stress known as Marangoni stress. These Marangoni stresses, in turn, could alter the stability behavior of GL interfacial mode. Indeed, earlier works by Whitaker (1964), Whitaker & Jones (1966), Anshus

& Acrivos (1967), and Lin (1970) all predicted that the presence of insoluble surfactant at free surface has a stabilizing effect on this GL mode and the critical Reynolds number increases for liquid film contaminated with surfactant in comparison to the clean film. The effect of soluble surfactant was also investigated by Ji & Setterwall (1994) and they observed the occurrence of an unstable surfactant mode for a vertical falling film. Blyth & Pozrikidis (2004*a*) presented the numerical solution of Orr-Sommerfeld eigenvalue problem for the gravity-driven flow of a liquid film loaded with insoluble surfactant for both zero and finite Reynolds number. They observed the existence of two normal modes in Stokes flow limit. The first is the usual Yih mode and the second is identified as Marangoni mode which occurs due to the spatial variations in surfactant concentration. Both modes remain stable in zero Reynolds number limit with the decay rate of Marangoni mode being significantly lower than the Yih (or GL) mode. Thus, Marangoni mode is the least stable mode in creeping flow limit (and at low Reynolds number). The Marangoni mode remains unaffected as Reynolds number increases above zero while the growth rate of Yih mode increases with Reynolds number and eventually Yih mode overtakes the Marangoni mode at low Reynolds number. The Yih mode finally becomes unstable beyond a critical Reynolds number and a low-wavenumber asymptotic analysis for Yih mode demonstrated that the presence of surfactant raises the critical Reynolds number for the onset of GL mode instability. The second mode, i.e. the Marangoni mode, was never found to be unstable and hence, the overall effect of surfactant was said to be stabilizing. In a related study, Pereira & Kalliadasis (2008) investigated the same problem in both linear and non-linear regime. The linear regime is examined in the framework of Orr-Sommerfeld formulation using both analytical solution in the limit of low wavenumbers and numerical solution for arbitrary wavenumbers. Their low-wavenumber analysis also revealed the existence of a second normal mode in addition to the usual Yih mode. This second mode originates from the surfactant transport equation and it is this mode which was referred as Marangoni mode in Blyth & Pozrikidis (2004*a*). However, they argued that this additional mode is simply a diffusional mode which would be present even in absence of Marangoni effect- i.e. for any species on GL interface and not necessarily a surfactant. The basis of their argument was that the growth rate was found to be proportional to surfactant diffusivity rather than Marangoni number. This mode

will continue to exist even for zero Marangoni number and it is the Marangoni number which characterizes the rate of change of surface tension with respect to concentration. They referred this mode as diffusional/concentration mode and observed that this second mode always remains stable. The characteristics of GL mode was found to be in agreement with the results of Blyth & Pozrikidis (2004*a*). The Marangoni/concentration mode was overlooked in several previous studies in context of film flows possibly because of stable behavior of this mode.

Frenkel & Halpern (2002) and Halpern & Frenkel (2003) were the first to discover the presence of a surfactant-induced unstable mode for the case of two-layer channel flow when the fluid-fluid interface is covered with a monolayer of surfactant. They demonstrated that in creeping flow limit, the usual fluid-fluid Yih type interfacial mode remains stable, while, an additional mode (called as Marangoni mode) originating due to the presence of surface tension gradients becomes unstable in Stokes flow limit. They showed that the simultaneous presence of surfactant and basic interfacial shear is sufficient to cause Marangoni mode instability even at zero Reynolds number. They suggested the absence of shear stress at GL interface as the reason for not observing the Marangoni mode instability for falling film configuration. Blyth & Pozrikidis (2004*b*) analyzed the stability of two-layer inclined channel flow in presence of an insoluble surfactant using a lubrication approximation and derived nonlinear evolution equations for interface position and surfactant concentration. Their linear stability results from lubrication flow model and Stoke's flow approximation confirmed the results of Frenkel & Halpern (2002) and Halpern & Frenkel (2003) that the presence of interfacial surfactant introduces a Marangoni mode instability for certain values of viscosity and thickness ratio of two fluid layers. Motivated by these observations, Wei analyzed the linear stability of surfactant-laden falling (Newtonian Wei (2005*a*) and viscoelastic Wei (2005*b*)) film down an inclined wall with shear imposed on the GL interface. He clearly demonstrated that depending on the direction of imposed shear, the Marangoni mode could be stable or unstable. The effect of imposed shear on GL mode was also discussed. Similar observations were made by Zhou *et al.* (2014) who investigated the role of imposed shear on the stability of viscoelastic contaminated film falling on the inner surface of a cylindrical tube. These studies re-consolidate the idea that the interfacial shear in the basic state must be non-zero for rendering Marangoni mode unstable. In

the present work, we focus on the effect of wall deformability on the stability of Marangoni mode and show that the Marangoni mode becomes unstable for sufficiently deformable wall even when the GL interface remains stress-free in the basic state. Mathematically, change of the type of substrate/wall (such as a deformable solid coating) leads to changes in boundary conditions at liquid-solid interface. A recent work related to examining the effect of change of type of substrate/wall has been reported by Anjalaiah *et al.* (2013). They carried out the stability analysis for surfactant laden film flow down a porous substrate and systematically examined the effect of porous wall characteristics on both GL and Marangoni modes. They proposed a strategy for stabilizing/destabilizing the GL interfacial mode by appropriately selecting porous wall characteristics, however, the Marangoni mode was always stable and no qualitative changes are observed for Marangoni mode because of variations in the properties of porous wall.

All the work cited in the brief review above is related to the stability of surfactant loaded liquid film falling down a rigid inclined wall. In the present work, we analyze the linear stability of a surfactant laden falling film but the film flows down a flexible inclined wall instead of a rigid inclined wall. When a fluid flows past a soft solid surface, the stresses exerted by the fluid create deformations in the solid layer and these deformations, in turn, could affect the fluid flow. This coupling between fluid and solid is known to cause an instability of liquid-solid (LS) interface in creeping flow limit (Eggert & Kumar 2004; Kumaran *et al.* 1994; Kumaran & Muralikrishnan 2000) as well as at finite Reynolds number (Gaurav & Shankar 2010*b*; Kumaran 2000; Neelamegam & Shankar 2015; Verma & Kumaran 2012*a*, 2013*b*). The physical configurations considered in these studies are Couette flow of a Newtonian liquid past a flexible surface (Eggert & Kumar 2004; Gkanis & Kumar 2003; Kumaran *et al.* 1994; Kumaran & Muralikrishnan 2000; Neelamegam *et al.* 2014) and pressure driven flow of a Newtonian fluid in a deformable channel or tube (Gaurav & Shankar 2009, 2010*b*; Gkanis & Kumar 2005; Neelamegam & Shankar 2015; Verma & Kumaran 2012*a*, 2013*b*). Note that all the configurations mentioned above involved a single fluid and a soft solid layer, and hence, the only deformable interface was LS interface which undergoes an instability when the solid layer becomes sufficiently soft. A very recent review of all these works related to instability of LS interface is presented by Shankar (2015) and Kumaran (2015). In contrast to

these studies, Shankar and co-workers (Adepu & Shankar 2007; Gaurav & Shankar 2007, 2010*a*, 2013; Jain & Shankar 2007, 2008; Shankar & Kumar 2004) examined the stability of various flow configurations past a soft solid layer which involved the presence of a fluid-fluid interface in addition to the deformable LS interface. For example, Shankar & Kumar (2004) analyzed the stability of two-layer Newtonian Couette flow past a deformable solid surface to investigate the effect of presence of deformable solid layer on fluid-fluid interfacial mode. It is well known that the fluid-fluid interface undergoes a long-wave instability due to jump in properties (like viscosity) across the interface (Joseph & Renardy 1993*a*,*b*). Shankar & Kumar (2004) demonstrated that it is possible to completely suppress this fluid-fluid interfacial mode without triggering the liquid-solid interfacial mode instability. A similar suppression of fluid-fluid interfacial mode using a deformable solid layer was shown to exist for several other configurations such as: free-surface flow of a single (Jain & Shankar 2007; Shankar & Sahu 2006) and two liquid layer film (Gaurav & Shankar 2010*a*) flowing down a flexible inclined plane, cylindrical liquid film flowing inside and outside of a tube coated with soft solid layer (Jain & Shankar 2008), core-annular flow in a flexible tube (Gaurav & Shankar 2013) etc. In all these studies, it was demonstrated that the fluid-fluid interfacial instability is suppressed when the solid becomes sufficiently soft (i.e as shear modulus of solid is decreased). As the solid becomes more and more deformable, both fluid-fluid and liquid-solid interface becomes unstable. Thus, there exists a window of stability in terms of shear modulus of solid where fluid-fluid interfacial mode is stabilized without exciting the LS interfacial mode. All these studies are summarized in a recent review by Gaurav & Shankar (2015). The central idea presented by works of Shankar and co-workers is that the fluid-fluid interfacial mode gets affected by the presence of deformable solid layer.

In direct relevance to the present work, there are few studies examining the linear stability of gravity-driven free surface (clean) film flows past a deformable solid surface (Gaurav & Shankar 2007; Gkanis & Kumar 2006; Shankar & Sahu 2006). The deformations in the solid layer are described by using a simple nonlinear neo-Hookean solid model (Gaurav & Shankar 2007; Gkanis & Kumar 2006). In the creeping flow limit, the Yih type GL mode remains suppressed, however, the liquid-solid interface becomes unstable at high wavenumbers for sufficiently

deformable solid layer (Gaurav & Shankar 2007; Gkanis & Kumar 2006). The Yih type GL mode becomes unstable above a critical Reynolds number for film flow down a rigid incline. Gaurav & Shankar (2007) demonstrated that the GL mode instability is suppressed for all wavenumbers for liquid film flow past a sufficiently flexible inclined wall for the parameters where the GL mode otherwise remains unstable in the rigid limit. They showed that there exists a wide window in terms of shear modulus of the solid layer where both GL and LS modes remain stable at all wavenumbers. Thus, the GL mode stability behavior is significantly altered by the presence of a deformable solid layer. It is expected that the presence of a deformable LS interface could also have a profound effect on Marangoni mode and this forms the subject of present investigation. The nonlinear stability and dynamics of falling liquid films over flexible inclined wall have also been investigated by using Benny-type coupled equations for film thickness and wall deflection (Matar *et al.* 2007; Peng *et al.* 2014). They used a simple forced membrane type equation which relates the restoring force with the normal force imposed by the fluid and the wall was restricted to move only in normal direction. Very recently, the effect of the presence of insoluble surfactant for a film falling down a flexible incline has been investigated (Peng *et al.* 2016) following the work of Matar *et al.* (2007). An integral method was used to derive a set of evolution equations for the film thickness, wall position, and surfactant concentration. A normal mode analysis of these equations revealed the dual role played by the flexible wall. A flexible wall with weak damping has a stabilizing effect while wall tension destabilizes flow. Further, the effect of surfactant was found to be stabilizing which is in agreement with previous studies (Blyth & Pozrikidis 2004*a*). However, they focused on the stability of Yih mode while the effect of flexible wall on Marangoni mode was not examined in the above-mentioned study (Peng *et al.* 2016).

The above discussion shows that most of the studies focused on the effect of surfactant or wall deformability on film flows with an objective to control GL interfacial mode instability. In case of contaminated film flows down a flexible inclined wall, the Marangoni mode could also get affected due to wall deformability and this aspect is not investigated in any of the previous studies. Thus, we examine the stability of a surfactant laden falling film down an incline which is coated with a deformable solid layer. Since, the focus is on the effect of wall deformability on

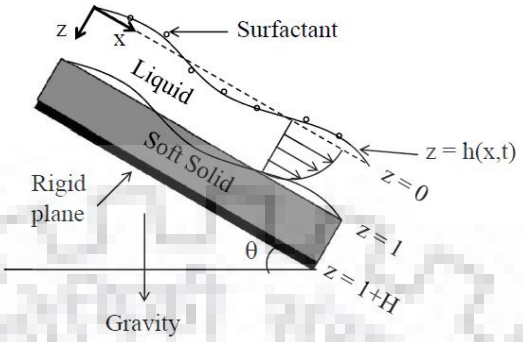

Figure 2.1: Schematic of the configuration considered in the present work: Surfactant-laden Newtonian liquid film falling down an inclined plane coated with a soft, deformable neo-Hookean solid layer.

Marangoni mode, we analyze the problem in creeping flow limit, thus, suppressing the Yih type GL mode instability. The rest of the chapter is arranged as follows: the problem description including the governing equations, linear stability analysis is given in Section 2.2. In Section 2.3, a low-wavenumber analysis is carried out to show the effect of the deformable solid layer on both GL and Marangoni modes with more attention on Marangoni mode. The low-wavenumber results are continued to finite and arbitrary wavenumbers in Section 2.4 and finally, key points are summarized in Section 2.5.

2.2 Problem formulation

2.2.1 Governing equations for fluid and solid

We consider the gravity-driven flow of a surfactant-laden Newtonian liquid layer (or film) down an inclined plane which is coated with an incompressible and impermeable deformable solid layer and is inclined at an angle θ with the horizontal surface (refer Figure 2.1). The solid (thickness HR, shear modulus E_s, and density ρ) is strongly attached to the rigid inclined plane at $z^* = (1+H)R$. The liquid layer (viscosity μ, and density ρ) is in contact with a passive gas and occupies a region

$0 \leq z^* \leq R$ in the undisturbed basic state.

The free surface of the film (exposed to a passive gas) is contaminated with a monolayer of insoluble surfactant with surface concentration $\Gamma^*(x^*,t^*)$. The surfactant molecules get convected and diffused over the free-surface but not into the bulk of the fluid, to locally alter the surface tension γ^*. We assume the densities of solid and liquid layers to be equal because the densities of commonly used elastomers are usually similar to those of common liquids. In the undisturbed steady state configuration, the gas-liquid (GL) interface remains flat with uniform surfactant concentration equal to Γ_0^* and a corresponding unperturbed surface tension as γ_0^*. The liquid layer is governed by conservation of mass (continuity) and momentum (Navier–Stokes) equations:

$$\boldsymbol{\nabla}^* \cdot \mathbf{v}^* = 0, \tag{2.1}$$

$$\rho[\partial_t^* \mathbf{v}^* + \mathbf{v}^* \cdot \boldsymbol{\nabla}^* \mathbf{v}^*] = \boldsymbol{\nabla}^* \cdot \mathbf{T}^* + \rho \mathbf{g}. \tag{2.2}$$

where, $\mathbf{v}^*$ and p^* are the velocity and pressure fields in the liquid layer; $\mathbf{T}^* = -p^*\mathbf{I} + \mu[\boldsymbol{\nabla}^* \mathbf{v}^* + (\boldsymbol{\nabla}^* \mathbf{v}^*)^T]$ is the total stress tensor for the liquid layer.

In perturbed state, at GL interface $z^* = h^*(x^*,t^*)$, the Marangoni stress induced by transportation of surfactant is balanced by hydrodynamic stress of the liquid layer and is given as:

$$\mathbf{n} \cdot \mathbf{T}^* = \boldsymbol{\nabla}_s{}^* \gamma^* - \gamma^* \mathbf{n}(\boldsymbol{\nabla}^* \cdot \mathbf{n}) \tag{2.3}$$

where, $\mathbf{n}$ is the unit normal vector,and $\boldsymbol{\nabla}_s{}^* = \boldsymbol{\nabla}^* - \mathbf{n}(\mathbf{n} \cdot \boldsymbol{\nabla}^*)$ is the component of gradient operator in the local plane of the interface. The convection-diffusion equation for surfactant transport Halpern & Frenkel (2003); Stone (1990) at GL interface is given as:

$$\frac{\partial \Gamma^*}{\partial t^*} + \boldsymbol{\nabla}_s{}^* \cdot (\Gamma^* \mathbf{v_s}^*) + \Gamma^* (\boldsymbol{\nabla}_s{}^* \cdot \mathbf{n})(\mathbf{v}^* \cdot \mathbf{n}) = D_s \boldsymbol{\nabla}_s^{2^*} \Gamma^* \tag{2.4}$$

where, $\mathbf{v_s}^*$ is the component of velocity vector in the interface defined as: $\mathbf{v}^* = \mathbf{v_s}^* + (\mathbf{v}^* \cdot \mathbf{n})\mathbf{n}$, and D_s is the surface diffusivity of surfactant. For small changes in surfactant concentration about the mean value Γ_0^*, the surface tension, and surfactant concentration are related as: $\gamma^* = \gamma_0^* - E(\Gamma^* - \Gamma_0^*)$, where, E refers to surface elasticity defined as $E = -(\partial \sigma^* / \partial \Gamma^*)_{\Gamma_0} > 0$. Finally, the kinematic condition at GL interface is: $\partial_t^* h^* + v_x^* \partial_x^* h^* = v_z^*$

We have used Eulerian (spatial) coordinates ($\mathbf{x}^* = x^*, y^*, z^*$) to describe the fluid model. Unlike the velocity distribution in case of liquid layer, the spatial variations of material points are of more importance in solid, and therefore, it is convenient to employ the Lagrangian approach to define the solid model and state the corresponding governing equations. The position vectors of material particles in the reference (or undeformed) state, $\mathbf{X}^* = (X^*, Y^*, Z^*)$ are considered the independent variables. Thus, the spatial coordinates (x^*, y^*, z^*) used for liquid coincides with the reference coordinates (X^*, Y^*, Z^*) in the unstressed configuration for the deformable solid. In the deformed state of solid, the spatial positions of the material particles $\mathbf{w}^* = (w_X^*, w_Y^*, w_Z^*)$, are expressed in this study as a function of those of the reference configuration: $\mathbf{w}^*(\mathbf{X}^*)$. The deformable solid layer is modeled as an incompressible neo-Hookean elastic solid and the mass and momentum conservation equations for the solid layer are given as (Holzapfel 2000; Malvern 1969):

$$\det(\mathbf{F}) = 1, \tag{2.5}$$

$$\rho \left[\frac{\partial^2 \mathbf{w}^*}{\partial t^{*2}} \right]_{\mathbf{X}^*} = \nabla^*_{\mathbf{X}^*} \cdot \mathbf{P}^* + \rho \mathbf{g}. \tag{2.6}$$

In the above equations, $\mathbf{F} = \nabla^*_{\mathbf{X}^*} \mathbf{w}^*$ is the deformation gradient tensor, and $\mathbf{P}^*$ is the first Piola-Kirchhoff stress tensor. Here, the subscript X^* indicates the gradient with respect to the reference coordinates. The first Piola-Kirchhoff stress tensor is related to Cauchy stress tensor by $\mathbf{P}^* = \mathbf{F}^{-1} \cdot \sigma^*$. The Cauchy stress tensor, $\boldsymbol{\sigma}^*$, for the neo-Hookean elastic solid is (Beatty & Zhou 1991; Destrade & Saccocmandi 2004; Fosdick & Yu 1996; Hayes & Saccocmandi 2002):

$$\boldsymbol{\sigma}^* = -p_s^* \mathbf{I} + E_s (\mathbf{F} \cdot \mathbf{F}^{\mathbf{T}} - \mathbf{I}) \tag{2.7}$$

where, E_s is the shear modulus of deformable solid layer and p_s^* is the pressure in the neo-Hookean solid.

At the liquid-solid (LS) interface, the velocities and stresses in liquid and the solid layer are continuous.

$$\mathbf{v}^* = \left(\frac{\partial \mathbf{w}^*}{\partial t^*} \right)_{X^*}, \tag{2.8}$$

$$\mathbf{n} \cdot \mathbf{T}^* + \gamma_{ls}^* \mathbf{n} (\nabla^* \cdot \mathbf{n}) = \mathbf{n} \cdot \boldsymbol{\sigma}^*, \tag{2.9}$$

where, γ_{ls}^* is the LS interfacial tension. A dot product of stress balance equation (2.9) with normal vector $\mathbf{n}$ gives normal stress balance and dot product with tangent

vector **t** gives tangential stress balance. Zero deformation conditions prevail at $z^* = (1+H)R$, as the flexible solid is strongly bonded to the rigid inclined plane: $\mathbf{w}^* = \mathbf{X}^*$.

The above system of equations is non-dimensionalized by using the following scales: R for lengths and displacements, unperturbed free surface velocity $V = \frac{\rho g R^2 \sin\theta}{2\mu}$ for velocities, $\mu V/R$ for stresses and pressure, Γ_0^* for surfactant concentration, and γ_0^* for surface tension. In the unperturbed steady state, the GL and LS interfaces remain flat. The non-dimensional velocity profile and pressure distribution in the liquid layer are given as:

$$\overline{v}_x(z) = \left(1 - z^2\right), \quad \overline{v}_z = 0, \quad \overline{p}(z) = (2\cot\theta)z, \tag{2.10}$$

where, overbar denotes various base-state physical quantities. The fluid base flow exerts shear stresses at the LS interface resulting in an unidirectional deformation in the solid layer, thereby creating a non-zero displacement in x-direction. The deformation and pressure fields for solid layer are given by:

$$\overline{w}_X = X + G[(1+H)^2 - Z^2], \quad \overline{w}_Z = Z, \quad \overline{p}_s = (2\cot\theta)Z. \tag{2.11}$$

In above equations, $G = \mu V/E_s R$ is the non-dimensional solid deformability parameter representing the ratio of viscous shear stresses in liquid to elastic stresses in the solid layer. $G \to 0$ represents the limit of a rigid surface.

2.2.2 Linear stability governing equations

A standard temporal linear stability analysis is performed in order to determine the stability of the present two layered configuration. All the dynamical quantities (velocities, displacement, pressure etc.) are perturbed about the base-state and are substituted in the governing equations and interfacial conditions. The resulting equations are then linearized to obtain a set of equations in terms of perturbation quantities. We consider two-dimensional perturbations (in the x and z directions) which are expanded in the form of Fourier modes,

$$f' = \tilde{f}(z)\exp[\mathrm{i}k(x-ct)], \tag{2.12}$$

where, f' is the small perturbation of any dynamical variable from its mean basic value, k is the wavenumber of perturbations, c is the complex wave speed and $\tilde{f}(z)$ is

the complex amplitude function of the disturbance. For the deformable solid, x and z are replaced by X and Z, respectively. If $c_i > 0$ (or $c_i < 0$), flow will be unstable (or stable). When the above form of perturbations is substituted in linearized governing equations and interfacial conditions, a set of equations is obtained in terms of amplitude functions and wave speed, c, that govern the stability of the system. The non-dimensional governing stability equations for liquid layer are:

$$\frac{\mathrm{d}\tilde{v}_z}{\mathrm{d}z} + \mathrm{i}k\tilde{v}_x = 0, \tag{2.13}$$

$$Re\left[\mathrm{i}k(\overline{v}_x - c)\tilde{v}_x + (\mathrm{d}_z\overline{v}_x)\tilde{v}_z\right] = -\mathrm{i}k\tilde{p} + \left[\frac{\mathrm{d}^2}{\mathrm{d}z^2} - k^2\right]\tilde{v}_x, \tag{2.14}$$

$$Re\left[\mathrm{i}k(\overline{v}_x - c)\tilde{v}_z\right] = -\frac{\mathrm{d}\tilde{p}}{\mathrm{d}z} + \left[\frac{\mathrm{d}^2}{\mathrm{d}z^2} - k^2\right]\tilde{v}_z. \tag{2.15}$$

The linearized equations for the neo-Hookean elastic solid are:

$$\frac{\mathrm{d}\tilde{w}_Z}{\mathrm{d}Z} + \mathrm{i}k\tilde{w}_X - (\mathrm{d}_Z\overline{w}_X)\,\mathrm{i}k\tilde{w}_Z = 0, \tag{2.16}$$

$$-\mathrm{i}k\tilde{p}_s + (2\cot\theta)\mathrm{i}k\tilde{w}_Z + \frac{1}{G}\left[-k^2 + \frac{\mathrm{d}^2}{\mathrm{d}Z^2}\right]\tilde{w}_X = -k^2c^2Re\,\tilde{w}_X, \tag{2.17}$$

$$(\mathrm{d}_Z\overline{w}_X)\,\mathrm{i}k\tilde{p}_s - (2\cot\theta)\mathrm{i}k\tilde{w}_X - \frac{\mathrm{d}\tilde{p}_s}{\mathrm{d}Z} + \frac{1}{G}\left[-k^2 + \frac{\mathrm{d}^2}{\mathrm{d}Z^2}\right]\tilde{w}_Z = -k^2c^2Re\,\tilde{w}_Z. \tag{2.18}$$

In above equations, $Re = \frac{\rho VR}{\mu}$ is the Reynolds number, and $G = \mu V/E_sR$ is the non-dimensional solid deformability parameter defined above.

The interfacial conditions at GL interface are obtained by Taylor-expanding the fluid dynamical variables about the base state. The linearized kinematic condition, surfactant transport equation and the stress balances at GL interface are:

$$\mathrm{i}k[\overline{v}_x(z=0) - c]\tilde{h} = \tilde{v}_z(z=0), \tag{2.19}$$

$$[\overline{v}_x(z=0) - c - \mathrm{i}kPe_{\mathrm{inv}}]\tilde{\Gamma} = -\tilde{v}_x(z=0), \tag{2.20}$$

$$-2\tilde{h} + \mathrm{d}_z\tilde{v}_x + \mathrm{i}k\tilde{v}_z = \mathrm{i}kMa\Sigma_{gl}\tilde{\Gamma}, \tag{2.21}$$

$$-\tilde{p} - (2\cot\theta)\tilde{h} + 2\frac{\mathrm{d}\tilde{v}_z}{\mathrm{d}z} = k^2\Sigma_{gl}\tilde{h}. \tag{2.22}$$

where $\tilde{\Gamma}$ is the amplitude of disturbance of surfactant concentration, $Ma = E\Gamma_0^*/\gamma_0^*$ is the Marangoni number, $Pe_{\mathrm{inv}} = D_s/VR$ is the inverse of Peclet number, and $\Sigma_{gl} = \gamma_0^*/\mu V$ is the nondimensional free-surface tension parameter.

While the Eulerian description is used for the liquid layer, a Lagrangian framework is used for expressing the dynamical variables in the solid layer. Thus, the treatment of interfacial conditions at perturbed LS interface will be slightly different compared to conditions at GL interface. The conditions at LS interface involve both Eulerian (in liquid layer) and Lagrangian (in solid layer) variables in contrast to conditions at GL interface where we have to deal only with Eulerian variables (in liquids). In Lagrangian description, a material particle in deformed state is identified on the basis of its position in unstressed reference configuration. This is also mentioned above in Section 2.2.1 where we said that the independent variables for the solid are the coordinates $\mathbf{X} = (X, Y, Z)$ of material particles in the reference (i.e. unstressed) configuration. Thus, a material point P_0 in solid layer at LS interface in unstressed configuration has a Lagrangian label as $(X, Z = 1)$. The label for this material point remains unchanged in stressed base state configuration or perturbed state configuration. Since, the independent variable labels are not changed, a Taylor series expansion about the unperturbed interface is not required for solid variables. On the other hand, Taylor expansion about the mean interface position is used for the Eulerian liquid variables in a similar fashion as followed at GL interface. The fundamental and mathematical details of the above process is explained in Gaurav & Shankar (2010*b*). The linearized conditions at LS interface are:

$$\tilde{v}_z = -\mathrm{i}kc\,\tilde{w}_Z\,, \tag{2.23}$$

$$\tilde{v}_x + (\mathrm{d}_z\bar{v}_x)_{z=1}\tilde{w}_Z = -\mathrm{i}kc\,\tilde{w}_X\,, \tag{2.24}$$

$$\frac{\mathrm{d}\tilde{v}_x}{\mathrm{d}z} + \mathrm{i}k\tilde{v}_z + (\mathrm{d}_z^2\bar{v}_x)\tilde{w}_Z = \frac{1}{G}\left\{(\mathrm{d}_Z\overline{w}_X)\frac{\mathrm{d}\tilde{w}_Z}{\mathrm{d}Z} + \frac{\mathrm{d}\tilde{w}_X}{\mathrm{d}Z} + \mathrm{i}k\tilde{w}_Z - (\mathrm{d}_Z\overline{w}_X)^2\mathrm{i}k\tilde{w}_Z\right\}, \tag{2.25}$$

$$-\tilde{p} + 2\frac{\mathrm{d}\tilde{v}_z}{\mathrm{d}z} + k^2\Sigma_{ls}\tilde{w}_Z = -\tilde{p}_s + \frac{2}{G}\frac{\mathrm{d}\tilde{w}_Z}{\mathrm{d}Z} + (2\cot\theta)\tilde{w}_Z\,. \tag{2.26}$$

where, $\Sigma_{ls} = \gamma_{ls}^*/\mu V$ is the nondimensional LS interfacial tension parameter. Finally, the boundary conditions at the rigid surface ($z = 1 + H$) are:

$$\tilde{w}_Z = 0,\ \tilde{w}_X = 0. \tag{2.27}$$

Equations (2.13)-(2.27) govern the linear stability of the two-layered system under consideration. A pseudo-spectral collocation method (Boyd 1999; Weideman

& Reddy 2000) and a numerical shooting procedure (Drazin & Reid 1981) is employed to evaluate the eigenvalues and neutral stability boundaries numerically. The numerical shooting procedure consists of determining linearly independent solutions of governing differential equations in liquid and solid layers by using a Runge-Kutta integrator. The numerical representation of the linearly independent solutions thus obtained are substituted in interfacial and boundary conditions to set up the characteristic matrix. The determinant of this matrix was set to zero to find out the complex wavespeed c. The characteristic equation is a nonlinear equation in c and a Newton-Raphson iterative procedure is used to solve the characteristic equation for c. More details of the exact procedure are explained in Shankar & Kumar (2004). Since, a Newton-Raphson method is used in numerical shooting procedure, it requires a good initial guess for converging to desired eigenvalue. The initial guess is determined using the pseudo-spectral collocation method. Briefly, the unknown variables ($\tilde{v}_z, \tilde{v}_x, \tilde{w}_X$ etc.) are represented as a truncated series of N Chebyshev polynomials and these expansions are substituted in the linearized governing equations for liquid and solid layer. The resulting equations are arranged on $N-8$ Gauss-Lobatto grid points and set to zero. The remaining 8 equations are generated using the linearized boundary and interfacial conditions. This yields a matrix eigen-value problem for eigenvalue c, which are obtained using the "polyeig" eigen-value solver in MATLAB. The details of implementation procedure are given in Weideman & Reddy (2000). We have verified that the eigenvalue c obtained from the spectral collocation method and numerical shooting procedure matches very well with the asymptotic solutions given in Section 2.3. To further check the validity of our numerical procedure, we have reproduced the results for stability of a clean film flowing down a neo-Hookean flexible inclined surface (Gaurav & Shankar 2007) and for stability of contaminated liquid film flowing down a rigid inclined plane (Blyth & Pozrikidis 2004*a*).

The linear stability of the flow configuration under consideration is governed by eight nondimensional parameters, namely, $Re, Ma, \theta, \Sigma_{gl}, Pe_{\text{inv}}, H, G$ and Σ_{ls}. Note that solid thickness H, wall deformability parameter G, and liquid-solid interfacial tension Σ_{ls} are the additional nondimensional parameters that appear in the problem because of the presence of the soft solid layer. We fix $\Sigma_{ls} = 0$ in this work because its effect on LS and GL modes is known (Gaurav & Shankar 2007; Gkanis & Kumar

2006) and our results indicate that it does not affect the stability of Marangoni mode. As mentioned in Section 2.1, we investigate results in creeping flow limit ($Re \to 0$) to suppress GL mode instability and focus on the effect of deformable solid coating (i.e effect of variation of G and H) on the stability of Marangoni mode. We fix Re identically equal to zero to recover creeping flow limit. In the scheme of nondimensionalization used in the present work, Re is identically equal to zero only when the bulk flow or the base velocity is zero. However, in this no flow situation, the Marangoni effect will be absent because a redistribution of surfactant will not be possible in absence of bulk fluid velocity. Thus, when we fix $Re = 0$ in this work, it simply refers to low-Re number creeping flow limit where the the inertial terms in the governing equations remain negligible in comparison to the contribution made by viscous and pressure terms. This does not necessarily means that the bulk flow velocity is identically zero, but it is sufficiently small such that the Re remains small. As an example, for flow of a viscous liquid film (with $\mu \sim 1$Pa s and $\rho \sim 10^3$kg/m^3) of thickness $R \sim 1$mm, the free surface velocity (characteristic velocity used for nondimensionalization) $V \sim \rho g R^2/\mu \sim 0.01$m/s. This corresponds to a $Re \sim 0.01$ and for such small values of Re, the contribution of inertial terms will be negligible in comparison with the viscous terms and we expect to recover these results in the limit of low Re by putting Re identically equal to zero. We have indeed verified this by generating results at $Re = 0.01$ and 0.1 and found that the results for $Re = 0$ are indistinguishable from results at $Re = 0.01$ or 0.1 (results not shown). The characteristic equation is quartic in c for $Re = 0$. Out of the four roots of this quartic characteristic equation, one corresponds to the GL interfacial mode, one to surfactant-induced Marangoni mode, and remaining two roots correspond to LS interfacial modes. Using our spectral code in low wavenumber limit ($k \sim 0.01 - 0.1$), we observed that the root corresponding to Marangoni mode remains stable in the rigid limit ($G \to 0$) and for low values of solid deformability parameter. However, it becomes unstable when nondimensional wall deformability parameter G increases above a critical value. The imaginary part of wave speed varies with k as $c_i \propto k^3$ for $k < 0.1$. This prompted us to investigate the effect of wall deformability on Marangoni mode in low wavenumber limit and hence, we present the low-k asymptotic analysis in the following section.

2.3 Low Wavenumber analysis

The long-wave analysis will be valid, in general, for $k \ll 1/(1+H)$, and this implies $k \ll 1$ for $H \sim O(1)$. All the nondimensional parameters are assumed to be $O(1)$ quantities which imply that they do not scale in any fashion with k. In the low-wavenumber limit, the complex wave speed is expanded in an asymptotic series in k: $c = c^{(0)} + kc^{(1)} + k^2c^{(2)} + k^3c^{(3)} + \cdots$, and the low-$k$ scaling of different variables are determined. For example, if we set $\tilde{v}_z \sim O(1)$ then continuity equation (Eq. (2.13)) and x-momentum (Eq. (2.14)), respectively, imply that $\tilde{v}_x \sim O(1/k)$ and $\tilde{p} \sim O(1/k^2)$. Thus, the velocities and the pressure in the liquid layer are expanded as:

$$\tilde{v}_z = \tilde{v}_z^{(0)} + k\tilde{v}_z^{(1)} + k^2\tilde{v}_z^{(2)} + k^3\tilde{v}_z^{(3)} + \cdots, \tag{2.28a}$$

$$\tilde{v}_x = \frac{1}{k}(\tilde{v}_x^{(0)} + k\tilde{v}_x^{(1)} + k^2\tilde{v}_z^{(2)} + k^3\tilde{v}_z^{(3)} + \cdots), \tag{2.28b}$$

$$\tilde{p} = \frac{1}{k^2}(\tilde{p}^{(0)} + k\tilde{p}^{(1)} + k^2\tilde{p}^{(2)} + k^3\tilde{p}^{(3)} + \cdots). \tag{2.28c}$$

Similarly, the Fourier coefficient of the GL interface deflection $\tilde{h} \sim O(1/k)$ (from Eq. (2.19)), surfactant surface concentration $\tilde{\Gamma} \sim O(1/k)$ (from Eq. (2.20)), and for solid layer: if $\tilde{w}_Z \sim O(1)$ this gives $\tilde{w}_X \sim O(1/k)$, $\tilde{p}_s \sim O(1/k^2)$ from governing equations (Eqs. (2.16) and (2.18)), respectively. All these variables are expanded according to their respective scalings and these expanded variables are substituted in the governing equations (Eqs. (2.13)-(2.18)) and boundary conditions (Eqs. (2.19)-(2.27)). The resulting equations are solved at each order in k. At leading order (i.e. $O(1)$), the governing equation for the liquid layer is:

$$\mathrm{d}_z^4\tilde{v}_z^{(0)} = 0. \tag{2.29}$$

and for solid layer is:

$$\mathrm{d}_Z^4\tilde{w}_Z^{(0)} = 0. \tag{2.30}$$

The conditions at GL interface ($z = 0$) are:

$$\mathrm{d}_z\tilde{v}_x^{(0)} - 2\tilde{h}^{(0)} = 0, \qquad \tilde{p}^{(0)} = 0. \tag{2.31a}$$

$$\mathrm{i}[\overline{v}_x - c^{(0)}]\tilde{h}^{(0)} = \tilde{v}_z^{(0)}, \qquad [\overline{v}_x - c^{(0)}]\tilde{\Gamma}^{(0)} = -\tilde{v}_x^{(0)}. \tag{2.31b}$$

where, Eqs. (2.31a) represent tangential and normal stress balances, respectively, and Eqs. (2.31b) refer to kinematic condition and surfactant transport equation. The leading order conditions at LS interface ($z = 1$) are:

$$\tilde{v}_z^{(0)} = 0, \quad \tilde{v}_x^{(0)} = 0, \tag{2.32a}$$

$$\mathrm{d}_z \tilde{v}_x^{(0)} = \frac{1}{G} \mathrm{d}_Z \tilde{w}_X^{(0)}, \quad \tilde{p}^{(0)} = \tilde{p_s}^{(0)}. \tag{2.32b}$$

Eqs. (2.32a) represent velocity continuity conditions, and Eqs. (2.32b) represent stress continuity at LS interface. Finally, the conditions at rigid surface ($z = 1 + H$) are: $\tilde{w}_Z^{(0)} = 0, \tilde{w}_X^{(0)} = 0$. The velocity field for the liquid layer at leading order can be obtained by integrating Eq. (2.29) and using conditions (2.31a), and (2.32a):

$$\tilde{v}_z^{(0)} = -\mathrm{i}(z-1)^2 \tilde{h}^{(0)}. \tag{2.33}$$

The leading order liquid velocity field in the above Eq. (2.33) is substituted in kinematic condition and surfactant transport equation (Eqs. (2.31b)) to obtain the leading order wave speed for GL mode, $c_{gl}^{(0)}$, and $\tilde{\Gamma}^{(0)}$:

$$c_{\mathrm{gl}}^{(0)} = 2, \qquad \tilde{\Gamma}^{(0)} = -2\tilde{h}^{(0)}. \tag{2.34}$$

Note that the GL mode is induced by interface fluctuation, $\tilde{h}^{(0)}$, which in turn causes a perturbation in surfactant concentration at this order as shown in Eq. (2.34) Wei (2005*a*). In addition to the GL interfacial mode, there exists another mode which is triggered by perturbation in surfactant concentration ($\tilde{\Gamma}^{(0)} \neq 0$) without necessarily having an interfacial deflection ($\tilde{h}^{(0)} = 0$). The leading order wave speed for this mode is determined by the leading order surfactant transport (second equation of Eq. (2.31b)) and by fixing $\tilde{h}^{(0)} = 0$:

$$c_{\mathrm{Ma}}^{(0)} = \bar{v}_x \,|_{z=0} = 1. \tag{2.35}$$

This mode is referred as Marangoni mode and our objective is to investigate the effect of the presence of deformable solid layer on this surfactant-induced Marangoni mode. Note that the leading order wave speed for both GL and Marangoni modes are obtained by using the governing equations for liquid layer, stress conditions at GL interface, kinematic condition (for GL mode), surfactant transport equation (for Marangoni mode), and leading order velocity continuity conditions at deformable

LS interface. However, the velocities at LS interface satisfies no slip conditions as in the case of rigid solid (refer Eqs. (2.32a)). Thus, solid deformations do not enter into the calculations of $c^{(0)}$ and hence, the leading order wave speed for both the modes remain identical to the case of flow past rigid incline. Further, as $c^{(0)}$ is real, we cannot determine the stability of the system at this order and it is required to perform calculations for next order in k. The leading order deformation field for solid layer can be obtained by integrating governing equation (2.30) along with stress continuity conditions Eq. (2.32b) and no deformation conditions at rigid surface ($\tilde{w}_Z^{(0)} = 0, \tilde{w}_X^{(0)} = 0$):

$$\tilde{w}_Z^{(0)} = -\mathrm{i}G(Z-1-H)^2\tilde{h}^{(0)}. \tag{2.36}$$

It is important to note that $\tilde{h}^{(0)} \neq 0$ for GL mode, thus, Eq. (2.36) shows that leading order deformation field is generated in solid layer due to liquid velocity field at this order. This is better understood if we refer to leading order stress continuity conditions at LS interface (Eq. (2.32b)). The stress conditions show that the leading order velocity field exerts a shear stress on solid layer at this order which in turn creates leading order deformations in the solid layer. Our subsequent analysis shows that these leading order solid deformations affect the first correction to velocity field through velocity continuity conditions at $O(k)$. Hence, we expect the effect of solid layer to appear at $O(k)$ for GL interfacial mode. In contrast to this, $\tilde{h}^{(0)} = 0$, and $\tilde{\Gamma}^{(0)} \neq 0$ for Marangoni mode. Thus, Eqs. (2.33) and (2.36), respectively show the absence of velocity field in liquid layer and deformation field in the solid layer. In the following, we show calculations at higher orders to determine stability of both GL and Marangoni modes.

At $O(k)$, the governing equations for liquid and solid layers are:

$$\mathrm{d}_z^4\tilde{v}_z^{(1)} = \mathrm{i}Re[(\bar{v}_x - c^{(0)})\mathrm{d}_z^2\tilde{v}_z^{(0)} - (\mathrm{d}_z^2\bar{v}_x)\tilde{v}_z^{(0)}], \tag{2.37a}$$

$$\mathrm{d}_Z^4\tilde{w}_Z^{(1)} + \mathrm{i}G(4Z\mathrm{d}_Z^3\tilde{w}_Z^{(0)} + 6\mathrm{d}_Z^2\tilde{w}_Z^{(0)}) = 0. \tag{2.37b}$$

The kinematic condition, surfactant transport equation, and stress conditions at GL

interface are:

$$\begin{aligned}
\mathrm{i}(\overline{v}_x - c^{(0)})\tilde{h}^{(1)} - \mathrm{i}c^{(1)}\tilde{h}^{(0)} &= \tilde{v}_z^{(1)}, && \text{(2.38a)}\\
(\overline{v}_x - c^{(0)})\tilde{\Gamma}^{(1)} &= (c^{(1)} + \mathrm{i}Pe_{\mathrm{inv}})\tilde{\Gamma}^{(0)} - \tilde{v}_x^{(1)}, && \text{(2.38b)}\\
\mathrm{d}_z\tilde{v}_x^{(1)} - 2\tilde{h}^{(1)} &= \mathrm{i}Ma\Sigma_{gl}\tilde{\Gamma}^{(0)}, && \text{(2.38c)}\\
\tilde{p}^{(1)} + (2\cot\theta)\tilde{h}^{(0)} &= 0. && \text{(2.38d)}
\end{aligned}$$

and the conditions at LS interface at $O(k)$ are:

$$\begin{aligned}
\tilde{v}_z^{(1)} &= -\mathrm{i}c^{(0)}\tilde{w}_Z^{(0)}, && \text{(2.39a)}\\
\tilde{v}_x^{(1)} &= 2\tilde{w}_Z^{(0)} - \mathrm{i}c^{(0)}\tilde{w}_X^{(0)}, , && \text{(2.39b)}\\
\mathrm{d}_z\tilde{v}_x^{(1)} &= \frac{1}{G}\mathrm{d}_Z\tilde{w}_X^{(1)} - 2\mathrm{d}_Z\tilde{w}_Z^{(0)} + 2\tilde{w}_Z^{(0)}, && \text{(2.39c)}\\
\tilde{p}^{(1)} &= \tilde{p}_s^{(1)}. && \text{(2.39d)}
\end{aligned}$$

The boundary conditions at $z = 1+H$ are: $\tilde{w}_Z^{(1)} = 0, \tilde{w}_X^{(1)} = 0$. The solution to Eq.(2.37a) for $\tilde{v}_z^{(1)}$ can be obtained by using Eqs. (2.38c) - (2.39b):

$$\begin{aligned}
\tilde{v}_z^{(1)} = (z-1)\Bigg[\frac{Re}{60}\left(z^3 - 3z^2 + 3z + 9\right) - 2GH^2 - \frac{\cot\theta}{3}\left(z^2 + z - 2\right)\Bigg]\tilde{h}^{(0)}\\
-c^{(0)}\left[\frac{Re}{12}\left(z^4 - 4z^3 + 8z - 5\right) + GH\left(2 + H - 2z\right)\right]\tilde{h}^{(0)}\\
+\frac{1}{2}(z-1)^2\left(Ma\Sigma_{gl}\tilde{\Gamma}^{(0)} - 2\mathrm{i}\tilde{h}^{(1)}\right). \quad \text{(2.40)}
\end{aligned}$$

2.3.1 The gas-liquid mode

The first correction to the complex wave speed for GL mode, $c_{gl}^{(1)}$ is calculated from $O(k)$ kinematic condition Eq.(2.38a) and is given as:

$$c_{\mathrm{gl}}^{(1)} = \mathrm{i}\left[\underline{\frac{8}{15}Re - \frac{2}{3}\cot\theta - 4GH} - Ma\Sigma_{gl}\right]. \quad \text{(2.41)}$$

The effect of presence of deformable solid layer on a clean GL interface in low-k limit has been discussed in detail by Shankar & Sahu (2006) and the underlined terms in the expression of $c_{gl}^{(1)}$ are identical to the result obtained by them. The term proportional to GH represents the soft solid contribution and the above expression for $c_{gl}^{(1)}$ shows that the effect of deformable solid layer is stabilizing for GL mode. The effect of presence of surfactant on GL interface stability in long-wave limit has

been studied by Blyth & Pozrikidis (2004*a*). In the above expression of $c_{gl}^{(1)}$, the last term proportional to Ma shows that the effect of adding a monolayer of surfactant is stabilizing for GL interfacial mode in agreement with previous studies (Blyth & Pozrikidis 2004*a*; Wei 2005*a*). While these results were already reported in separate studies, we present it here for the sake of completeness of the problem.

2.3.2 The surfactant/Marangoni mode

The interface deflection at leading order $\tilde{h}^{(0)} = 0$ and the leading order wave speed $c_{\mathrm{Ma}}^{(0)} = \bar{v}_x \mid_{z=0} = 1$ for Marangoni mode. Thus, Eq. (2.38a) implies that $\tilde{v}_z^{(1)} \mid_{z=0} = 0$. Substituting this condition in the expression of $\tilde{v}_z^{(1)}$ given in Eq. (2.40) yields:

$$Ma\Sigma_{gl}\tilde{\Gamma}^{(0)} = 2\mathrm{i}\tilde{h}^{(1)}. \tag{2.42}$$

The above condition implies that velocity field is zero at this order for Marangoni mode and the leading order concentration fluctuation has created a nonzero surface deflection $\tilde{h}^{(1)}$ at $O(k)$. Under this no flow situation at $O(k)$, the surfactant transport equation (2.38b) gives the first correction to wave speed as:

$$c_{\mathrm{Ma}}^{(1)} = -\mathrm{i}Pe_{\mathrm{inv}}. \tag{2.43}$$

The first correction to wave speed shows that the surfactant diffusivity has a stabilizing effect on Marangoni mode. However, the effect of surfactant diffusion is usually neglected because of low values of diffusivity coefficient. Thus, Pe_{inv} is taken as zero in several earlier studies (Gao & Lu 2007; Halpern & Frenkel 2003; Samanta 2014; Wei 2005*a*), and the Marangoni mode remains neutrally stable at this order. While we do not take $Pe_{\mathrm{inv}} = 0$ in presenting the analysis, we will show it later that for realistic estimates of Pe_{inv}, the effect of surfactant diffusivity usually remains insignificant.

More importantly, we carry out further calculations at higher orders in k to investigate the destabilization of Marangoni mode due to wall deformability as reported in previous section. Since flow in liquid layer is absent at this order ($\tilde{v}_z^{(1)} = 0, \tilde{v}_x^{(1)} = 0, \tilde{p}^{(1)} = 0$), the governing equation for solid (Eq. (2.37b)), and boundary conditions (Eq. (2.32b)) and no deformation conditions at rigid surface are all homogeneous, thus leading to no deformations in the solid layer ($\tilde{w}_Z^{(1)} = \tilde{w}_X^{(1)} = 0$). Considering no

deformations in solid and no flow in liquid until $O(k)$, the governing equations for liquid and solid layer at $O(k^2)$ are:

$$\mathrm{d}_z^4 \tilde{v}_z^{(2)} = 0, \qquad \mathrm{d}_z^4 \tilde{w}_Z^{(2)} = 0. \tag{2.44}$$

The conditions at GL interface are:

$$\begin{aligned}
\mathrm{i}(\overline{v}_x - c_{\mathrm{Ma}}^{(0)})\tilde{h}^{(2)} - \mathrm{i}c_{\mathrm{Ma}}^{(1)}\tilde{h}^{(1)} &= \tilde{v}_z^{(2)}, && \text{(2.45a)}\\
(\overline{v}_x - c_{\mathrm{Ma}}^{(0)})\tilde{\Gamma}^{(2)} - (c_{\mathrm{Ma}}^{(1)} + \mathrm{i}Pe_{\mathrm{inv}})\tilde{\Gamma}^{(1)} - c_{\mathrm{Ma}}^{(2)}\tilde{\Gamma}^{(0)} &= -\tilde{v}_x^{(2)}, && \text{(2.45b)}\\
\mathrm{d}_z\tilde{v}_x^{(2)} - 2\tilde{h}^{(2)} &= \mathrm{i}Ma\Sigma_{gl}\tilde{\Gamma}^{(1)}, && \text{(2.45c)}\\
\tilde{p}^{(2)} + (2\cot\theta)\tilde{h}^{(1)} &= 0. && \text{(2.45d)}
\end{aligned}$$

At LS interface, we have:

$$\begin{aligned}
\tilde{v}_z^{(2)} &= 0, && \text{(2.46a)}\\
\tilde{v}_x^{(2)} &= 0, && \text{(2.46b)}\\
\mathrm{d}_z\tilde{v}_x^{(2)} &= \frac{1}{G}\mathrm{d}_Z\tilde{w}_X^{(2)}, && \text{(2.46c)}\\
\tilde{p}^{(2)} &= \tilde{p}_s{}^{(2)}. && \text{(2.46d)}
\end{aligned}$$

and finally no deformation conditions at rigid surface:

$$\tilde{w}_Z^{(2)} = 0, \qquad \tilde{w}_X^{(2)} = 0. \tag{2.47}$$

The second correction to the liquid velocity field is obtained by integrating the first equation in (2.44) and using interfacial conditions (2.45c)-(2.46b), along with kinematic condition (2.45a) to give:

$$\tilde{v}_z^{(2)} = \frac{\mathrm{i}}{6}Ma\Sigma_{\mathrm{gl}}(z-1)^2(3Pe_{\mathrm{inv}} + z\cot\theta)\tilde{\Gamma}^{(0)}. \tag{2.48}$$

The second correction to the wave speed $c^{(2)}$ is calculated using Eq. (2.45b),

$$c_{\mathrm{Ma}}^{(2)} = Ma\Sigma_{\mathrm{gl}}\left(Pe_{\mathrm{inv}} - \frac{1}{6}\cot\theta\right), \tag{2.49}$$

The above expression shows that $c_{\mathrm{Ma}}^{(2)}$ is real and does not contribute in determining the stability of Marangoni mode. Further, the effect of solid layer does not appear in the expression of $c_{\mathrm{Ma}}^{(2)}$ which is expected as no solid deformations exist up to $O(k)$ for Marangoni mode. However, since velocity field exists at $O(k^2)$, it will exert

stresses at LS interface (refer Eqs. (2.46c) and (2.46d)) which in turn will cause deformations in the solid layer. Thus, we expect the solid contribution to occur in next order calculations. The governing equation for solid (second Eq. in (2.44)) is solved using Eqs. (2.46c)-(2.47) and is given as:

$$\tilde{w}_Z^{(2)} = \frac{\mathrm{i}}{6} GMa\Sigma_{\mathrm{gl}}(Z-1-H)^2\left[3Pe_{\mathrm{inv}} + (Z+2H)\cot\theta\right]\tilde{\Gamma}^{(0)}. \tag{2.50}$$

The liquid governing equation at next higher order is:

$$\mathrm{d}_z^4\tilde{v}_z^{(3)} = \mathrm{i}Re\left[-(\mathrm{d}_z^2\overline{v}_x)\tilde{v}_z^{(2)}\right]. \tag{2.51}$$

The conditions at GL interface are:

$$\mathrm{i}\left[(\overline{v}_x - c_{\mathrm{Ma}}^{(0)})\tilde{h}^{(3)} - c_{\mathrm{Ma}}^{(1)}\tilde{h}^{(2)} - c_{\mathrm{Ma}}^{(2)}\tilde{h}^{(1)}\right] = \tilde{v}_z^{(3)}, \tag{2.52a}$$

$$(\overline{v}_x - c_{\mathrm{Ma}}^{(0)})\tilde{\Gamma}^{(3)} - (c_{\mathrm{Ma}}^{(1)} + \mathrm{i}Pe_{\mathrm{inv}})\tilde{\Gamma}^{(2)} - c_{\mathrm{Ma}}^{(2)}\tilde{\Gamma}^{(1)} - c_{\mathrm{Ma}}^{(3)}\tilde{\Gamma}^{(0)} = -\tilde{v}_x^{(3)}, \tag{2.52b}$$

$$\mathrm{d}_z\tilde{v}_x^{(3)} - 2\tilde{h}^{(3)} = \mathrm{i}Ma\Sigma_{\mathrm{gl}}\tilde{\Gamma}^{(2)}, \tag{2.52c}$$

$$\tilde{p}^{(3)} + (2\cot\theta)\tilde{h}^{(2)} = 0. \tag{2.52d}$$

and at liquid-solid interface, $z = 1$:

$$\tilde{v}_z^{(3)} = -\mathrm{i}c_{\mathrm{Ma}}^{(0)}\tilde{w}_Z^{(2)}, \tag{2.53a}$$

$$\tilde{v}_x^{(3)} = 2\tilde{w}_Z^{(2)} - \mathrm{i}c_{\mathrm{Ma}}^{(0)}\tilde{w}_X^{(2)}. \tag{2.53b}$$

The governing equation for liquid layer Eq. (2.51) is solved along with interfacial conditions at GL interface, (2.52c) and (2.52d), and conditions at LS interface, (2.53a) and (2.53b). Note that the solid contribution enters into the velocity field via the velocity continuity conditions at LS interface (Eqs. (2.53a) and (2.53b)). On using the kinematic condition (Eq. (2.52a)), the third correction to velocity in liquid layer is given as:

$$\tilde{v}_z^{(3)} = f_1 + f_2 + f_3. \tag{2.54}$$

where

$$f_1 = \frac{ReMa\Sigma_{\mathrm{gl}}}{2520}\left[\left(2z^6 - 7z^4 + 16z - 11\right)\cot\theta + 21Pe_{\mathrm{inv}}\left(2z^4 - 5z^3 + 7z - 4\right)\right]z\tilde{\Gamma}^{(0)},$$

$$f_2 = \frac{Ma\Sigma_{\mathrm{gl}}GH}{6}\left\{\left[2(H^2 - H - 1)z + 3H + 2\right]\cot\theta + 3Pe_{\mathrm{inv}}(Hz - 2z + 2)\right\}z\tilde{\Gamma}^{(0)},$$

$$f_3 = \frac{Ma\Sigma_{\mathrm{gl}}(z-1)^2}{6}\left[\mathrm{i}z\tilde{\Gamma}^{(1)} + \left(\frac{1}{2}Ma\Sigma_{\mathrm{gl}} + Pe_{\mathrm{inv}}(z-2) - \frac{2}{3}z\cot\theta\right)\right]\tilde{\Gamma}^{(0)}\cot\theta$$
$$+\frac{Ma\Sigma_{\mathrm{gl}}(z-1)^2Pe_{\mathrm{inv}}}{2}\left[\mathrm{i}\tilde{\Gamma}^{(1)} + (Pe_{\mathrm{inv}} - Ma\Sigma_{\mathrm{gl}})\tilde{\Gamma}^{(0)}\right].$$

Note that both solid thickness (H) and solid deformability parameter (G) occur in the liquid velocity field at this order which implies that the velocity perturbations get altered due to the presence of solid layer at this order. Thus, we expect that the $c_{\mathrm{Ma}}^{(3)}$ will also get affected by the wall deformability at this order. The third correction to wave speed is again determined from surfactant transport equation, Eq. (2.52b), and is given as:

$$\begin{aligned} c_{\mathrm{Ma}}^{(3)} &= \mathrm{i}\frac{Ma\Sigma_{\mathrm{gl}}}{30}\left\{\left[5(3H+2)\cot\theta + Pe_{\mathrm{inv}}\right]GH + \left[25\cot\theta - Re - 30(Pe_{\mathrm{inv}} - Ma\Sigma_{\mathrm{gl}})\right]Pe_{\mathrm{inv}}\right\} \\ &\quad -\mathrm{i}\frac{Ma\Sigma_{\mathrm{gl}}\cot\theta}{2520}\left(11Re + 420Ma\Sigma_{\mathrm{gl}} + 280\cot\theta\right). \end{aligned} \tag{2.55}$$

The above expression shows that $c_{\mathrm{Ma}}^{(3)}$ is purely imaginary and hence contribute in determining the stability of the system. The solid contribution is represented by the terms proportional to GH and it is clear from the above equation that these terms occur with a positive sign which implies that the soft solid has a destabilizing contribution for Marangoni mode. We set $Pe_{\mathrm{inv}} = 0$ in order to suppress the stabilizing contribution occurring at $O(k)$ (recall $c_{\mathrm{Ma}}^{(1)} = -\mathrm{i}Pe_{\mathrm{inv}}$) and hence, stability of Marangoni mode is completely determined by $c_{\mathrm{Ma}}^{(3)}$. If we further set $Re = 0, \theta = \pi/4$, the expression for $c_{\mathrm{Ma}}^{(3)} = \frac{\mathrm{i}Ma\Sigma_{gl}}{9}\left[-1 - 1.5Ma\Sigma_{gl} + (3GH + 4.5GH^2)\right]$. This expression clearly shows that the Marangoni mode remains stable for $H = 0$ and could become unstable by appropriately choosing values of solid thickness H and solid deformability parameter G. For example, if we set $Ma = 1, \Sigma_{gl} = 0.5$ and $H = 10$, Marangoni mode becomes unstable to long-wave perturbations for $G \gtrsim 0.003$, while for $H = 5$, the value of G above which stable to unstable transition of Marangoni mode occurs decreases and it becomes unstable for $G \gtrsim 0.01$. Note that $c_{\mathrm{Ma}}^{(3)} \propto Ma = \frac{\Gamma_0^*}{\sigma_0^*}\left(-\frac{\partial\sigma^*}{\partial\Gamma^*}\right)_{\Gamma_0^*}$ and we have set $Pe_{\mathrm{inv}} = 0$ in writing down the expression given above. This implies that the instability will be present only if the species present at the interface is a surfactant whose spatial variations in concentration will cause a gradient in surface tension and hence results in the generation of Marangoni stresses. This is in contrast to the observation made by Pereira & Kalliadasis (2008) for liquid film flow down a rigid inclined wall. They pointed out the existence of an additional normal mode due to the presence of any species at the interface and not necessarily a surfactant. They put forward this argument because the growth rate was found to be proportional to Pe_{inv} at $O(k)$ and was not related to Ma at this order. Recall $c_{\mathrm{Ma}}^{(1)} = -\mathrm{i}Pe_{\mathrm{inv}}$ in our analysis as well, however,

for $Pe_{\text{inv}} = 0$, while this contribution at $O(k)$ is absent, a contribution at higher order in k is present which is proportional to Ma and could become unstable because of the presence of a deformable liquid-solid interface.

The above analysis clearly shows that the instability of Marangoni mode due to wall deformability occurs at $O(k^3)$ and thus growth rate $\sim kc_i \sim O(k^4)$. On the other hand, the stabilizing contribution proportional to Pe_{inv} occurs at $O(k)$ with decay rates $\sim O(k^2)$. We fix $Pe_{\text{inv}} = 0$ to suppress this stabilizing contribution and focus on the estimates of growth rate of Marangoni mode instability triggered because of the presence of soft solid layer. If we take $H = 5, G = 0.05, Re = 0, \theta = \pi/4, Ma = 1$, and $\Sigma_{\text{gl}} = 0.5$, the above equation gives $c_{\text{Ma}}^{(3)} = 0.25i \sim O(0.1)$. The non-dimensional growth rate $kc_i \sim k^4 c_{\text{Ma}}^{(3)} \sim 10^{-9}$ for $k = 0.01$ and this contribution is destabilizing due to presence of soft solid layer. Note that if $H = 0$ and/or $G = 0$ with all other parameters kept at the same value, $c_{\text{Ma}}^{(3)} = -0.09i$ which is negative and hence stabilizing in the rigid limit. The unstable growth rates obtained here in low-k limit are significantly smaller than the unstable growth rates observed for Yih type free-surface mode for which the low-k instability is typically observed at $O(k)$ (with growth rate $\sim O(k^2)$) (Yih 1963, 1967). However, note that inertia is always required to excite Yih's interfacial mode. In contrast, the Marangoni mode becomes unstable due to presence of deformable wall at $Re = 0$. Further, it is the maximum growth rate that will ultimately dominate the stability of the system. Our numerical results in Section 2.4 show that the growth rates increase by at least three to four order of magnitudes depending on the solid thickness and deformability.

Let us now focus our attention on the comparison of stabilizing contribution of Pe_{inv} occurring at $O(k)$ and destabilizing contribution of soft solid at $O(k^3)$ for Marangoni mode. The inverse of Peclet number for film flow considered here can be estimated as follows: $Pe_{\text{inv}} = D_s/VR \sim \frac{D_s \mu}{\rho g R^3}$. The typical value of diffusion coefficient lies between $D_s \sim 10^{-8} - 10^{-10}\text{m}^2/\text{s}$ depending on the surfactant molecule and the liquid. If we set $\rho \sim 10^3 \text{kg/m}^3$, $g \sim 10\text{m/s}^2$, $R \sim 10^{-3}\text{m}$, and $D_s \sim 10^{-9}\text{m}^2/\text{s}$, this gives $Pe_{\text{inv}} \sim 10^{-4}\mu$. Thus, Pe_{inv} can vary from 10^{-7} for water type liquid ($\mu \sim 10^{-3}$Pa-s) to $Pe_{\text{inv}} \sim 10^{-4}$ for a very viscous liquid of $\mu \sim 1$Pa-s (assuming $D_s = 10^{-9}$ m^2/s, even though we expect D_s to decrease with increase in μ). As noted above, the non-dimensional growth rate corresponding to the destabilizing contribution of the soft solid layer is $kc_i \sim k^4 c_{\text{Ma}}^{(3)} \sim 10^{-9}$ for $k = 0.01$ for

$H = 5, G = 0.05, Re = 0, \theta = \pi/4, Ma = 1$, and $\Sigma_{gl} = 0.5$. On the other hand, the order of decay rate obtained at $O(k)$ calculations due to diffusive effect of surfactant molecules is $\sim k^2 Pe_{inv} \sim 10^{-4} Pe_{inv}$ for $k \sim 0.01$. Thus, the decay rates could vary from $10^{-11} - 10^{-8}$ depending on the value of inverse of Peclet number. This implies that for relatively lower values of Pe_{inv}, we expect that the destabilizing contribution due to the presence of soft solid will dominate the stability of Marangoni mode. On the other hand, for $Pe_{inv} \gtrsim 10^{-4}$, the destabilizing contribution obtained at $O(k^3)$ due to wall deformability could be comparable to the stabilizing contribution at $O(k)$ and either of the two contributions could dominate the stability of Marangoni mode depending on the relative magnitudes of Pe_{inv} and soft solid variables (H and G). This will become more clear if we write down the expression for imaginary part of wave speed in low-k regime: $c_{Ma}^{(i)} = k c_{Ma}^{(1)} + k^3 c_{Ma}^{(3)} = -\mathrm{i} k Pe_{inv} + \frac{k^3 \mathrm{i}}{2520}(-245 + 420GH + 630GH^2 + 1680Pe_{inv} + 1260GHPe_{inv} - 1260Pe_{inv}^2)$ keeping $Re = 0, \theta = \pi/4, Ma = 1, \Sigma_{gl} = 0.5$. If $Pe_{inv} = 10^{-7}, H = 5, G = 0.05$, and $k = 0.01$ this gives $c_{Ma}^{(i)} = 2.55 \times 10^{-7}$. On the other hand, if $Pe_{inv} = 10^{-4}$ and keeping all other parameters same as above, $c_{Ma}^{(i)} = -7.43 \times 10^{-7}$ which implies that stabilizing contribution due to surfactant diffusivity dominates the destabilization due to solid layer deformability and hence Marangoni mode remains stable. However, if we increase solid thickness from $H = 5$ to $H = 10$ for $Pe_{inv} = 10^{-4}$, we find that $c_{Ma}^{(i)} = 2.36 \times 10^{-7}$ which implies that the soft solid contribution dominates and Marangoni mode is rendered unstable by wall deformability.

2.4 Results and discussion

The results presented in Section 2.3 demonstrated that the Marangoni mode becomes unstable for long-wave perturbations when solid deformability parameter increases beyond a critical value. Further, inertia is not required to trigger this surfactant mode instability. The low-k results for Marangoni mode presented in Section 2.3 are continued numerically to finite and arbitrary wavenumbers. Figure 2.2 shows growth rate versus wavenumber plot depicting the effect of increasing solid deformability parameter (G) on Marangoni mode for $Re = 0, H = 5$, and $Ma = 1$. The Marangoni mode remains stable for all wavenumbers in the rigid limit ($G \to 0$) and for sufficiently low values of wall deformability parameter. However, when G increases beyond a critical value, the Marangoni mode becomes unstable in the

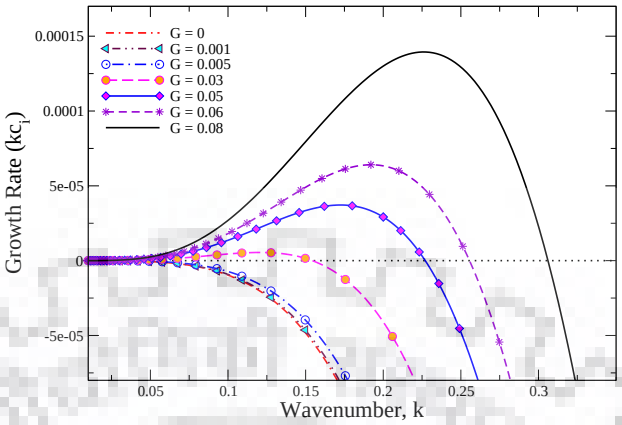

Figure 2.2: Effect of solid layer deformability on Marangoni mode illustrating destabilization of Marangoni mode on increasing the values of G. Growth-rate vs. k for $Re = 0, H = 5, Ma = 1, Pe_{\text{inv}} = 0, \Sigma_{\text{gl}} = 0.5, \Sigma_{\text{ls}} = 0, \theta = 45^\circ$

low-wavenumber limit and positive growth rates are obtained up to $k \sim O(0.1)$. The range of unstable wavenumbers increases with increase in solid deformability parameter. As noted in Section 2.3, the growth rates remain significantly low ($\sim 10^{-9}$) in low-k limit, but are three to four order of magnitudes higher for $k \sim 0.1$. Figure 2.2 shows that the maximum growth rate for Marangoni mode is obtained for $k \sim 0.1$ and this maximum value increases with increase in solid deformability parameter. The maximum nondimensional growth rate obtained for $G \sim 0.01$ is $\sim 10^{-5}$ at $k \sim 0.1$. This is still smaller by at least two order of magnitudes, as compared to the unstable growth rate obtained for Yih's free surface GL mode. However, the GL free surface mode becomes unstable in presence of inertia when Reynolds number increases above a critical value. On the other hand, the Marangoni instability triggered due to wall deformability is present even in the creeping flow limit ($Re = 0$). Thus, we expect Marangoni mode to dominate the stability of the system at lower values of Re for which the GL mode remains stable. We also investigated the effect of varying wall deformability parameter G on GL interfacial mode and observed that the GL mode does not become unstable for any value of G. Further, increasing Ma has a stabilizing effect on this GL interfacial mode (numerical results not shown) which is in agreement with previous studies Blyth & Pozrikidis (2004*a*). One of the root corresponding to LS mode becomes unstable in high wavenumber

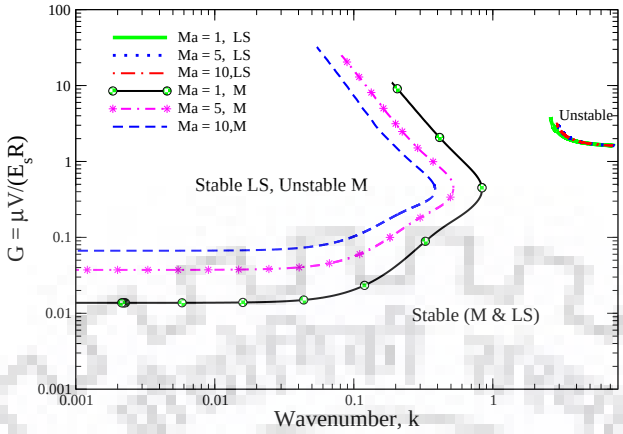

Figure 2.3: Neutral stability curves for $Re = 0, H = 5, Pe_{\text{inv}} = 0, \Sigma_{\text{gl}} = 0.5, \Sigma_{\text{ls}} = 0, \theta = 45^\circ$

limit for higher values of $G \sim O(1)$ as has also been observed in previous studies (Gaurav & Shankar 2007, 2010*a*). Thus, the flow remains stable in rigid limit and for lower values of G. However, with an increase in G, the Marangoni mode becomes unstable first followed by short wave instability of LS interface at sufficiently higher values of G.

Figure 2.3 shows the neutral stability diagram demarcating stable and unstable regions in G vs. k plane for $Re = 0$, and $H = 5$ for different values of Marangoni number. This figure clearly depicts that all three modes (GL, Marangoni, and LS) remain stable for lower values of G. For $Ma = 1$, as G increases above the neutral curve shown by solid line, the perturbations corresponding to Marangoni mode becomes unstable in low-k limit and the unstable region extends up to finite wavenumbers whose exact value depends on G. The effect of increasing Ma is stabilizing as shown by shifting of neutral curves upward for values of $Ma = 5$ and 10. Figure 2.3 also shows the neutral curves corresponding to short-wave instability of LS interface which occurs due to jump in normal stress in the base state across the liquid-solid interface (Gkanis & Kumar 2003). We extensively searched the parameter space (H, G, Ma etc.) and never observed a GL mode instability in creeping flow limit. The new feature that evolved out of Figure 2.2 and Figure 2.3 is the destabilization of Marangoni mode solely due to the presence of deformable solid layer. This is different from the destabilization of liquid-liquid interface for the case of planar

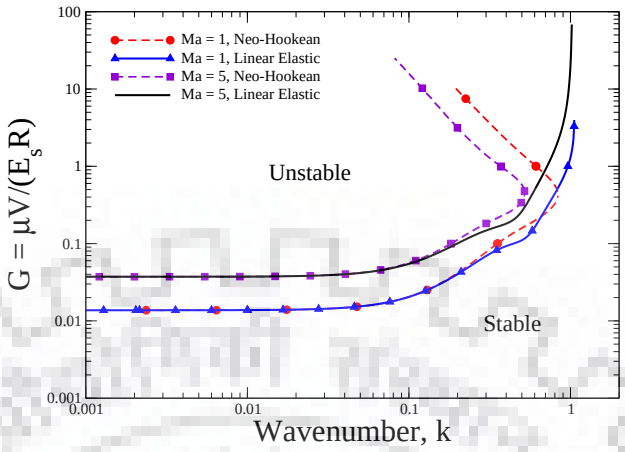

Figure 2.4: Neutral stability curves for Marangoni mode for both linear elastic and neo-Hookean solid model: G vs. k for $Re = 0, H = 5, Ma = 1, Pe_{\text{inv}} = 0, \Sigma_{gl} = 0.5, \Sigma_{ls} = 0$, and $\theta = 45^{\circ}$.

two layer channel flow, as observed by Halpern & Frenkel (2003), where a non-zero interfacial shear in base state must be present to cause destabilization of Marangoni mode. Halpern & Frenkel (2003) pointed out that the Marangoni mode does not become unstable for the case of falling film configuration because the GL interface remains stress-free in the basic state. In this context, Wei (2005*a*) analyzed the effect of imposed shear on GL interface and demonstrated that stability of Marangoni mode for film flows is determined by the direction of imposed shear relative to the direction in which gravity acts. Marangoni mode becomes unstable when the imposed shear assists gravity while it remains stable when imposed shear opposes gravity. In contrast to these studies, the stresses at GL interface in the base state remain zero in the present work which suggests that the destabilization is triggered solely due to the alteration of boundary conditions at LS interface.

It is worth to comment at this point regarding the choice of solid model and the extent to which the above observed destabilization of Marangoni mode due to wall deformability will depend on the solid model. In the present work, we have used a neo-Hookean constitutive relation for representing the dynamics of deformable solid layer. Several earlier studies related to stability of flow past deformable surfaces have modeled the soft solid layer using a linear elastic constitutive relation (Kumaran 2000; Shankar & Kumar 2004; Shankar & Sahu 2006). We have also

performed some preliminary calculations for a simple linear elastic model which can be recovered as a special case of neo-Hookean solid model in the limit of small deformation gradients (Macosko 1994; Malvern 1969). We have observed that the qualitative prediction of destabilization of Marangoni mode due to wall deformability holds for linear elastic solid as well. While there are some quantitative differences in the predictions based on the two solid models, the critical value of wall deformability parameter G still remains almost identical for both solid models. This is shown in Figure 2.4 which presents the neutral stability diagram for Marangoni mode for both solid models. The neutral curves for two solid models differ at finite wavenumbers for which the nondimensional wall deformability parameter $G \sim O(1)$ or higher. Higher values of G implies more soft solid which in turn implies that solid can undergo large and finite deformations, and deformation gradients due to the stress exerted by liquid layer. However, linear elastic model is strictly valid only for small displacement gradients and it is necessary to use a nonlinear constitutive stress-strain relationship to get an accurate picture of stability of the system (Gaurav & Shankar 2007, 2010*b*; Gkanis & Kumar 2003, 2006). The neo-Hookean solid model is a generalization of Hooke's law valid for finite displacement gradients, and this generalization results in a nonlinear stress-deformation relationship (Macosko 1994). This nonlinearity in the constitutive relation results in several additional coupling terms between the base state deformation and the perturbation quantities and these additional terms are present in the governing equations of solid when a neo-Hookean model is used but remain absent for a linear elastic model (Gaurav & Shankar 2007, 2009, 2010*b*; Gkanis & Kumar 2003, 2005). These terms become important for higher values of G (for which we expect large and finite deformation gradients) and thus, we observe the differences between the solid models at $k \sim O(1)$ when G becomes an $O(1)$ quantity. Further, the neo-Hookean model exhibits a first normal stress difference in base state which is known to cause a short wave instability of liquid-solid interfacial mode (Gkanis & Kumar 2003) (Refer the LS mode curves on the top Right side of Figure 2.3). This normal stress difference is absent for linear elastic solid and hence, the short wave liquid-solid unstable mode is not captured using linear model. Due to these reasons,we expect the results obtained using neo-Hookean solid model to be more accurate than predicted using linear model. Other complex nonlinear constitu-

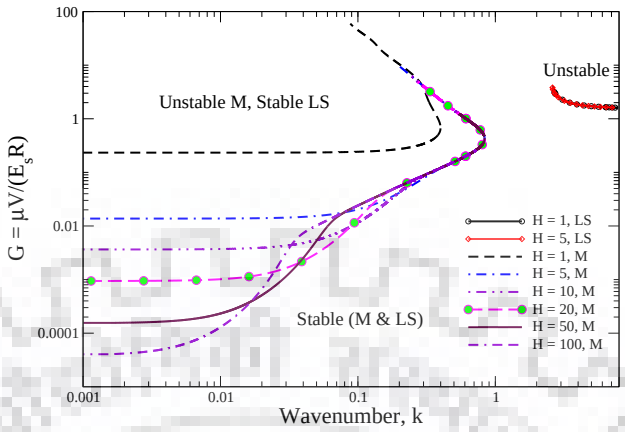

Figure 2.5: Neutral stability curves for different values of solid thickness. Data for $Re = 0, Pe_{\text{inv}} = 0, Ma = 1, \Sigma_{\text{gl}} = 0.5, \Sigma_{\text{ls}} = 0, \theta = 45^{\circ}$

tive relations like Mooney Rivlin model are also available for soft solids and these can also be reduced to the neo-Hookean or linear elastic solid model. We expect to observe similar destabilization of Marangoni mode using these models as well. The neo-Hookean model is one of the simplest model which accounts for constitutive nonlinearities and is also shown to a provide a good (if not perfect) fit to the experimental data on real rubber samples Macosko (1994). Further, recent studies conducted by Verma & Kumaran (2013*b*) on flow in flexible microchannel, and Neelamegam *et al.* (2014) on viscous flow past soft gels in a parallel plate rheometer compared experimental results for flow transition with the linear stability calculations made using neo-Hookean solid model. Both these studies found a reasonably good agreement between experimental observations and theoretical predictions. In light of these experimental observation, we believe that neo-Hookean model is an appropriate and simple to use solid model for capturing the essential physics related to flow transitions.

Figure 2.5 shows the neutral stability curves for both Marangoni and LS modes for different values of solid thickness. The short wave LS mode neutral curves remain unaffected by variation of H which is in agreement with several previous studies (Gaurav & Shankar 2007; Gkanis & Kumar 2003). In contrast, the neutral curves corresponding to Marangoni mode shifts downwards with increase in solid thickness. This illustrates that the critical value of G required for triggering

Marangoni mode instability decreases with increasing H. We further investigated the effect of variation of solid thickness on the growth rate of unstable Marangoni mode for a given value of solid deformability parameter. Note that the expression of $c_{\mathrm{Ma}}^{(3)}$ given in Section 2.3 shows that the magnitude of $c_{\mathrm{Ma}}^{(3)}$ increases with increase in both G and H. For example, the expression for third correction to wave speed when parameter values are set as in Figure 2.5 (except H and G) is $c_{\mathrm{Ma}}^{(3)} = \mathrm{i}(-0.0972222 + 0.166667GH + 0.25GH^2)$. This expression clearly shows that the growth rate increases monotonically with increase in H for long-wave perturbations. However, the trend for variation of growth rate with solid thickness is not monotonous when these low-k results are continued to finite wavenumbers. For example, Figure 2.6(a) shows growth rate vs. wavenumber plot for $G = 0.05$ for different values of H. If we focus on the maximum growth rate (or most unstable mode), we observe that the maximum growth rate first increases when H is increased from $H = 3$ to $H = 8$ and then decreases as solid thickness increases from $H = 10$ to $H = 20$. These data suggest that for a given G, there will be an optimum solid thickness for which the growth rate for Marangoni mode will be maximum. In order to further verify this, we constructed several growth rate vs. wavenumber plots for different values of G and varied solid thickness for each G. The maximum growth rate, obtained at a given G for different values of H, is plotted against H as shown in Figure 2.6(b). This figure clearly shows that for a given G, maximum growth rate first increases to a maximum value with increase in H, then decreases and finally approaches to a constant value at sufficiently large H. Both the value of H at which growth rate becomes maximum and H at which it becomes constant increases with decrease in solid deformability parameter G.

Figure 2.7 shows the effect of inverse of Peclet number (or equivalently, surfactant diffusivity) on Marangoni and LS mode neutral stability curves. Recall that the effect of surfactant diffusivity was found to be stabilizing in low-k limit ($c_{\mathrm{Ma}}^{(1)} = -\mathrm{i}Pe_{\mathrm{inv}}$). Figure 2.7 demonstrates that the neutral stability curves corresponding to Marangoni mode at $Pe_{\mathrm{inv}} = 0$ and $Pe_{\mathrm{inv}} = 10^{-6}$ almost overlap each other for all wavenumbers. As Pe_{inv} is increased to 10^{-5} and 10^{-4}, the Marangoni mode neutral curves start turning upward showing a strong stabilizing effect on low-wavenumber perturbations. However, still, the effect on critical value of G required to cause destabilization of Marangoni mode is marginal. For example, the

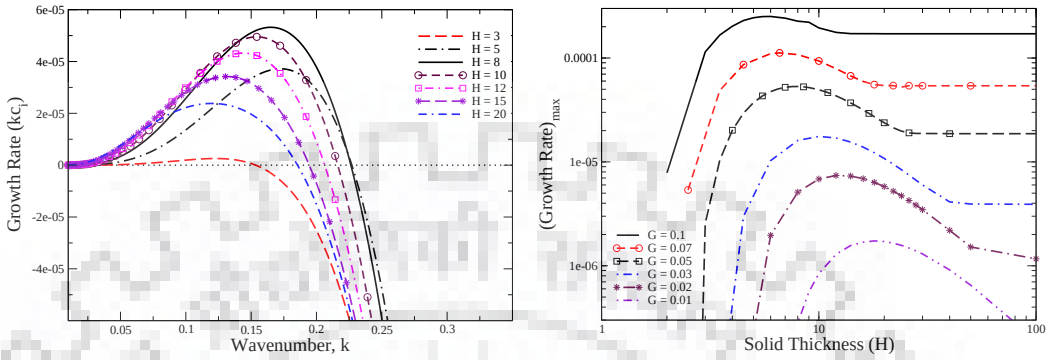

(a) Growth rate vs. k (b) Maximum growth rate vs. H

Figure 2.6: Data showing the effect of solid layer thickness on growth rate of Marangoni mode: Data for $G = 0.05, Re = 0, Ma = 1, Pe_{\text{inv}} = 0, \Sigma_{\text{gl}} = 0.5, \Sigma_{\text{ls}} = 0$, and $\theta = 45°$.

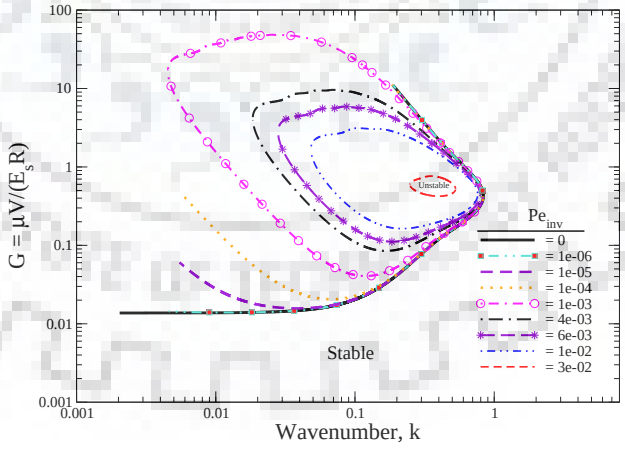

Figure 2.7: Effect of inverse Peclet number on neutral stability curves. Data for $Re = 0, H = 5, Ma = 1, \Sigma_{\text{gl}} = 0.5, \Sigma_{\text{ls}} = 0, \theta = 45°$

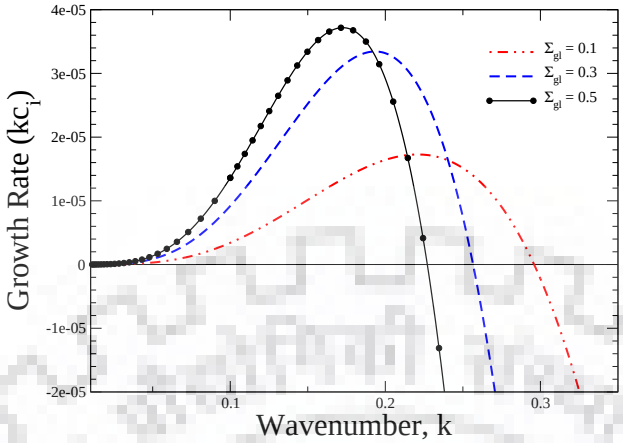

Figure 2.8: Effect of surface tension (Σ_{gl}) on the growth rate of Marangoni mode. Data for $Re = 0, H = 5, G = 0.05, Pe_{inv} = 0, Ma = 1, \Sigma_{ls} = 0, \theta = 45^{\circ}$

---

critical $G \approx 0.013$ for $Pe_{inv} = 0$ while critical G increases marginally to 0.02 for $Pe_{inv} = 10^{-4}$. As Pe_{inv} is further increased to 10^{-3}, the neutral stability curve forms a loop and Marangoni mode is unstable with in the region enclosed by this loop. The area enclosed by such loops decrease with increase in Pe_{inv} and finally vanishes for $Pe_{inv} \gtrsim 0.01$. Thus, the Marangoni instability induced by solid deformability is suppressed by strong surfactant diffusion. However, it is important to note that the results presented for $Pe_{inv} > 10^{-4}$ are certainly not relevant to the case of insoluble surfactant, in which case, the surfactant diffusivity values are usually small. Higher values of Pe_{inv} could be observed for the case of soluble surfactant (for example refer Karapetsas & Bontozoglou (2013)) but this is beyond the scope of the present work.

Figure 2.8 shows the growth rate versus wavenumber plot depicting the effect of increasing surface tension (Σ_{gl}) on the Marangoni mode for the parameters $Re = 0, H = 5, G = 0.05, Pe_{inv} = 0, Ma = 1, \Sigma_{ls} = 0, \theta = 45^{\circ}$. The growth rate of unstable Marangoni mode remains significantly low ($\sim 10^{-9}$) for low-wavenumber but it is two to three times higher at order of $k(\sim 0.1)$. The maximum growth rate of unstable Marangoni mode increases while corresponding wavenumber decreases with increasing the value of surface tension (Σ_{gl}).

Figure 2.9 is plotted between growth rate of Marangoni mode and wavenumber which shows the effect of angle (θ) on the stability of Marangoni mode for the data

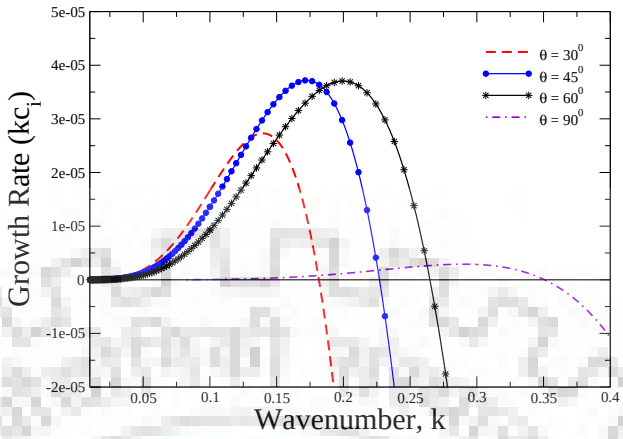

Figure 2.9: Effect of inclination of a plane (θ) on the growth rate of Marangoni mode. Data for $Re = 0, H = 5, G = 0.05, Pe_{\text{inv}} = 0, Ma = 1, \Sigma_{\text{gl}} = 0.5, \Sigma_{\text{ls}} = 0$

$Re = 0, H = 5, G = 0.05, Pe_{\text{inv}} = 0, Ma = 1, \Sigma_{\text{gl}} = 0.5, \Sigma_{\text{ls}} = 0$. The growth rate of unstable Marangoni mode is significantly low for low-wavenumber but it increases and becomes maximum at order of wavenumber ($k \sim 0.1$). The effect of angle (θ) on the Marangoni mode is stabilizing for low-wavenumber and destabilizing for finite wavenumber. The maximum positive growth rate of Marangoni mode at order of $k(\sim 0.1)$ increases with increasing the value of angle (θ) but it decreases with increasing the angle (θ) above a critical value. At angle ($\theta = 90^{\circ}$), the unstable growth rate of Marangoni mode becomes very weak or negligible (≈ 0) for low-wavenumber but it increases significantly very low in finite wave limit. With increasing the value of angle (θ), the value of critical wavenumber at which unstable Marangoni mode becomes stable also increases.

Figure 2.10 is a neutral stability curve which shows the effect of surface tension (Σ_{gl}) on the Marangoni mode for the data $Re = 0, H = 5, Pe_{\text{inv}} = 0, Ma = 1, \Sigma_{\text{ls}} = 0, \theta = 45^{\circ}$. The effect of Σ_{gl} on the LS mode is not shown here because it has been investigated in previous studies (Gaurav & Shankar 2007, 2010*a*). The Marangoni mode is stable in longwave for a low values of G but transition from stable to unstable occurs when the values of G increases above a critical value ($G_c = 0.009, 0.011,$ and 0.013 corresponding $\Sigma_{\text{gl}} = 0.1, 0.3,$ and 0.5). Here, the analytical solution and numerical solution both produces similar values of critical G for corresponding values of surface tension (Σ_{gl}). The values of critical G increases with increasing the

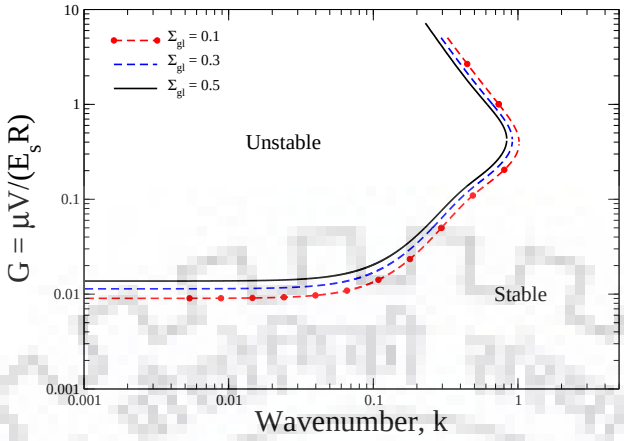

Figure 2.10: Neutral stability curves for different values of surface tension (Σ_{gl})solid thickness. Data for $Re = 0, H = 5, Pe_{inv} = 0, Ma = 1, \Sigma_{ls} = 0, \theta = 45^{\circ}$

values of surface tension at GL interface. If longwave results extend upto finite wave by using numerical solution then also we find equivalent results and effects. Thus, the effect of surface tension (Σ_{gl}) on the Marangoni mode is stabilizing because critical value of G increases and unstable $G-k$ region decreases simultaneously with increasing the values of Σ_{gl}.

Figure 2.11 shows effect of angle (θ) on the the neutral stability curves of Marangoni mode for the data $Re = 0, H = 5, Pe_{inv} = 0, Ma = 1, \Sigma_{gl} = 0.5, \Sigma_{ls} = 0$. The flow system is stable (or Marangoni mode) for lower values of deformability parameter G but becomes unstable at higher values of G. Next, The effect of angle (θ) on the Marangoni mode is destabilizing because the critical value of G decreases with increasing the angle, as a results unstable $G-k$ region increases. This Marangoni mode instability can also be shown by the analytical expression for low-wavenumber, $G_c = (21 + 28Cot\theta)/3570$ which gives the value of $G_c = 0.0194, 0.0104$, and 0.0058 corresponding to the value of $\theta = 30^{\circ}, 60^{\circ}$, and 90°. Here, it clear that the critical values of deformability parameters decreases as increasing in angle of inclination of a deformable surface in longwave. If these longwave results extend upto finite wave numerically then we also find the destabilizing effect of angle but also observe the small increment in the value of G_c. The results at higher values of wavenumber and G are equivalent to the discussion given for previous neutral stability curves or figures.

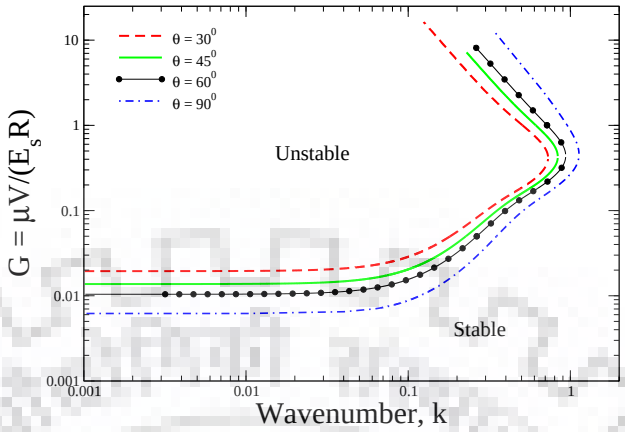

Figure 2.11: Neutral stability curves for different values of inclination of plane (θ). Data for $Re = 0, H = 5, Pe_{\text{inv}} = 0, Ma = 1, \Sigma_{\text{gl}} = 0.5, \Sigma_{\text{ls}} = 0$

2.5 Conclusions

The linear stability of a surfactant-laden liquid film flowing down a flexible inclined wall is analyzed in the creeping flow limit with a major focus on the role of wall deformability on the stability behavior of surfactant-induced Marangoni mode. Both the surfactant-induced Marangoni mode and the gas-liquid interfacial mode remain stable for film flowing down a rigid inclined wall in the zero Reynolds number limit. We have demonstrated that the Marangoni mode becomes unstable when the nondimensional wall deformability parameter $G = \mu V / E_s R$ increases above a critical value. The critical value of G required for triggering Marangoni mode instability decreases with increase in solid thickness, while for a given G, there exist an optimum solid thickness for which the growth rate for unstable Marangoni mode is maximum. The deformability of solid layer has an additional stabilizing effect on already stable GL interfacial mode in creeping flow limit. The liquid-solid interface also becomes unstable for high wavenumber perturbations, but at higher values of G as compared to the G values required for destabilization of Marangoni mode. Thus, the Marangoni mode is the most unstable mode in creeping flow limit for a contaminated liquid film flowing down a deformable inclined wall. As shown by Blyth & Pozrikidis (2004*a*), even though the Marangoni mode remains the dominant mode for film flow down a rigid inclined wall in zero and low Reynolds number limit, but it was never observed to become unstable. On the other hand, this mode does

become unstable on imposing a shear stress at GL interface (Wei 2005*a*). In contrast to these studies, the Marangoni mode instability is observed here solely due to the presence of a sufficiently deformable wall even when the GL interface remains stress-free in its basic state.

Finally, we provide some dimensional estimates of parameters for which the Marangoni instability observed here can be realized in experiments. Since the surfactant diffusivity is usually small, we set $Pe_{\text{inv}} = 0$. The Marangoni number varies between $O(0.01-1)$ for low to moderate values of surfactant concentration and hence, we fix $Ma = 1$. For $H \sim 10$, $G \gtrsim 0.001$ for triggering the Marangoni mode instability. If we set $\rho \sim 10^3 \text{kg/m}^3, R \sim 10^{-3}\text{m}$ and $\mu \sim 1$ Pa-s, then $G \gtrsim 0.001$ implies that shear modulus of solid layer $E_s \lesssim 10^4$ Pa for observing soft solid induced Marangoni mode instability for surfactant laden film flows down a deformable inclined wall.

Chapter 3

Manipulation and control of instabilities for surfactant-laden liquid film flowing down an inclined plane using a deformable solid layer

Abstract

We analyzed the linear stability of surfactant-laden liquid film with free surface flowing down an inclined plane under the action of gravity when the inclined plane is coated with a deformable solid layer. For flow past a rigid incline and in presence of inertia, the gas- liquid (GL) interface is prone to a free surface instability and the presence of surfactant is known to stabilize the free surface mode when Marangoni number increases above a critical value. The rigid surface configuration also admits a surfactant induced Marangoni mode which remains stable for film flows with the free surface. This Marangoni mode was observed to become unstable for surfactant covered film flow past flexible inclined plane in creeping flow limit when the wall is made sufficiently deformable. In view of these observations, we investigate the following two aspects. First, what is the effect of inertia on Marangoni mode instability induced by wall deformability? Second, and more importantly, whether it is possible to use a deformable solid coating to obtain stable flow for surfactant covered film for cases when the Marangoni number is below the critical value

required for stabilization of free surface instability. In order to explore the first question, we continued the growth rates for Marangoni mode from creeping flow limit to finite Reynolds numbers (Re) and observed that while the increase in Reynolds number has a small stabilizing effect on growth rates, the Marangoni mode still remains unstable for finite Reynolds numbers as long as the wall is sufficiently deformable. The Marangoni mode remains the dominant mode for zero and small Reynolds numbers until the GL mode also becomes unstable with an increase in Re. Thus, for a given set of parameters and beyond a critical Re, there is an exchange of dominant mode of instability from Marangoni to free surface GL mode. With respect to the second important aspect, our results clearly demonstrate that for cases when the stabilizing contribution of surfactant is not sufficient for suppressing GL mode instability, a deformable solid coating could be employed to suppress free surface instability without triggering Marangoni or liquid-solid interfacial modes. Specifically, we have shown that for a given solid thickness, as the shear modulus of the solid layer decreases (i.e. the solid becomes more deformable) the GL mode instability is suppressed. With further decrease in shear modulus, the Marangoni and liquid-solid interfacial modes become unstable. Thus, there exists a stability window in terms of shear modulus where the surfactant-laden film flow remains stable even when the Marangoni number is below the critical value required for free surface instability suppression. Further, when the Marangoni number is greater than the critical value so that the GL mode remains stable in rigid limit or with the deformable wall, the increase in wall deformability or solid thickness triggers Marangoni mode instability and thus, renders a stable flow configuration into an unstable one. Thus, we show that the soft solid layer can be used to manipulate and control the stability of surfactant-laden film flows.

3.1 Introduction

Liquid film flow with free surface occurs in various engineering applications such as coating flows (Wenstein & Ruschak 2004), distillation units, condensers, falling film reactors, microfluidics etc.(Craster & Matar 2009; Squires & Quake 2005), as well as in biological systems such as pulmonary fluid mechanics (Grotberg & Jensen 2004; Halpern & Grotberg 1993). It is well known that the liquid film

flowing down a rigid inclined plane undergoes a free surface instability, and subsequently displays a variety of complex spatiotemporal wave patterns (Chang & Demekhin 2002). The occurrence of waves is desirable in heat and mass transfer applications, while, in other instances such as coating flows, surface waves are undesirable as they lead to non-uniform coating thickness. Thus, manipulation and control of free surface instability (and interfacial instabilities, in general) remains a crucial aspect for several technological applications. The liquid film flow is usually accompanied by surface active agents or surfactants which play a critical role in different applications (Goerke 1998; Morrow & Mason 2001; Quere *et al.* 1997). Previous studies have demonstrated the suppression of free surface instability for liquid film flowing down a rigid inclined plane using a monolayer of an insoluble surfactant at gas-liquid (GL) interface (Blyth & Pozrikidis 2004*a*; Pereira & Kalliadasis 2008; Wei 2005*a*). An additional stable normal mode also appears due to transport of surfactant species along the GL interface and this additional mode is referred as surfactant/Marangoni mode in literature. These observations suggest that the surfactants can be used to suppress/control the free surface instability. In relation to suppression of free surface instability, Shankar and coworkers (Gaurav & Shankar 2007; Jain & Shankar 2007; Sahu & Shankar 2016; Shankar & Sahu 2006) have shown the possibility of using a deformable wall to obtain a stable flow of clean (i.e. devoid of surfactant layer) liquid film when the liquid film otherwise remains unstable for flow past a rigid inclined wall. Very recently, we analyzed the stability of surfactant-laden liquid film flowing down an inclined plane when the inclined plane is coated with a soft solid layer. The stability of the system was investigated in creeping flow limit (i.e., Reynolds number Re = 0) and in this Re = 0 limit, the free surface or GL mode instability remains absent. We demonstrated that the additional surfactant mode which remains stable for flow past rigid inclined wall becomes unstable when the wall is made sufficiently deformable. In view of this wall deformability induced destabilization of Marangoni mode, we re-examine the stability of surfactant covered liquid film flow down an inclined plane coated with a soft solid layer in presence of inertia (Re = 0) to investigate whether the suppression predicted by Shankar and coworkers for a clean film holds for surfactant-laden liquid film as well or not? In the following, we briefly discuss relevant literature and motivate the context of the present study.

Earlier theoretical studies on the linear stability of clean liquid film flowing down a rigid inclined plane demonstrated that the free surface or GL interface becomes unstable for longwave perturbations when Reynolds number increases above a critical value (Benjamin 1957; Lin 1967; Yih 1963). This instability is referred as free surface or GL mode instability in the present work. In presence of surfactant at an interface, the interfacial tension depends on the surface concentration of surfactant and the convective motion of surfactant results in non-uniform distribution of surfactant at the interface. This non-uniform distribution leads to surfactant concentration gradient which, in turn, results in variation of surface tension along the interface. As a consequence, the additional term corresponding to Marangoni stress appears in tangential stress balance and this could have a stabilizing or destabilizing effect on an interfacial mode. For the case of a single liquid film with free surface falling down a rigid inclined plane, this additional Marangoni stress has a stabilizing influence on GL interfacial mode (Anshus & Acrivos 1967; Blyth & Pozrikidis 2004*a*; Pereira & Kalliadasis 2008; Whitaker 1964; Whitaker & Jones 1966). Blyth & Pozrikidis (2004*a*)(also see, Pereira & Kalliadasis (2008)) analyzed the stability of surfactant covered liquid film flowing down a rigid inclined plane by using an Orr-Sommerfeld formulation. They clearly demonstrated the presence of two normal modes in creeping flow limit: the usual GL interfacial mode and the Marangoni mode which originates due to the convective motion of surfactant along with the interface. The Marangoni mode remains the least stable mode for zero and low Reynolds numbers. With an increase in Reynolds number, the growth rate of GL mode increases while the growth rate of Marangoni mode remains unaffected. The GL mode eventually overtakes Marangoni mode and finally becomes unstable. Thus, an exchange of dominant mode of instability from Marangoni mode at low Reynolds number to GL mode above a critical Reynolds number is observed by Blyth & Pozrikidis (2004*a*). We show the subtle differences that occur in change of dominant mode with change in Reynolds number for surfactant-contaminated liquid film flowing down a deformable inclined wall instead of a rigid inclined plane. More importantly, in relation to the effect of surfactant on free surface instability, the neutral curves presented by Blyth & Pozrikidis (2004*a*) in Reynolds number vs. wavenumber plane clearly demonstrate that the presence of surfactant increases the critical Reynolds number for the onset of GL mode instability as compared to the

critical Reynolds number observed for a clean film. In other words, there exists a critical Marangoni number above which the free surface instability is suppressed.

In the context of effect of surfactant on the stability of interfacial flow systems, it is important to mention the work of Frenkel & Halpern (2002) and Halpern & Frenkel (2003) who first uncovered the instability of Marangoni/surfactant mode for an interfacial flow system. They analyzed the linear stability of two-layer channel flow in creeping flow limit with surfactant monolayer present at the fluid-fluid interface. The usual Yih type (Yih 1967) interfacial mode remains stable in creeping flow limit while the additional Marangoni mode becomes unstable for certain values of viscosity and thickness ratio of two fluid layers. They demonstrated that basic interfacial shear is necessary to destabilize the Marangoni mode. Blyth & Pozrikidis (2004*b*) investigated the stability of inclined two-layer channel flow in presence of interfacial surfactant and derived non-linear evolution equations for interface location and surfactant concentration using lubrication approximation. They confirmed the results of Frenkel & Halpern (2002) and Halpern & Frenkel (2003) related to Marangoni mode instability. Halpern & Frenkel (2003) suggested the absence of interfacial shear as the reason for not observing the Marangoni mode instability for a free surface flow of liquid film down an inclined plane. Wei examined the stability of surfactant-laden (Newtonian (Wei 2005*a*) and viscoelastic (Wei 2005*b*)) liquid film flow down an inclined plane with an imposed shear applied at GL interface. Their results clearly demonstrated that the Marangoni mode can be rendered unstable for non-zero values of imposed shear at GL interface, and thus, supporting the idea that basic interfacial shear must be present for triggering Marangoni mode instability.

Several strategies have been explored by different authors to control and suppress free surface instabilities. For example, imposing in-plane horizontal oscillations for single (Lin & Chen 1997; Lin *et al.* 1996) and two-liquid film with free surface (Jiang & Lin 2005), and heating of the inclined wall to impose a linear temperature gradient (Demekhin *et al.* 2006) have been explored in the context of controlling free surface and interfacial instabilities. While these studies suggested active methodologies (e.g. imposing external oscillations or heating) for controlling instabilities, Shankar and coworkers explored the possibility of using a passive deformable solid layer to suppress and manipulate interfacial instabilities for a di-

verse class of flow configurations (for example, see a recent review by Gaurav & Shankar (2015)). When a fluid flows past a soft, deformable solid surface, the stress exerted by fluid creates deformations in the solid layer and these deformations in turn could alter the fluid flow. This coupling between the fluid and solid layer can have a profound impact on the stability of a composite fluid-solid system. For example, Shankar & Kumar (2004) analyzed the stability of two layer plane Couette flow past a linear elastic solid layer, and showed for the first time that the presence of solid layer can stabilize the fluid-fluid interfacial instability caused due to jump in viscosity across the interface. However, an additional liquid-solid (LS) interface that can deform is also present for such composite fluid-solid systems. It is well established, both by theory and experiments, that this deformable LS interface becomes unstable in creeping flow limit (Eggert & Kumar 2004; Kumaran *et al.* 1994; Kumaran & Muralikrishnan 2000) as well as at finite Reynolds number (Gaurav & Shankar 2010*b*; Kumaran 2000; Neelamegam & Shankar 2015; Verma & Kumaran 2012*a*, 2013*b*). This instability of liquid-solid interface is referred as LS mode in the present work.

In direct relevance to the present work, Shankar & Sahu (2006) analyzed the stability of a clean Newtonian liquid film falling down an inclined plane coated with a soft solid layer. They defined a deformability parameter for the soft solid layer as $G = \mu V/E_s R$, where μ is the viscosity of a fluid, V is the free surface velocity, R is the thickness of a liquid film, and E_s is the shear modulus of the soft solid layer. The rigid solid limit is recovered by fixing $G = 0$, and higher values of G correspond to more soft solid layer. Their results clearly demonstrated that for a given solid thickness, when the deformability parameter G increases above a critical value, the free surface instability is suppressed for those values of Reynolds number for which the GL mode otherwise remains unstable when the liquid film flows past a rigid incline. With further increase in G, the liquid-solid (LS) interface as well as the GL interface become unstable. Thus, there exists a stable gap in terms of parameter G where all modes remain stable. A similar suppression of free surface instability was also shown by Jain & Shankar (2007) for a visco-elastic liquid film. While the works of both Shankar & Sahu (2006) and Jain & Shankar (2007) used a simple linear elastic constitutive relation for modeling the deformable solid layer, Gaurav & Shankar (2007) used a non-linear neo-Hookean solid model for the soft

solid layer and demonstrated the presence of stability window in a manner similar to the work of Shankar & Sahu (2006). The importance of using a non-linear neo-Hookean solid model over a linear elastic model to accurately capture the stability characteristics for composite fluid-solid systems has been highlighted in several previous studies (Gaurav & Shankar 2007, 2009, 2010*b*; Gkanis & Kumar 2003, 2005, 2006). Based on these observations, we have used a neo-Hookean constitutive relation to represent the dynamics of deformable solid layer in the present work.

The stability of a surfactant-covered liquid film flowing past an inclined plane which is lined with a deformable solid layer is examined recently by Tomar *et al.* (2017) in creeping flow limit ($Re = 0$). Since, a free surface, a surfactant monolayer, and a deformable LS interface are present, there is a possibility of any of the three modes (GL, Marangoni, and/or LS) becoming unstable for this system. The GL or free surface mode was never observed to become unstable in creeping flow limit irrespective of whether the wall is rigid or deformable. For a given solid thickness, the Marangoni mode remains stable in rigid limit $G \to 0$ in agreement with previous studies (Blyth & Pozrikidis 2004*a*; Pereira & Kalliadasis 2008), and for lower values of G. As this deformability parameter G increases beyond a threshold value, the Marangoni mode becomes unstable first, and with further increase in G, the LS interface also becomes unstable. Thus, the Marangoni mode remains the dominant mode of instability for creeping flow of surfactant loaded liquid film past a deformable inclined wall. In this chapter, we examine the same problem in presence of inertia as we examined in chapter 2 for creeping flow limit. As mentioned earlier that in presence of inertia, the GL mode can also become unstable above a critical Reynolds number. The presence of surfactant is known to suppress the free surface instability when Marangoni number is above a critical value, and the deformable solid layer also has a stabilizing effect on this GL mode instability. Thus, we intuitively expect that the liquid film in presence of deformable solid layer and surfactant monolayer will be a more stable system in comparison to either of (i) a clean liquid film flowing past a rigid incline, or (ii) a contaminated liquid film past a rigid incline, or (iii) a clean liquid film flowing past an inclined wall coated with deformable solid layer. This is indeed true for GL interfacial mode as will be demonstrated in the present work. The deformable solid layer (together with the surfactant layer) suppresses the GL mode instability when G increases

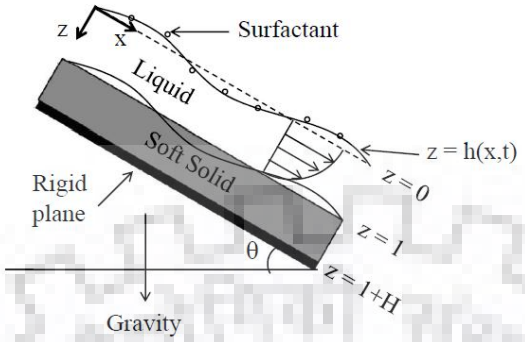

Figure 3.1: Sketch of gravity-driven surfactant-laden liquid film flowing down an inclined neo-Hookean solid surface.

above a critical value. However, with further increase in deformability parameter, the Marangoni mode can also become unstable. Thus, in light of this new observation related to wall induced instability of Marangoni mode, a pertinent question is whether it is possible to obtain stable film flow using a deformable solid coating particularly when the surfactant contribution is not sufficient enough to completely suppress the GL mode instability? We examine the stability characteristics of the composite system (contaminated liquid film flow past an inclined wall coated with deformable solid layer) to answer the above-posed questions. The description of the flow configuration and governing equations are given in Section 3.2, results are discussed in Section 3.3, and the findings are finally summarized in Section 3.4.

3.2 Problem Formulation

3.2.1 Governing equations for fluid and solid

The system under consideration (Figure 3.1) consists of a Newtonian liquid film (thickness R, viscosity μ, and density ρ) falling freely due to gravity down a soft/deformable solid layer. The flexible wall (thickness HR, shear modulus E_s , and density ρ) is firmly fixed to an inclined plane at $z^* = (1+H)R$ which makes an angle θ with the horizontal. Note that the densities of both solid and liquid layers

are assumed to be identical for simplicity. The free surface is exposed to a passive gas and wrapped by a monolayer of insoluble surfactant with surface concentration $\Gamma^*(x^*,t^*)$. The gas-liquid (GL) interface remains flat in base state with a constant surfactant concentration Γ_0^*, and a corresponding base state surface tension as γ_0^*. The governing equations for the liquid are Navier-Stokes continuity and momentum balance:

$$\nabla^* \cdot \mathbf{v}^* = 0, \tag{3.1}$$

$$\rho[\partial_t^* \mathbf{v}^* + \mathbf{v}^* \cdot \nabla^* \mathbf{v}^*] = \nabla^* \cdot \mathbf{T}^* + \rho \mathbf{g}. \tag{3.2}$$

where, $\mathbf{v}^*$ and p^* are the velocity and pressure fields in the liquid layer; $\mathbf{T}^* = -p^*\mathbf{I} + \mu[\nabla^*\mathbf{v}^* + (\nabla^*\mathbf{v}^*)^T]$ is the total stress tensor for the liquid layer.

The stress balance at GL interface, in presence of surfactant layer, is given as:

$$\mathbf{n} \cdot \mathbf{T}^* = \nabla_s{}^* \gamma^* - \gamma^* \mathbf{n}(\nabla^* \cdot \mathbf{n}) \tag{3.3}$$

where, $\mathbf{n}$ is the unit normal vector,and $\nabla_s{}^* = \nabla^* - \mathbf{n}(\mathbf{n} \cdot \nabla^*)$ is the component of a gradient operator in the local plane of the interface. The convection-diffusion equation for surfactant transport (Halpern & Frenkel 2003; Stone 1990) at GL interface is given as:

$$\frac{\partial \Gamma^*}{\partial t^*} + \nabla_s{}^* \cdot (\Gamma^* \mathbf{v_s}{}^*) + \Gamma^* (\nabla_s{}^* \cdot \mathbf{n})(\mathbf{v}^* \cdot \mathbf{n}) = D_s \nabla_s^{2^*} \Gamma^* \tag{3.4}$$

where, $\mathbf{v_s}{}^*$ is the component of the velocity vector in the interface defined as: $\mathbf{v}^* = \mathbf{v_s}{}^* + (\mathbf{v}^* \cdot \mathbf{n})\mathbf{n}$, and D_s is the surface diffusivity of surfactant. For small changes in surfactant concentration about the mean value Γ_0^*, the surface tension, and surfactant concentration are related as: $\gamma^* = \gamma_0^* - E(\Gamma^* - \Gamma_0^*)$, where, E refers to surface elasticity defined as $E = -(\partial\sigma^*/\partial\Gamma^*)_{\Gamma_0} > 0$. Finally, the kinematic condition at GL interface is: $\partial_t^* h^* + v_x^* \partial_x^* h^* = v_z^*$

Unlike the flow patterns in liquid, the behaviour of deformable solid is analyzed by studying the spatial movements of material points. Therefore, it is convenient (following Gkanis & Kumar (2003)) to use the Lagrangian coordinates to describe governing equations for the solid layer. The undeformed configuration is considered the reference state and hence, the position vector of material points in this unstressed reference state $\mathbf{X}^* = (X^*, Y^*, Z^*)$ are treated as the independent variables. In the deformed state of the solid, the spatial position vector of the material particles

$\mathbf{w}^* = (w_X^*, w_Y^*, w_Z^*)$ can be expressed as a function of reference coordinates: $\mathbf{w}^*(\mathbf{X}^*)$. The deformable solid layer is modeled as an impermeable and incompressible neo-Hookean elastic solid, and the mass and momentum conservation equations for the neo-Hookean solid layer are given as (Holzapfel 2000; Malvern 1969):

$$\det(\mathbf{F}) = 1, \tag{3.5}$$

$$\rho \left[\frac{\partial^2 \mathbf{w}^*}{\partial t^{*2}}\right]_{\mathbf{X}^*} = \nabla^*_{\mathbf{X}^*} \cdot \mathbf{P}^* + \rho \mathbf{g}. \tag{3.6}$$

In the above equations, $\mathbf{F}$ is the deformation gradient tensor defined as $\mathbf{F} = \nabla^*_{\mathbf{X}^*}\mathbf{w}^*$ and $\mathbf{P}^*$ is the first Piola-Kirchhoff stress tensor, related to Cauchy stress tensor by $\mathbf{P}^* = \mathbf{F}^{-1} \cdot \sigma^*$. The Cauchy stress tensor, $\boldsymbol{\sigma}^*$, for the neo-Hookean elastic solid is (Beatty & Zhou 1991; Destrade & Saccocmandi 2004; Fosdick & Yu 1996; Hayes & Saccocmandi 2002):

$$\boldsymbol{\sigma}^* = -\hat{p}_s^* \mathbf{I} + E_s(\mathbf{F} \cdot \mathbf{F}^{\mathbf{T}}) \tag{3.7}$$

where, E_s is the shear modulus of deformable solid layer and $\hat{p}_s$ is the pressure-like function related to actual pressure in the neo-Hookean solid as $\hat{p}_s = p_s + E_s$.

At the liquid-solid (LS) interface, the velocities and stresses in liquid and the solid layer are continuous.

$$\mathbf{v}^* = \left(\frac{\partial \mathbf{w}^*}{\partial t^*}\right)_{X^*}, \tag{3.8}$$

$$\mathbf{n} \cdot \mathbf{T}^* + \gamma_{ls}^* \mathbf{n}(\nabla^* \cdot \mathbf{n}) = \mathbf{n} \cdot \boldsymbol{\sigma}^*, \tag{3.9}$$

where, γ_{ls}^* is the LS interfacial tension and $\mathbf{n}$ is the unit normal vector to LS interface. As the deformable solid is firmly adhered to a rigid surface, zero deformation conditions prevail at $z^* = (1+H)R$: $\mathbf{w}^* = \mathbf{X}^*$.

The above system of equations is nondimensionalized by using the following scales: R for lengths and displacements, unperturbed free surface velocity $V = \frac{\rho g R^2 \sin\theta}{2\mu}$ for velocities, $\mu V/R$ for stresses and pressure, Γ_0^* for surfactant concentration, and γ_0^* for surface tension. In the unperturbed steady state, the GL and LS interfaces remain flat. The non-dimensional velocity profile and pressure distribution in the liquid layer are given as:

$$\bar{v}_x(z) = \left(1 - z^2\right), \quad \bar{v}_z = 0, \quad \bar{p}(z) = (2\cot\theta)z, \tag{3.10}$$

Various base-state physical quantities are denoted by an overbar. The fluid base velocity exerts shear stress at the LS interface, thereby creating unidirectional deformations in the solid layer with a non-zero displacement in x-direction. The deformation and pressure fields for solid layer are given as:

$$\overline{w}_X = X + G[(1+H)^2 - Z^2], \quad \overline{w}_Z = Z, \quad \overline{p}_s = (2\cot\theta)Z. \tag{3.11}$$

3.2.2 Linearised governing equations

We perform a standard temporal linear stability analysis in which infinitesimally small perturbations are imposed over the base state for all the dynamical variables in fluid and solid layers. These perturbed variables are substituted in governing equations and boundary conditions, and the resulting equations are then linearized to obtain a set of equations in terms of perturbation variables. The perturbations are assumed to be two-dimensional and are expanded in the form of Fourier modes:

$$f' = \tilde{f}(z)\exp[\mathrm{i}k(x-ct)], \tag{3.12}$$

where, f' is the small perturbation of any dynamical variable, k is the (real) wavenumber of perturbations, c is the complex wave speed and $\tilde{f}(z)$ is the complex amplitude function of the disturbance. For the deformable solid, x and z are replaced by X and Z, respectively. If $c_i > 0$ (or $c_i < 0$), flow will be unstable (or stable). On the substitution of above form of perturbations in linearized governing equations and boundary conditions, we obtain a set of equations in terms of amplitude functions and wave speed, c, which govern the stability of the composite system. The non-dimensional governing stability equations for the liquid layer are:

$$\frac{\mathrm{d}\tilde{v}_z}{\mathrm{d}z} + \mathrm{i}k\tilde{v}_x = 0, \tag{3.13}$$

$$Re\left[\mathrm{i}k(\overline{v}_x - c)\tilde{v}_x + (\mathrm{d}_z\overline{v}_x)\tilde{v}_z\right] = -\mathrm{i}k\tilde{p} + \left[\frac{\mathrm{d}^2}{\mathrm{d}z^2} - k^2\right]\tilde{v}_x, \tag{3.14}$$

$$Re\left[\mathrm{i}k(\overline{v}_x - c)\tilde{v}_z\right] = -\frac{\mathrm{d}\tilde{p}}{\mathrm{d}z} + \left[\frac{\mathrm{d}^2}{\mathrm{d}z^2} - k^2\right]\tilde{v}_z. \tag{3.15}$$

The linearized equations for the neo-Hookean elastic solid are:

$$\frac{\mathrm{d}\tilde{w}_Z}{\mathrm{d}Z} + \mathrm{i}k\tilde{w}_X - (\mathrm{d}_Z\overline{w}_X)\,\mathrm{i}k\tilde{w}_Z = 0\,, \quad (3.16)$$

$$-\mathrm{i}k\tilde{p}_s + (2\cot\theta)\mathrm{i}k\tilde{w}_Z + \frac{1}{G}\left[-k^2 + \frac{\mathrm{d}^2}{\mathrm{d}Z^2}\right]\tilde{w}_X = -k^2c^2Re\,\tilde{w}_X\,, \quad (3.17)$$

$$(\mathrm{d}_Z\overline{w}_X)\,\mathrm{i}k\tilde{p}_s - (2\cot\theta)\mathrm{i}k\tilde{w}_X - \frac{\mathrm{d}\tilde{p}_s}{\mathrm{d}Z} + \frac{1}{G}\left[-k^2 + \frac{\mathrm{d}^2}{\mathrm{d}Z^2}\right]\tilde{w}_Z = -k^2c^2Re\,\tilde{w}_Z\,. \quad (3.18)$$

Where, $Re = \frac{\rho VR}{\mu}$ is the Reynolds number, and $G = \mu V/E_sR$ is the non-dimensional solid deformability parameter representing the ratio of viscous shear stress in liquid to elastic stress in solid layer. $G \to 0$ represents the limit of a rigid solid.

The interfacial conditions at GL interface are obtained by Taylor-expanding the fluid dynamical variables about the base state. The linearized kinematic condition, surfactant transport equation and the stress balances at GL interface are:

$$\begin{aligned}
\mathrm{i}k[\overline{v}_x(z=0) - c]\tilde{h} &= \tilde{v}_z(z=0)\,, & (3.19)\\
[\overline{v}_x(z=0) - c - \mathrm{i}kPe_{\text{inv}}]\tilde{\Gamma} &= -\tilde{v}_x(z=0)\,, & (3.20)\\
-2\tilde{h} + \mathrm{d}_z\tilde{v}_x + \mathrm{i}k\tilde{v}_z &= \mathrm{i}kMa\Sigma_{gl}\tilde{\Gamma}, & (3.21)\\
-\tilde{p} - (2\cot\theta)\tilde{h} + 2\frac{\mathrm{d}\tilde{v}_z}{\mathrm{d}z} &= k^2\Sigma_{gl}\tilde{h}. & (3.22)
\end{aligned}$$

where $\tilde{\Gamma}$ is the amplitude of disturbance of surfactant concentration, $Ma = E\Gamma_0^*/\gamma_0^*$ is the Marangoni number, $Pe_{\text{inv}} = D_s/VR$ is the inverse of Peclet number, and $\Sigma_{gl} = \gamma_0^*/\mu V$ is the nondimensional free-surface tension parameter.

The treatment of interfacial conditions at LS interface which involves both Eulerian and Lagrangian variables will be slightly different as compared to the treatment of interfacial conditions at GL interface where only Eulerian variables are involved. Gaurav & Shankar (2010*b*) suggested that a Taylor series expansion is not required for solid (Lagrangian) variables because a material particle's Lagrangian label do not change in deformed state (pre-stressed base state or perturbed state). The independent variables used to label/identify a material particle always remain the coordinates in unstressed configuration (i.e. $\mathbf{X} = (X,Y,Z)$). On the other hand, the fluid variables were Taylor expanded about the base state in Gaurav & Shankar (2010*b*). However, the Taylor series expansion of fluid quantities were carried out only in the direction normal to the flow. Very recently, Patne *et al.* (2017) suggested that the Taylor expansion of fluid variables must be carried out in both flow and normal to

flow directions to make the Lagrangian formulation of Gaurav & Shankar (2010*b*) consistent. They referred the Lagrangian formulation of Gaurav & Shankar (2010*b*) as old L2 formulation, and the modified consistent formulation (with Taylor expansion of fluid variables at LS interface in both flow and cross-flow directions) as proposed consistent L2 formulation or simply L2 formulation. They have also proposed another consistent Lagrangian formulation and referred it as L3 formulation. The undeformed state, deformed base state, and perturbed state are the three states that remain important in L3 formulation, and the deformed base state is used as the reference state in L3 formulation. Note that the unstressed or undeformed state remains the reference configuration in L2 formulation. Patne *et al.* (2017) used specific cases of plane-Couette flow past neo-Hookean solid and Hagen-Poiseuille flow through a neo-Hookean tube to demonstrate the consistency between L3 and modified L2 (or simply L2) formulations. They have shown that the L3 formulation gives the same results as obtained by using L2 formulation which confirms the consistency of two Lagrangian formulations. In the present work, we have used an L2 formulation (as proposed in Patne *et al.* (2017)) where the two states that are important in formulating the problem are undeformed state and the perturbed state with undeformed state being the reference configuration. It is important to remark here that for the flow configuration considered in the present work, the fluid base state remains independent of flow (x -) direction (refer Eq. (3.10)). Hence, no additional terms are expected due to Taylor expansion of fluid variables in x - direction in addition to Taylor expansion in normal (z -) direction. This implies that the modified L2 and old L2 formulations remain identical for the problem considered in the present work. However, for general class of problems related to flow past deformable solid surfaces, the correct way to write down LS interfacial conditions is the L2 (or L3) approach as discussed in Patne *et al.* (2017). Following the procedure outlined in Patne *et al.* (2017) for L2 formulation, the linearized conditions at LS interface are given as:

$$\tilde{v}_z = -\mathrm{i}kc\,\tilde{w}_Z \,, \tag{3.23}$$

$$\tilde{v}_x + (\mathrm{d}_z\overline{v}_x)_{z=1}\tilde{w}_Z = -\mathrm{i}kc\,\tilde{w}_X \,, \tag{3.24}$$

$$\frac{\mathrm{d}\tilde{v}_x}{\mathrm{d}z} + \mathrm{i}k\tilde{v}_z + (\mathrm{d}_z^2\overline{v}_x)\tilde{w}_Z = \frac{1}{G}\left\{(\mathrm{d}_Z\overline{w}_X)\frac{\mathrm{d}\tilde{w}_Z}{\mathrm{d}Z} + \frac{\mathrm{d}\tilde{w}_X}{\mathrm{d}Z} + \mathrm{i}k\tilde{w}_Z - (\mathrm{d}_Z\overline{w}_X)^2\mathrm{i}k\tilde{w}_Z\right\} \,, \tag{3.25}$$

$$-\tilde{p} + 2\frac{\mathrm{d}\tilde{v}_z}{\mathrm{d}z} + k^2\Sigma_{ls}\tilde{w}_Z = -\tilde{p}_s + \frac{2}{G}\frac{\mathrm{d}\tilde{w}_Z}{\mathrm{d}Z} + (2\cot\theta)\tilde{w}_Z \,. \tag{3.26}$$

where, $\Sigma_{ls} = \gamma^*_{ls}/\mu V$ is the nondimensional LS interfacial tension parameter. Finally, the boundary conditions at the rigid surface ($z = 1 + H$) are:

$$\tilde{w}_Z = 0,\ \tilde{w}_X = 0. \tag{3.27}$$

Equations (3.13)-(3.27) govern the linear stability equations for a composite liquid-solid system. We used a pseudo-spectral collocation method and a numerical shooting procedure as we have discussed in chapter 2 to numerically evaluate the eigenvalues and neutral stability boundaries.

3.3 Results and discussion

As mentioned in introduction that for a given solid thickness, the Marangoni mode becomes unstable in creeping flow limit when the wall deformability parameter increases above a critical value. One of the objectives of the work presented in this chapter is to examine the effect of variation of Reynolds number on the growth rate of the Marangoni mode instability. Further, for a given solid thickness and wall deformability parameter, the GL mode can also become unstable with increase in Reynolds number. Thus, it is of interest to know which mode remains the critical mode of instability as Reynolds number increases from zero to finite values. The other more important aspect we examine is the following. It is known that for film flow past a rigid incline, the presence of surfactant suppresses the GL mode instability when Marangoni number increases above a critical value. However, when Marangoni number remains below this threshold value, is it possible to use a deformable solid layer to obtain stable flow configuration? We first briefly discuss the effect of deformable solid layer on GL and Marangoni modes in long-wavelength limit. The long-wave analysis has been discussed in detail in chapter 2, however, we briefly present long wave results for the sake of completeness and this discussion of low-k results sets the context of presenting numerical results in a clear manner.

3.3.1 Long-wave results

The results of long wavelength asymptotic analysis remains valid for $k \ll 1/(1+H)$ in general, and for $k \ll 1$ for $H \sim O(1)$. The wave speed c is expanded in an asymptotic series in k: $c = c^{(0)} + kc^{(1)} + k^2c^{(2)} + k^3c^{(3)} + \cdots$. All the dynamical

variables are expanded according to their respective scalings and the expanded variables are substituted in governing equations and boundary conditions. The resulting equations are solved at each order in k to determine the effect of deformable solid layer for both GL and Marangoni mode. For GL or free surface mode, calculations up to an $O(k)$ are sufficient to determine the stability of the composite system. The leading order wave speed $c^{(0)}$ and first correction to wave speed $c^{(1)}$ for GL interfacial mode are given as:

$$c_{\mathrm{gl}}^{(0)} = 2, \qquad c_{\mathrm{gl}}^{(1)} = \mathrm{i}\left[\underline{\frac{8}{15}Re - \frac{2}{3}\cot\theta - 4GH} - Ma\Sigma_{gl}\right]. \tag{3.28}$$

The leading order wave speed is real and the first correction to wave speed is purely imaginary. Hence, the stability of GL interfacial mode is determined by $c_{gl}^{(1)}$. The underlined terms in the expression of $c_{gl}^{(1)}$ would be present for a clean liquid film, the term proportional to Ma appears because of the presence of surfactant monolayer, and the term proportional to GH represents the soft solid contribution. The expression of $c_{gl}^{(1)}$ clearly shows that soft solid layer has a stabilizing contribution (term proportional to GH) in addition to the stabilizing contribution of surfactant layer (term proportional to Ma). The leading order wave speed for Marangoni mode is also real ($c_{Ma}^{(0)} = 1$), and hence, the Marangoni mode is neutrally stable at this order. The first correction to wave speed is $c_{\mathrm{Ma}}^{(1)} = -\mathrm{i}Pe_{\mathrm{inv}}$. $c_{Ma}^{(1)}$ is purely imaginary, proportional to Pe_{inv} , and occurs with a negative sign which implies that this contribution is stabilizing. However, as noted in several previous studies (Blyth & Pozrikidis 2004*a*; Halpern & Frenkel 2003; Samanta 2014) the value of Pe_{inv} is usually negligible, and hence, we set $Pe_{\mathrm{inv}} = 0$. Subsequent analysis reveals that the third correction to wave speed determines the stability of Marangoni mode. The $c_{Ma}^{(2)}$ is also found to be real, and the expression for $c_{Ma}^{(3)}$ (with $Pe_{\mathrm{inv}} = 0$) is given as:

$$c_{\mathrm{Ma}}^{(3)} = \mathrm{i}\frac{Ma\Sigma_{\mathrm{gl}}\cot\theta}{2520}\left[420(3H+2)GH - (11Re + 420Ma\Sigma_{\mathrm{gl}} + 280\cot\theta)\right]. \tag{3.29}$$

The above expression of $c_{Ma}^{(3)}$ clearly shows that the term proportional to GH is destabilizing while all other terms are stabilizing at this order. This implies that for a given inclination, Re, Ma, and Σ_{gl}; this surfactant mode could be rendered unstable by manipulating the properties of soft solid layer (G and H). The above discussion suggests that the stability of contaminated liquid film flowing past a deformable inclined wall will be governed by the competition between the GL and Marangoni

mode instability. At this point, it is worth to comment about the appearance of any additional non-trivial contribution due to the use of non-linear neo-Hookean solid model as compared to the simple linear elastic solid model which is used in several previous studies related to the effect of deformable wall on the stability of fluid-fluid interfaces (Gaurav & Shankar 2007; Sahu & Shankar 2016; Shankar & Kumar 2004; Shankar & Sahu 2006). This issue is important because it is known that up to $O(k)$, the linearized neo-Hookean solid equations reduce to those for a linear elastic solid in low-wavenumber limit (Gaurav & Shankar 2007). However, the Marangoni mode instability is captured at $O(k^3)$ calculations, and thus, several additional contributions from neo-Hookean solid could be expected to be present in the low-k analysis. We have performed the low-k analysis using both neo-Hookean and linear elastic solid models, and observed that the low-k analysis remains identical for both the solid models for Marangoni mode up to $O(k^3)$. The exact details of the low-k analysis which show how the two solid models remain identical up to $O(k^3)$ calculations are presented in previous chapter. The numerical results presented in previous chapter using the two solid models also confirm the same. Briefly, the low-k analysis reveals that the velocity field in the fluid and the deformation field in the solid remain absent up to $O(k)$. The additional terms that appear at $O(k^2)$ or $O(k^3)$ due to the use of neo-Hookean constitutive relation involve solid variables at $O(1)$ or $O(k)$, and hence, these additional terms remain absent.

3.3.2 Numerical results

The expression of $c_{Ma}^{(3)}$ given in Eq. (3.29) clearly shows that for a given solid thickness H, the Marangoni mode becomes unstable when deformability parameter G increases above a critical value. The growth rate characteristics of this wall deformability induced Marangoni mode instability were presented in chapter 2 for $Re = 0$. We start by investigating the effect of Reynolds number on this Marangoni mode instability. Figure 3.2(a) shows the growth rate vs. wavenumber data as a function of Reynolds number for $H = 5, G = 0.05, Ma = 1, \theta = 45^\circ$ and $\Sigma_{gl} = 0.5$. For these values of parameters, the critical value of G above which the Marangoni mode becomes unstable is given by $c_{Ma}^{(3)} = 0$, which yields $G_{crit} = 0.01372 + 0.0003Re$. This implies that for $Re \sim O(1)$, the change in G_{crit} with variations in Re will be negligible. Thus, we set $G = 0.05$ in Figure 3.2(a) and varied

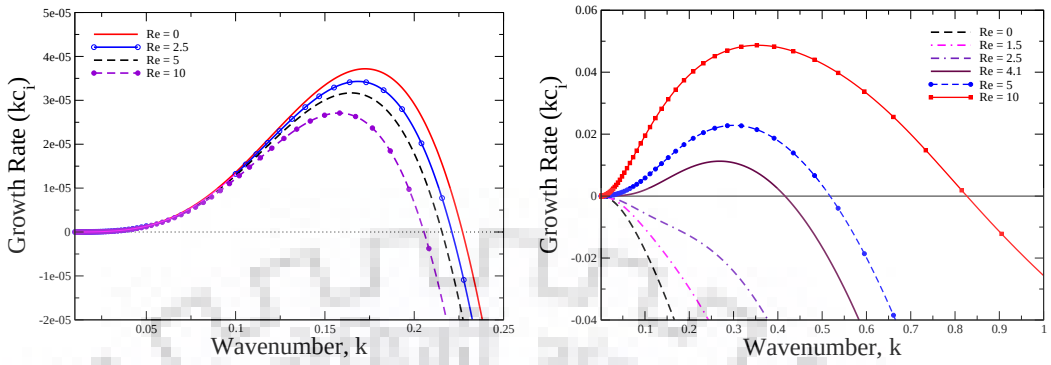

(a) Growth rate vs. k for Marangoni mode (b) Growth rate vs. k for GL mode

Figure 3.2: Growth rate vs. wavenumber data for different values of Reynolds number for (a) Marangoni mode and (b) GL mode. Data for $H = 5, G = 0.05, Ma = 1, Pe_{\text{inv}} = 0, \Sigma_{\text{gl}} = 0.5, \Sigma_{\text{ls}} = 0$, and $\theta = 45^\circ$.

Re from 0 to 10. Similar conclusion regarding the negligible change in growth rates of Marangoni mode with variations in *Re* can be drawn from the expression of $c_{Ma}^{(3)}$ in low-k limit for a given value of H and G. Figure 3.2(a) depicts the continuation of growth rates from low wavenumber values to finite and arbitrary wavenumbers as a function of *Re*. While there is visibly no significant variations in growth rates at low wavenumbers, the maximum growth rate that occurs at $k \sim O(0.1)$ decreases with increase in *Re* from 0 to 10. However, the more important observation is that the Marangoni mode still remains unstable at finite $Re \sim O(1-10)$. Figure 3.2(b) shows the growth rate for GL mode for different values of *Re* for the same set of parameters as taken for Figure 3.2(a). For these values of parameters, the expression of $c_{gl}^{(1)}$ in Eq. (3.28) shows that the GL mode becomes unstable when $Re > 4.06$ in low-k limit. Figure 3.2(b) clearly demonstrates that the GL mode remains stable for all wavenumbers from *Re* = 0 to 4. With further increase in *Re*, for example *Re* = 4.1 or higher, the GL mode becomes unstable and the maximum growth occurs at finite wavenumber. Thus, for $Re \geq 4.06$, both GL and Marangoni modes remain unstable. When both modes remain unstable, a comparison of growth rates of both GL and Marangoni mode reveals that the maximum growth rate of GL mode is two to three orders of magnitude larger than the Marangoni mode. Thus, for sufficiently higher values of *Re*, GL mode remains the most unstable mode. On the other hand, for lower values of *Re* in presence of soft solid layer and surfactant, the Marangoni

mode is the critical mode of instability. It is important to point out that the LS interfacial modes can also become unstable, however, the LS mode instability is usually observed at higher values of $G(\geq 0.1)$. We have verified using our spectral code, which resolves the complete spectrum of eigenvalues for a given number of Chebyshev polynomials, that for the range of parameters considered in Figure 3.2, GL and Marangoni mode are the two least stable or most unstable modes.

Figure 3.2 depicts the situation when either one or both the modes (GL and Marangoni) remain unstable. We next try to explore the parameter sets where all the modes remain stable. Let us focus our attention for the moment on the expression of $c_{gl}^{(1)}$. For $\theta = \pi/4, \Sigma_{\text{gl}} = 0.5, Re = 1.5$ and H and/or $G = 0$ (i.e. in absence of deformable solid layer), the expression of $c_{gl}^{(1)}$ gives the critical value of $Ma = 0.27$ above which the GL mode can be made stable (solely) due to the presence of surfactant layer. Thus, if we set Marangoni number below 0.27, the stabilizing effect due to surfactant is not sufficient enough to suppress GL mode instability. However, the expression of $c_{gl}^{(1)}$ shows that the presence of deformable solid layer provides an additional stabilizing contribution for GL interfacial mode. This expression shows that for given parameters and solid thickness, the GL mode instability is suppressed in low-k limit when G increases above a critical value. On the other hand, the low-k results for Marangoni mode shows that the Marangoni mode becomes unstable when G is sufficiently increased for a given solid thickness. Thus, a pertinent question is whether there exists a window in terms of parameter G where the system remains stable? The long-wave results suggest that it is indeed possible to choose appropriate values of H and G such that both Marangoni and GL mode simultaneously remain stable. For example, if we set $Re = 1.5, Ma = 0.25 (< Ma_{crit}|_{H=0} = 0.27), \Sigma_{\text{gl}} = 0.5, \theta = \pi/4$, and $H = 0$; the first correction to wave-speed is positive ($c_{gl}^{(1)} = 0.00833$), which implies that GL mode remains unstable for $H = 0$.

In presence of deformable solid layer with nondimensional thickness $H = 2$, the expression of $c_{gl}^{(1)}$ shows that the GL mode instability can be suppressed in low-k limit for $G > 0.00104$. Further, the expression of $c_{Ma}^{(3)}$ shows that the Marangoni mode becomes unstable when $G > 0.05$. This value of G above which Marangoni mode becomes unstable due to wall deformability is at least an order of magnitude higher than G value above which GL mode perturbations are stabilized in low-k

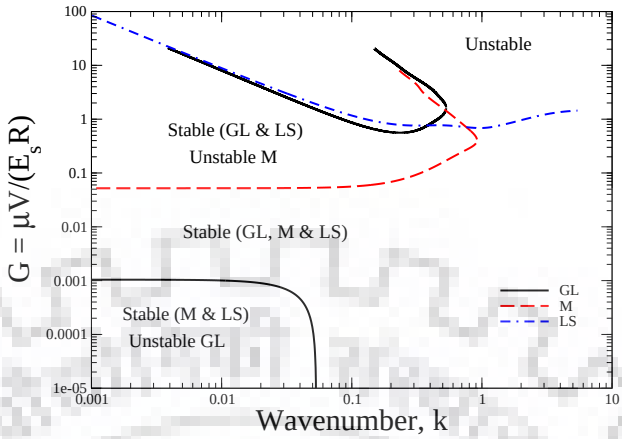

Figure 3.3: Neutral stability curves for showing stability window for $H = 2, Re = 1.5, Ma = 0.25, Pe_{\text{inv}} = 0, \Sigma_{\text{gl}} = 0.5, \Sigma_{\text{ls}} = 0, \theta = 45^{\circ}$.

limit. Thus, for low wavenumber disturbances, there exists a sufficient gap in terms of parameter G where GL mode perturbations are suppressed without exciting the Marangoni mode instability. Further, the LS interface can also become unstable for finite wavenumber perturbations with increase in wall deformability parameter. Keeping in view of all the above aspects (i.e. GL, Marangoni, and LS modes instabilities), we construct the neutral stability curves in G vs. k plane to explore the regions where the film flow configuration remains stable.

Figure 3.3 presents the neutral stability diagram for $H = 2, Re = 1.5$, and $Ma = 0.25$. In agreement with the discussion above, the GL interface remains unstable for $Ma = 0.25$ in the rigid wall limit $(G \to 0)$. As wall deformability parameter G increases above the lower neutral curve, there is a transition from unstable GL mode perturbations to stable GL perturbations. With further increase in G, we encounter a second neutral curve corresponding to the destabilization of Marangoni mode due to the presence of soft solid layer. There exist two more neutral curves above this Marangoni mode curve showing the destabilization of GL and LS interfaces at sufficiently higher values of G. The destabilization of GL mode (or interfacial mode in general) at higher values of G had been reported in several previous studies (Gaurav & Shankar 2007, 2010*a*; Jiang & Lin 2005; Shankar & Kumar 2004; Shankar & Sahu 2006). The destabilization of LS interface when the solid becomes sufficiently soft had also been investigated extensively in last two decades, see, for example,

two recent reviews by Kumaran (2015) and Shankar (2015) . More importantly, this figure shows that there exists a sufficient gap between the lower GL mode neutral curve and the Marangoni mode neutral curve where all interfacial modes (GL and LS), and Marangoni mode remain stable. Thus, Figure 3.3 demonstrates that it is possible to achieve a stable flow configuration by suitably selecting wall deformability parameter G when the surfactant layer does not provide sufficient stabilizing contribution. We have ensured by using our spectral code that all the eigenvalues remain stable with in the stability window observed in Figure 3.3.

Figure 3.4(a) shows the effect of varying solid thickness on the width of stable gap for the same set of parameters as used in Figure 3.3. Our results in terms of G vs. k neutral curves for a wide variety of parameters suggest that the width of stable region is determined by the lower GL and Marangoni mode neutral curves. Hence, we have not presented neutral curves corresponding to destabilization of GL and LS modes in Figure 3.4 (as well in all the figures given later in this work). Figure 3.4(a) demonstrates that the stable gap is present for higher values of H as well. A comparison of the data presented in Figure 3.3 and Figure 3.4(a) shows that the width of stable region decreases with increase in value of solid thickness. For example, the critical value of G above which GL mode becomes stable (while all other modes remain stable) is 0.00104 for $H = 2$ (See Figure 3.3). The critical value of G for Marangoni mode neutral curve is 0.052 and we have already shown that all modes remain stable in between these two values (i.e., G_{crit} for GL mode stability and G_{crit} for the Marangoni mode destabilization). Thus, the gap ratio for which the system remains stable for $H = 2$ from Figure 3.3 is $0.052/0.00104 \approx 50$. This gap ratio reduces to around 23 for $H = 5$ and to approximately 12 for $H = 10$ (refer Figure 3.4(a)). This implies that the width of stability window decreases on increasing the solid thickness.

Figure 3.4(b) shows the neutral curves for two values of solid thickness when Ma is decreased from 0.25 (in Figure 3.4(a) or Figure 3.3) to 0.2. A comparison of gap ratios for $H = 2$ and $H = 5$ again verifies that the width of stability window decreases with increase in solid thickness. Further, the stable region for $Ma = 0.2$ is smaller than for $Ma = 0.25$ for the same value of solid thickness. For example, as mentioned above in reference to Figure 3.3, the stable gap ratio for $H = 2$ and $Ma = 0.25$ is approximately 50. On the other hand, when $Ma = 0.2$ and $H = 2$,

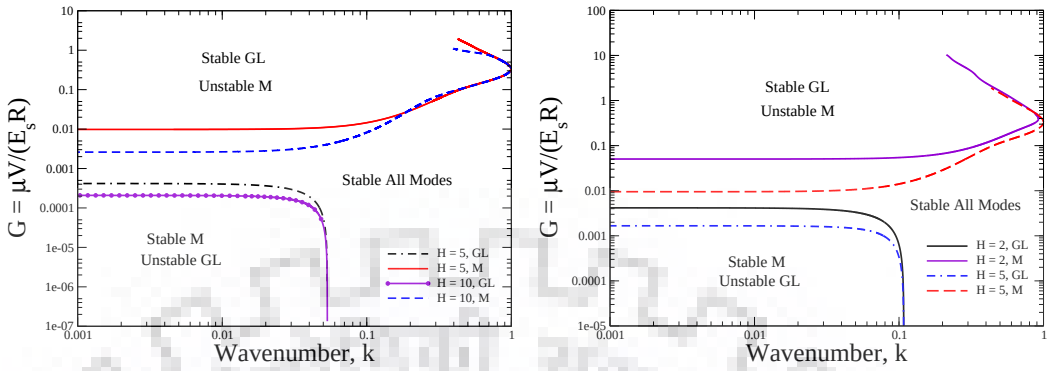

(a) $Ma = 0.25, H = 5$ and 10 (b) $Ma = 0.2, H = 2$ and 5

Figure 3.4: Neutral stability curves for for $Re = 1.5, Pe_{\text{inv}} = 0, \Sigma_{\text{gl}} = 0.5, \Sigma_{\text{ls}} = 0$, and $\theta = 45^{\circ}$.

Figure 3.4(b) shows that the gap ratio is reduced to 12. The significant reduction in width of stable region occurs mainly because of smaller stabilizing contribution of surfactant at lower values of Marangoni number. This results in increase of critical value of G required to stabilize GL interface while the critical G required to destabilize Marangoni mode is marginally affected. This can be verified from Figure 3.4 which shows that for $H = 5$, the $G_{crit} \approx 0.0017$ for stabilizing GL interface with $Ma = 0.2$, and $G_{crit} \approx 0.00042$ for $Ma = 0.25$. Thus, there is a substantial increase in the critical value of deformability parameter for lower GL mode neutral curve with decrease in Marangoni number. On the other hand, the G_{crit} for Marangoni mode neutral curve is only slightly altered from 0.0095 for $Ma = 0.2$ to 0.0098 for $Ma = 0.25$. It is worth to point out that both Figure 3.3 and Figure 3.4 demonstrate that the critical values of G for lower GL mode neutral curve and Marangoni mode neutral curve (both of which collectively determine the stability window) can be obtained from the low-k expressions of $c_{gl}^{(1)}$ and $c_{Ma}^{(3)}$, respectively. Thus, we can comment about the stability window for a given set of parameter values by simply examining low-wavenumber results.

For further decrease in the value of Marangoni number to 0.1 with same parameters as in Figure 3.4, the critical value of G for lower GL and Marangoni mode neutral curves are reported in Table 3.1 for different values of solid thickness. Table 3.1 clearly shows that the width of stability window is relatively small for $H = 2$ (as compared to width of stable gap for $H = 2$, and $Ma = 0.2$ or 0.25), and decreases

Table 3.1: Critical value of G for lower GL mode and Marangoni mode neutral curves for $Re = 1.5, Ma = 0.1, Pe_{\text{inv}} = 0, \Sigma_{\text{gl}} = 0.5, \Sigma_{\text{ls}} = 0$ and $\theta = 45^\circ$.

H	G_{crit} for GL mode	G_{crit} for Marangoni mode	Gap ratio = $(G_{Ma}/G_{GL})_{crit}$
2	0.0104	0.0472	4.53
5	0.0042	0.0089	2.12
10	0.00208	0.00236	1.13
15	0.00139	0.00107	0.77

with increase in solid thickness. In fact, for $H = 10$, the two critical values which determine the stable gap are very close to each other and for $H = 15$, the stability window vanishes as evident by gap ratio value less than unity. Recall that for parameters used in above figures and Table 3.1, the critical Marangoni number in absence of deformable solid layer ($H = 0$ and/or $G = 0$) for making GL mode stable is given as $Ma_{crit}|_{H=0} = 0.27$. The results presented above in terms of neutral stability diagrams and Table 3.1 demonstrate the potential of deformable solid layer in obtaining stable flow configuration for values of $Ma < Ma_{crit}|_{H=0}$. However, as Marangoni number decreases sufficiently below $Ma_{crit}|_{H=0}$, the stability window becomes smaller and finally vanishes for higher values of solid thickness.

The results presented above demonstrated the possibility of using a soft solid layer to obtain stable flow configuration when the stabilizing effect of surfactant is not sufficient enough in rigid limit. Next, we present results when $Ma > Ma_{crit}|_{H=0}$ for which the liquid film falling down a rigid incline remains stable due to sufficient stabilizing contribution of surfactant monolayer. Figure 3.5 presents neutral stability curves for $Ma = 1 (> Ma_{crit}|_{H=0})$ for three different values of solid thickness to elucidate the role of wall deformability in this case. The neutral curves corresponding to all the modes are shown for $H = 2$, while for $H = 5$ and 10, only the most unstable Marangoni mode is depicted in Figure 3.5. Since, the GL interface remains stable at first place in rigid limit for $Ma = 1$, the lower GL mode neutral curve remains absent for any value of solid thickness. As the value of G increases, the Marangoni mode becomes unstable first followed by destabilization of GL and LS

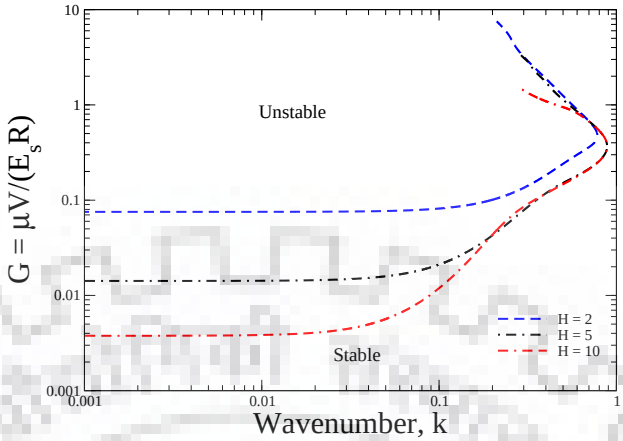

Figure 3.5: Neutral stability curves for the case when surfactant contribution is sufficient for suppressing GL mode instability. Data for three different values of $Re = 1.5, Ma = 1, Pe_{inv} = 0, \Sigma_{gl} = 0.5, \Sigma_{ls} = 0$, and $\theta = 45^{\circ}$.

modes at sufficiently higher values of wall deformability parameter G. As expected, the critical value of G above which Marangoni mode becomes unstable decreases with increase in solid thickness. Thus, the system which remains stable in rigid limit can be rendered unstable by using a deformable solid layer. Such a feature could be possibly utilized in applications which demand high heat and mass transfer rates.

Figure 3.6 shows the effect of surface tension (Σ_{gl}) on the neutral stability curves for the data $Re = 1.5, H = 2, Ma = 1, Pe_{inv} = 0, \Sigma_{ls} = 0$, and $\theta = 45^{\circ}$. The surface tension (Σ_{gl}) shows the stabilizing effect on both, gas-liquid and Marangoni mode in longwave which can be shown by the analytical expression $G_c = 0.01667 - 0.125\Sigma_{gl}$ for GL mode and $G_c = 0.04412 + 0.0625\Sigma_{gl}$ for Marangoni mode respectively for above given data (in figure 3.6). If this longwave results are extended numerically upto finite wave then we also find a stabilizing effect of Σ_{gl} on both mode. Our results form analytical solution are equivalent to the results which we obtained from numerical solution (see figure 3.6) that is why it is clear from both the analysis that the critical value of G is increased for the Marangoni mode and is decreased for the GL mode (see table 3.2 for analytical and figure 3.6 for numerical solutions), as a result, stable gap or window exist between them. The stable gap (stability window) or gap ratio is increased with increasing the value of Σ_{gl} (see table 3.2) and lower neutral curve of GL mode fade out at $\Sigma_{gl} = 0.5$ so the system becomes

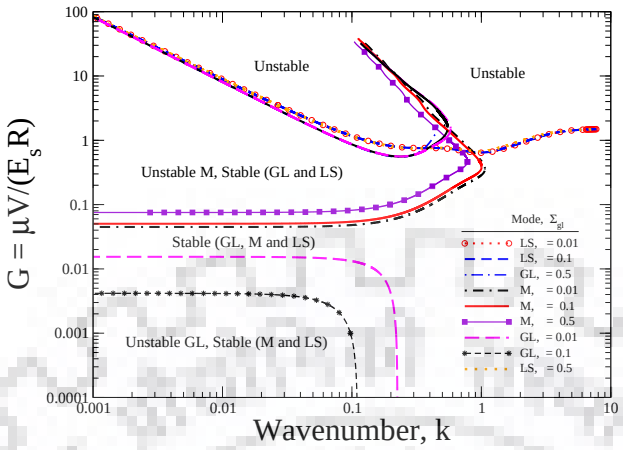

Figure 3.6: Neutral stability curves for the data: $Re = 1.5, H = 2, Ma = 1, Pe_{\text{inv}} = 0, \Sigma_{\text{ls}} = 0$, and $\theta = 45^{\circ}$.

Table 3.2: Critical value of G for lower GL mode and Marangoni mode neutral curves for $Re = 1.5, H = 2, Ma = 1, Pe_{\text{inv}} = 0, \Sigma_{\text{ls}} = 0$ and $\theta = 45^{\circ}$.

Σ_{gl}	G_{crit} for GL mode	G_{crit} for Marangoni mode	Gap ratio = $(G_{Ma}/G_{GL})_{crit}$
0.01	0.014434	0.04405	3.0518
0.1	0.00418	0.049731	11.869
0.5	disappear	finite	—

completely stable for $G_c < 0.05$. Here, it is predicted that the surface tension (Σ_{gl}) shows a stabilizing effect on both the mode (GL and Marangoni) but LS mode remains unaltered.

Figure 3.7 shows the effect of inverse of Peclet number on the neutral stability curves for the data $Re = 1.5, H = 2, Ma = 1, \Sigma_{\text{gl}} = 0.1, \Sigma_{\text{ls}} = 0$. The neutral stability curves of GL and LS mode remains unaltered by varying the value of inverse of Peclet number. On the other hand, if we increase the value of Pe_{inv} then the value of deformability parameter G is increased and Marangoni mode curve shifts upward, as a result, unstable $G-k$ region is decreased. At a certain value of Pe_{inv} Marangoni mode curve forms a loop and the unstable region reduces drastically, if we further increase the value of Pe_{inv} then above a certain value (or critical value),

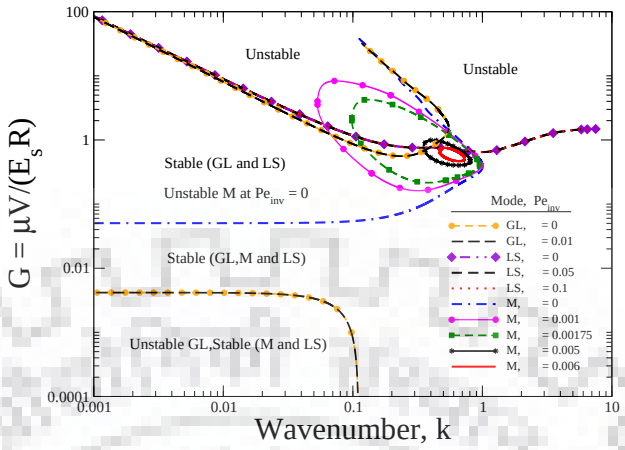

Figure 3.7: Neutral stability curves data for different values of Pe_{inv} : $Re = 1.5, H = 2, Ma = 1, \Sigma_{\text{gl}} = 0.1, \Sigma_{\text{ls}} = 0$.

the Marangoni mode curve is disappeared. As a result, the stability window is increases where the flow system becomes completely stable with increasing the value of P_{inv}. Note that the higher values of Pe_{inv} are not useful for experimental purpose.

Figure 3.8(a) shows the effect of angle of inclination (θ) on the GL mode for the data $Re = 1.5, H = 2, Pe_{\text{inv}} = 0, \Sigma_{\text{gl}} = 0.1, \Sigma_{\text{ls}} = 0$. For the low values of deformability parameter (G), the GL mode is unstable for all the angles of inclination (θ) which are given in the figure in long and finite wave limit but it (GL mode) is completely stable for the low value of angle of inclination ($\theta = 30^\circ$). For $\theta = 45^\circ$ and 60°, the transition from unstable to stable flow occurs at G_c = 0.004 and 0.038 respectively for GL mode. Here, it is clear that the critical G is increased with the angle of inclination of the plane (θ), as a result, destabilization of GL mode occurs. Figure 3.8(b) shows the effect of angle (θ) on the neutral stability curves of Marangoni mode for the same datas as given in Figure 3.8(a). The Marangoni mode is completely stable at low values of deformability parameter but the destabilization occurs when the value of angle (θ) is increased (critical value of G is decreased with increasing the agnle (θ), as a result, unstable $G-k$ region is decreased) for low and finite wave number. At $\theta = 45^\circ$, the critical value of deformability parameter (G_c) for GL and Marangoni mode is 0.004 and 0.05 respectively then the gap ratio will be $\approx$12.5. At $\theta = 60^\circ$, the G_c for GL and Marangoni mode is 0.0388 and 0.0322 then the gap ratio will be $\approx$ 0.83. Here, it is clear that the value of gap ratio ($\sim$ stability window) is

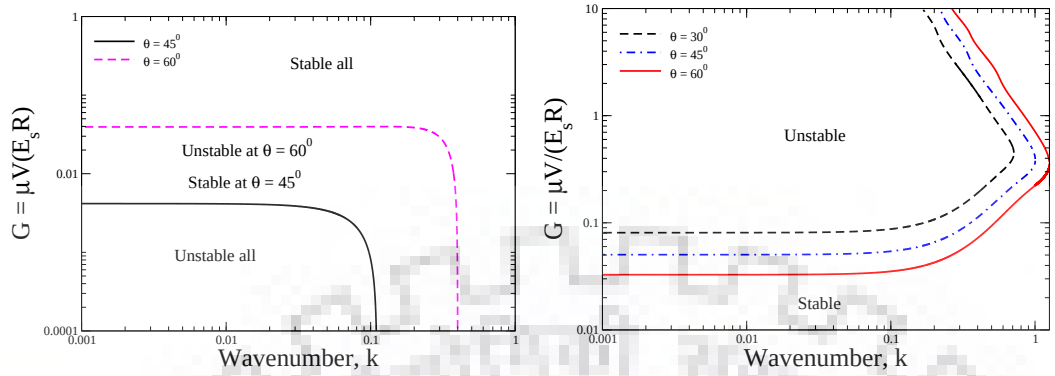

(a) GL mode (b) Marangoni mode

Figure 3.8: Neutral stability curves for the data: $Re = 1.5, H = 2, Pe_{\text{inv}} = 0, \Sigma_{\text{gl}} = 0.1, \Sigma_{\text{ls}} = 0$.

decreased with increasing the angle (θ) and this window is disappeared completely with further increasing the angle of inclination of a plane. Thus the angle (θ) shows the destabilizing effect on both the modes (GL and Marangoni), as a results, stability window is decreased. Here, it can be predicted that the decreasing the angle of inclination of a plane (θ) is in favour to achieve a stable flow configuration where the flow remains completely stable.

3.4 Conclusions

The linear stability of surfactant-laden liquid film flowing down an inclined plane coated with a deformable solid layer is analyzed using an Orr-Sommerfeld type formulation. Previous studies have demonstrated the suppression of free surface instability for the flow of a clean liquid film by employing a soft solid layer. The primary aim of the work of this chapter is to re-examine the potential of soft solid layer in suppressing the free surface instability for a surfactant loaded liquid film without triggering any other modes of instabilities. The concern regarding the excitation of other modes of instabilities arise mainly because of recently observed destabilization of Marangoni mode due to wall deformability for the same flow configuration as considered in the chapter 2. Further, the liquid-solid interface can also become unstable on increasing wall deformability parameter for a diverse class of flow con-

figurations (Shankar 2015). In addition to all the above mentioned aspects, it is well known that the presence of surfactant suppresses the free surface instability when Marangoni number increases above a critical value for film flow past a rigid incline (Blyth & Pozrikidis 2004*a*). However, in several physical situations, it is quite possible that the Marangoni number remains below this critical value and hence, a complete suppression of free surface instability is not possible for flow past rigid inclined surfaces. For such cases (i.e .when $Ma < Ma_{crit}$), we have demonstrated that it is indeed possible to obtain stable flow by employing a soft solid layer. The neutral stability curves in G vs. k plane demonstrate that for a given solid thickness, there exists a sufficient window in terms of wall deformability parameter G where the free surface instability is suppressed without triggering any other mode of instability. The width of stability window decreases with increase in solid thickness primarily due to destabilization of Marangoni mode at lower values of G. For a given Reynolds number, the width of stability window also decreases with decrease in Marangoni number and when the Marangoni number is sufficiently decreased below the critical value, the stable gap vanishes. For cases when Marangoni number is above the critical value required for stabilization of gas-liquid mode in rigid limit (i.e. the GL mode remains stable in first place), the deformable solid coating can render the flow unstable when G increases above a threshold value to destabilize the Marangoni mode. This feature could be potentially useful for increasing heat and mass transfer rates by manipulating the solid coating properties without changing any other parameter like Reynolds number.

Finally, we provide some typical estimates for the physical parameters where the predicted suppression can be observed in experiments. The Marangoni number varies between $O \sim (0.01 - 10)$ for low to sufficiently high values of surfactant concentration. We set $Ma \sim O(0.1)$ as most of our results concerning instability suppression are presented for this range of Marangoni numbers. Figure 3.4 shows the neutral stability data for $Re \sim O(1)$, and G remains $\sim O(0.001)$ within the stable gap. If we set $\rho \sim 10^3 kg/m^3$, $R \sim 10^{-3}$m, $\mu \sim 0.01$ Pa-s and $\sigma \sim 0.01$ N/m, then $Re \sim O(1)$ and $\Sigma_{gl} \sim O(1)$. For these values, $G \sim 0.001$ implies that the shear modulus of solid layer $E_s \sim 10^4$ Pa to obtain stable flow of surfactant-laden liquid film down a flexible inclined plane.

Chapter 4

Conclusion

We examined the linear stability of liquid film flowing down an inclined plane in presence of monolayer of insoluble surfactant at free surface when the inclined plane is coated with an incompressible and impermeable deformable neo-Hookean solid layer for creeping flow and finite *Re* limit. In this analysis, we assumed that the (i) base flow is steady state, fully developed and unidirectional (ii) fluid is Newtonian and incompressible. In creeping flow limit, we focus on the effect of various parameters (soft solid thickness as well as deformability of a solid) on the surfactant-induced Marangoni mode. The Marangoni and GL mode remain stable for the gravity-driven contaminated liquid film flowing down an inclined rigid plane in creeping (or $Re \sim 0$) flow limit (Blyth & Pozrikidis 2004*a*). If the rigid plane is coated with a neo-Hookean solid layer then Marangoni mode is destabilized when the deformability parameter increases above its critical value for a fixed value of soft solid thickness. In context of soft solid, we find that the critical value of deformability parameter G required for triggering the Marangoni mode instability is decreased with increasing in soft solid thickness. There is also an existence of an optimum solid thickness for fixed value of G for which unstable growth rate of surfactant (or Marangoni) mode is obtained maximum. Here, deformability parameter G shows an additional stabilizing effect on the GL mode perturbations in the creeping flow ($Re \sim 0$) limit. LS mode also becomes unstable above a critical value of G(at high wavenumber) which is higher than a critical values of G required for triggering Marangoni mode instability. In this case, we find that the Marangoni mode is a dominating mode for a surfactant-laden liquid layer flowing down an inclined

plane in creeping flow limit. Here, Marangoni mode becomes unstable due to sufficiently increase in deformability of a solid even when gas-liquid mode remians stable.

We extended our above discussed creeping flow problem to finite *Re* and observed the tremendous effect of various parameters on the flow system (importantly on the stability window where flow remains completely stable). For creeping flow, we have investigated that the Marangoni mode is destabilized when rigid plane is coated with a soft solid and such type of Marangoni mode instabilities are suppressed upto an optimum value by increasing the Marangoni number (see chapter 2). In this study, We re-investigated the potential of deformable solid layer to suppress the free surface instabilities for insoluble surfactant loaded liquid film flowing down an inclined deformable solid surface without triggering any other modes of instabilities. In this study , LS mode also remains unstable at higher value of G for high wavenumber but the stability of GL and Marangoni modes are affected greatly by altering the various parameters. The free surface instabilities can be suppressed by increasing the Marangoni number beyond a critical values as it is shown in previous studies (Blyth & Pozrikidis 2004*a*). On the other hand, in many physical cases, when the Marangoni number remains below its critical value then it is not possible to suppress the free surface instabilities completely for the contaminated Newtonian liquid layer (film) flowing down an inclined rigid plane. For this type of case, we used a soft solid and have shown the stabilizing effect of soft solid layer on the free surface instabilities to a sets of parameters where flow remains completely stable. We have demonstrated stabilizing effect of soft solid on the free surface instabilities by using a new parameter that is known as gap ratio $(G_{Ma}/G_{GL})_{crit}$. Here, we find that the gap ratio is decreased with increasing in solid thickness H (see G vs. k curves) however stability window exist. This stability gap also shows that the critical value of G for both, Marangoni and GL modes is decreased. As a result, Marangoni mode is destabilized but free surafce (or GL) mode is stabilized. This stability window (or gap ratio) is also decreased with decreasing the Marangoni number but it is vanished when the Marangoni number is decreased below its critical value. The destabilization of Marangoni mode due to presence of soft solid coating can be used to enhance heat and mass transfer rate without changing many parameters except soft solid properties like deformability, thickness etc.

References

ADEPU, J. & SHANKAR, V. 2007 Suppression or enhancement of interfacial instability in two-layer plane couette flow of fene-p fluids past a deformable solid layer. *J. Non-Newtonian Fluid Mech.* **141**, 43–58.

ANJALAIAH & USHA, R. 2015 Effects of velocity slip on the inertialess instability of a contaminated two-layer film flow. *Acta Mechanica* **226** (9), 3111–3132.

ANJALAIAH, USHA, R. & MILLET, S. 2013 Thin film flow down a porous substrate in the presence of an insoluble surfactant: Stability analysis. *Phy. Fluids* **25** (2), 022101 (1–26).

ANSHUS, BRYON. E. & ACRIVOS, A. 1967 The effect of surface active agents on the stability characteristics of falling liquid films. *Chem. Eng. Sci.* **22** (3), 389–393.

BANDARU, P. & KUMARAN, V. 2016 Ultra-fast microfluidic mixing by soft-wall turbulence. *Chem. Eng. Sci.* **149**, 156–168.

BANDYOPADHYAY, D., SHARMA, A. & SHANKAR, V. 2008 Instabilities and pattern miniaturization in confined and free elastic-viscous bilayers. *J. Chem. Phys.* **128**, 154909.

BASSOM, A. P., BLYTH, M. G. & PAPAGEORGIOU, D. T. 2012 Using surfactants to stabilize two-phase pipe flows of core-annular type. *J. Fluid Mech.* **704**, 333–359.

BEATTY, M. F. & ZHOU, Z. 1991 Universal motion for a class of viscoelastic materials of differential type. *Continuum Mech. Thermodyn.* **3**, 169–191.

BENJAMIN, T. B. 1957 Wave formation in laminar flow down an inclined plane. *J. Fluid Mech.* **2**, 554–574.

BLYTH, M. G. & BASSOM, A. P. 2013 Stability of surfactant-laden core-annular flow and rod-annular flow to non-axisymmetric modes. *J. Fluid Mech.* **716**, 716 R13–12.

BLYTH, M. G. & POZRIKIDIS, C. 2004*a* Effect of surfactant on the stability of flow down an inclined plane. *J. Fluid Mech.* **521**, 241–250.

BLYTH, M. G. & POZRIKIDIS, C. 2004*b* Effect of surfactants on the stability of two-layer channel flow. *J. Fluid Mech.* **505**, 59–86.

BOYD, J. P. 1999 *Chebyshev and Fourier Spectral Methods*, 2nd edn. Springer-Verlag.

CARVALHO, M. S. & SCRIVEN, L. E. 1997 Deformable roll coating flows: steady state and linear perturbation analysis. *J. Fluid Mech.* **339**, 143–172.

CASSIDY, K. J., HALPERN, D., RESSLER, B. G. & GROTBERG, J. B. 1999 Surfactant effects in model airway closure experiments. *Journal of Applied Physiology* **87**, 415–427.

CHANG, H.-C. & DEMEKHIN, E. A. 2002 *Complex Wave Dynamics on Thin Films*. Amsterdam: Elsevier.

CHATTOPADHYAY, GEETANJALI & USHA, R. 2016 On the yih–marangoni instability of a two-phase plane poiseuille flow in a hydrophobic channel. *Chem. Engg. Sc.* **145**, 214–232.

CHEN, K. P. 1993 Wave formation in the gravity-driven low-Reynolds number flow of two liquid films down an inclined plane. *Phys. Fluids A* **5** (12), 3038–3048.

CRASTER, R. V. & MATAR, O. K. 2009 Dynamics and stability of thin liquid films. *Rev. Mod. Phys.* **81**, 1131–1198.

DEMEKHIN, E. A., KALLIADASIS, S. & VELARDE, M. G. 2006 Suppressing falling film instabilities by Marangoni forces. *Phys. Fluids* **18**, 042111 (1–16).

DESTRADE, M. & SACCOCMANDI, G. 2004 Finite–amplitude inhomogeneous waves in Mooney–Rivlin viscoelastic solids. *Wave Motion* **40**, 251–262.

DRAZIN, P.G. & REID, W.H. 1981 *Hydrodynamic Stability*. Cambridge: Cambridge University Press.

EGGERT, M. D. & KUMAR, S. 2004 Observations of instability, hysterisis, and oscillation in low-Reynolds number flow past polymer gels. *J. Colloid Interface Sci.* **274**, 234–242.

FOSDICK, R. L. & YU, J. H. 1996 Thermodynamics, stability and non–linear oscillations of viscoelastic solids – I. Differential type solids of second grade. *Int. J. Non–Linear Mech.* **31**, 495–516.

FRENKEL, A. L. & HALPERN, D. 2002 Stokes-flow instability due to interfacial surfactant. *Phys. Fluids* **14**, L45–L48.

GAO, P. & LU, X. 2007 Effect of surfactants on the inertialess instability of a two-layer film flow. *J. Fluid Mech.* **591**, 495–507.

GAUGLITZ, P.A & RADKE, C .J. 1988 An extended evolution equation for liquid film breakup in cylindrical cappilaries. *Chemical Engineering Science* **43**, 1457–1465.

GAURAV & SHANKAR, V. 2007 Stability of gravity-driven free-surface flow past a deformable solid layer at zero and finite Reynolds number. *Phys. Fluids* **19**, 024105.

GAURAV & SHANKAR, V. 2009 Stability of fluid flow through deformable neo-Hookean tubes. *J. Fluid Mech.* **627**, 291–322.

GAURAV & SHANKAR, V. 2010*a* Role of wall deformability on interfacial instabilities in gravity-driven two-layer flow with a free surface. *Phys. Fluids* **22**, 094103.

GAURAV & SHANKAR, V. 2010*b* Stability of pressure-driven flow in a deformable neo-Hookean channel. *J. Fluid Mech.* **659**, 318–350.

GAURAV & SHANKAR, V. 2013 Manipulation of instabilities in core-annular flows using a deformable solid layer. *Phys. Fluids* **25**, 014104.

GAURAV & SHANKAR, V. 2015 Manipulation of interfacial instabilities by using a soft, deformable solid layer. *Sadhana* **40** (3), 1033–1048.

GKANIS, V. & KUMAR, S. 2003 Instability of creeping Couette flow past a neo-Hookean solid. *Phys. Fluids* **15**, 2864–2471.

GKANIS, V. & KUMAR, S. 2005 Stabilty of pressure-driven creeping flows in channels lined with a nonlinear elastic solid. *J. Fluid Mech.* **524**, 357–375.

GKANIS, V. & KUMAR, S. 2006 Instability of gravity-driven free-surface flow past a deformable elastic solid. *Phys. Fluids* **18**, 044103.

GOERKE, J. 1998 Pulmonary surfactant: functions and molecular composition. *Biochimica et Biophysica Acta (BBA) - Molecular Basis of Disease* **1408** (23), 79 – 89.

GOREN, S. L. 1961 The instability of an annular liquid thread. *J. Fluid Mech.* **12**, 309–319.

GROTBERG, J. B. & JENSEN, O. E. 2004 Biofluid mechanics in flexible tubes. *Ann. Rev. Fluid Mech.* **36**, 121–147.

GAD-EL HAK, M. 2003 Drag reduction using compliant walls. In *IUTAM symposium on flow past highly compliant boundaries and in collapsible tubes* (ed. P. W. Carpenter & T. J. Pedley), chap. 9, pp. 191–229. The Netherlands: Kluwer Academic.

HALPERN, DAVID & FRENKEL, ALEXANDER L 2003 Destabilization of a creeping flow by interfacial surfactant: linear theory extended to all wavenumbers. *Journal of Fluid Mechanics* **485**, 191–220.

HALPERN, D & GROTBERG, JB 1993 Surfactant effects on fluid-elastic instabilities of liquid-lined flexible tubes: a model of airway closure. *J. Biomech Eng.* **115** (3), 271–277.

HALPERN, D. & GROTBERG, J. B. 1992 Fluid-elastic instabilities of liquid-lined flexible tubes. *J. Fluid Mech.* **244**, 615–632.

HAMMOND, P. S. 1983 Nonlinear adjustment of a thin annular film of viscous fluid surrounding a thread of another within a circular cylindrical pipe. *J. Fluid Mech.* **137**, 363–384.

HAYES, M. A. & SACCOCMANDI, G. 2002 Finite–amplitude waves superimposed on pseudoplanar motions for Mooney–Rivlin viscoelastic solids. *Non Linear Mechanics* **37**, 1139–1146.

HOLZAPFEL, G. A. 2000 *Nonlinear Solid Mechanics*. Chichester, UK: John Wiley.

JAIN, A. & SHANKAR, V. 2007 Instability suppression in viscoelastic film flows down an inclined plane lined with a deformable solid layer. *Phys. Rev. E* **76**, 046314 (1–14).

JAIN, A. & SHANKAR, V. 2008 Elastohydrodynamic suppression of free-surface instabilities in annular liquid film flow outside wires and inside tubes,. *Ind. Engg. Chem. Res.* **47**, 6473–6485.

JI, WEI & SETTERWALL, FREDRIK 1994 On the instabilities of vertical falling liquid films in the presence of surface-active solute. *J. Fluid Mech.* **278**, 297–323.

JIANG, W. Y. & LIN, S. P. 2005 Enhancement or suppression of instability in a two-layered liquid film flow. *Phys. Fluids* **17**, 054105.

JOSEPH, D.D. & RENARDY, Y.Y. 1993*a* *Fundamentals of Two-Fluid Dynamics : Part 1, Mathematical Theory and Applications*. New York: Springer-Verlag.

JOSEPH, D.D. & RENARDY, Y.Y. 1993*b* *Fundamentals of Two-Fluid Dynamics : Part 2, Lubricated Transport, Drops and Miscible Liquids*. New York: Springer-Verlag.

KARAPETSAS, G. & BONTOZOGLOU, V. 2013 The primary instability of falling films in the presence of soluble surfactants. *J. Fluid Mech.* **729**, 123–150.

KUMARAN, V. 1995 Stability of the viscous flow of a fluid through a flexible tube. *J. Fluid Mech.* **294**, 259–281.

KUMARAN, V. 2000 Classification of instabilities in flow past flexible surfaces. *Current Sci.* **79**, 766–773.

KUMARAN, V. 2003 Hydrodynamic stability of flow through compliant channels and tubes. In *IUTAM symposium on flow past highly compliant boundaries and in collapsible tubes* (ed. P. W. Carpenter & T. J. Pedley), chap. 5, pp. 95–118. The Netherlands: Kluwer Academic.

KUMARAN, V. 2015 Experimental studies on the flow through soft tubes and channels. *Sadhana* **40** (3), 911–923.

KUMARAN, V., FREDRICKSON, G. H. & PINCUS, P. 1994 Flow induced instability of the interface between a fluid and a gel at low Reynolds number. *J. Phys. II France.* **4**, 893–904.

KUMARAN, V. & MURALIKRISHNAN, R. 2000 Spontaneous growth of fluctuations in the viscous flow of a fluid past a soft interface. *Phys. Rev. Lett.* **84**, 3310–3313.

KWAK, S. & POZRIKIDIS, C. 2001 Effect of surfactants on the instability of a liquid thread or annular layer part i: Quiescent fluids. *Int. J. of Multiphase Flow* **27**, 1–37.

LIN, S. P. 1967 Instability of liquid film flowing down an inclined plane. *Phys. Fluids* **10**, 308.

LIN, S. P. 1970 Stabilizing effects of surface-active agents on a film flow. *AIChE* **16** (3), 375–379.

LIN, S. P. & CHEN, J. N. 1997 Elimination of three-dimensional waves in a film flow. *Phys. Fluids* **9**, 3926–3928.

LIN, S. P., CHEN, J. N. & WOODS, D. R. 1996 Suppression of instability in a liquid film flow. *Phys. Fluids* **8**, 3247–3252.

MACOSKO, C.W. 1994 *Rheology: Principles, Measurements, and Applications*. New York: VCH.

MAJUMDER, A., TIWARI A.K. KORADA K. & GHATAK, A. 2010 Microchannel induced surface bulging of a soft elastomeric layer. *Journal of Adhesion Science and Technology* **24**, 26812692.

MALVERN, L. E. 1969 *Introduction to the Mechanics of a Continuous Medium*. Englewood Cliffs, NJ: Prentice-Hall.

MATAR, O. K., CRASTER, R. V. & KUMAR, S. 2007 Falling films on flexible inclines. *Phys. Rev. E* **76**, 056301 (1–17).

MATAR, O. K. & KUMAR, S. 2004 Rupture of a surfactant-sovered thin liquid film on a flexible wall. *SIAM J. Appl. Math.* **64** (6), 2144–2166.

MORROW, N. R. & MASON, G. 2001 Recovery of oil by spontaneous imbibition. *Current Opinion in Colloid and Interface Science* **6**, 321 – 337.

MUKHERJEE, R & SHARMA, A. 2015 Instability, self-organization and pattern formation in thin soft films. *Soft Matter* **11**, 8717–8740.

NEELAMEGAM, R., GIRIBABU, D. & SHANKAR, V. 2014 Instability of viscous flow over a deformable two-layered gel: Experiments and theory. *Phys. Rev. E* **90**, 043004 (1–13).

NEELAMEGAM, R. & SHANKAR, V. 2015 Experimental study of the instability of laminar flow in a tube with deformable walls. *Phys. Fluids* **27**, 024102 (1–18).

PATNE, R., GIRIBABU, D. & SHANKAR, V. 2017 Consistent formulations for stability of fluid flow through deformable channels and tubes. *J. Fluid Mech.* **827**, 31–66.

PENG, J., JIANG, L. Y., ZHUGE, W. L. & ZHANG, Y. J. 2016 Falling film on a flexible wall in the presence of insoluble surfactant. *J. Eng. Math.* **97**, 33–48.

PENG, JIE, ZHANG, YANG-JUN & ZHUGE, WEI-LIN 2014 Falling film on flexible wall in the limit of weak viscoelasticity. *J. Non-Newtonian Fluid Mech.* **210**, 85 – 95.

PENG, J. & ZHU, K. 2010 Linear instability of two-fluid Taylor-Couette flow in the presence of surfactant. *J. Fluid Mech.* **651**, 357–385.

PEREIRA, ANTONIO & KALLIADASIS, SERAFIM 2008 Dynamics of a falling film with solutal marangoni effect. *Phys. Rev. E* **78**, 036312.

PICARDO, JASON R., RADHAKRISHNA, T. G. & PUSHPAVANAM, S. 2016 Solutal marangoni instability in layered two-phase flows. *J. Fluid Mech.* **793**, 280–315.

POZRIKIDIS, C. 2003 Effect of surfactants on film flow down a periodic wall. *J. Fluid Mech.* **496**, 105–127.

QUERE, D., DE RYCK, A. & RAMDANE, O. O. 1997 Liquid coating from a surfactant solution. *Europhys. Lett.* **37** (4), 305.

SAHU, S. & SHANKAR, V. 2016 Passive manipulation of free-surface instability by deformable solid bilayers. *Phys. Rev. E* **94**, 013111 (1–14).

SAMANTA, ARGHYA 2014 Effect of surfactants on the instability of a two-layer film flow down an inclined plane. *Phys. Fluids* **26** (9), 094105.

SHANKAR, V. 2004 Stability of two-layer viscoelastic plane Couette flow past a deformable solid layer. *J. Non-Newtonian Fluid Mech.* **117**, 163–182.

SHANKAR, V. 2005 Stability of two-layer viscoelastic plane Couette flow past a deformable solid layer: Implications of fluid viscoscity stratification. *J. Non-Newtonian Fluid Mech.* **125**, 143–158.

SHANKAR, V. 2015 Stability of fluid flow through deformable tubes and channels: An overview. *Sadhana* **40** (3), 925–943.

SHANKAR, V. & KUMAR, L 2004 Stability of two-layer Newtonian plane Couette flow past a deformable solid layer. *Phys. Fluids* **16**, 4426–4442.

SHANKAR, V. & KUMARAN, V. 1999 Stability of non-parabolic flow in a flexible tube. *J. Fluid Mech.* **395**, 211–236.

SHANKAR, V. & KUMARAN, V. 2000 Stability of fluid flow in a flexible tube to non-axisymmetric disturbances. *J. Fluid Mech.* **408**, 291–314.

SHANKAR, V. & KUMARAN, V. 2001*a* Asymptotic analysis of wall modes in a flexible tube revisited. *Euro. Phys. J. B.* **19**, 607–622.

SHANKAR, V. & KUMARAN, V. 2001*b* Weakly nonlinear stability of viscous flow past a flexible surface. *J. Fluid Mech.* **434**, 337–354.

SHANKAR, V. & KUMARAN, V. 2002 Stability of wall modes in fluid flow past a flexible surface. *Phys. Fluids* **14**, 2324–2338.

SHANKAR, V. & SAHU, A. K. 2006 Suppression of instability in liquid flow down an inclined plane by a deformable solid layer. *Phys. Rev. E* **73**, 016301 (1–12).

SHRIVASTAVA, A., CUSSLER, E. L. & KUMAR, S. 2008 Mass transfer enhancement due to a soft elastic boundary. *Chem. Engg. Sc.* **63**, 4302–4305.

SQUIRES, T. M. & QUAKE, S. R. 2005 Microfluidics: Fluid physics at the nanoliter scale. *Rev. Mod. Phys.* **77**, 977–1026.

STONE, H. A. 1990 A simple derivation of the time-dependent convective-diffusion equation for surfactant transport along a deforming interface. *Phys. Fluids A: Fluid Dynamics* **2** (1), 111–112.

TOMAR, DHARMENDRA S., BAINGNE, MAHENDRA & SHARMA, GAURAV 2017 Stability of gravity-driven free surface flow of surfactant-laden liquid film flowing down a flexible inclined plane. *Chemical Engineering Science* **165**, 216 – 228.

VERMA, M.K.S., MAJUMDER A. & GHATAK, A. 2006 2006 Embedded template-assisted fabrication of complex microchannels in pdms and design of a microfluidic adhesive. *Langmuir* **22**, 10291–10295.

VERMA, M. K. S. & KUMARAN, V. 2012*a* A dynamical instability due to fluid-wall coupling lowers the transition Reynolds number in flow through flexible tube. *J. Fluid Mech.* **705**, 322–347.

VERMA, M. K. S. & KUMARAN, V. 2012*b* A dynamical instability due to fluid-wall coupling lowers the transition Reynolds number in the flow through a flexible tube. *J. Fluid Mech.* **705**, 322–347.

VERMA, M. K. S. & KUMARAN, V. 2013*a* A multifold reduction in the transition Reynolds number, and ultra-fast mixing, in a micro-channel due to a dynamical instability induced by a soft wall. *J. Fluid Mech.* **727**, 407–455.

VERMA, M. K. S. & KUMARAN, V. 2013*b* A multifold reduction in transition Reynolds number, and ultra fast mixing, in a micro-channel due to dynamical instability induced by soft wall. *J. Fluid Mech.* **727**, 407–455.

WEI, H., H. 2007 Role of base flows on surfactant-driven interfacial instabilities. *Phys. Rev. E* **75**, 036306.

WEI, H-H 2005*a* Effect of surfactant on the long-wave instability of a shear-imposed liquid flow down an inclined plane. *Phys. Fluids* **17**, 012103.

WEI, H-H 2005*b* Stability of a viscoelastic falling film with surfactant subjected to interfacial shear. *Phys Rev E* **71**, 066306.

WEIDEMAN, J. A. & REDDY, S. C. 2000 A Matlab differentiation matrix suite. *ACM Trans. Math. Software* **26**, 465–519.

WENSTEIN, S. J. & RUSCHAK, K. J. 2004 Coating flows. *Annu. Rev. Fluid Mech.* **36**, 29–53.

WHITAKER, STEPHEN 1964 Effect of surface active agents on the stability of falling liquid films. *Ind. Eng. Chem. Fun.* **3** (2), 132–142.

WHITAKER, STEPHEN & JONES, L. O. 1966 Stability of falling liquid films. effect of interface and interfacial mass transport. *AIChE* **12** (3), 421–431.

YIH, C.-S 1963 Stability of liquid flow down an inclined plane. *Phys. Fluids* **6**, 321–334.

YIH, C.-S. 1967 Instability due to viscosity stratification. *J. Fluid Mech.* **27**, 337–350.

ZHOU, ZHI-QIANG, PENG, JIE, ZHANG, YANG-JUN & ZHUGE, WEI-LIN 2014 Instabilities of viscoelastic liquid film coating tube in the presence of surfactant. *J. Non-Newtonian Fluid Mech.* **204**, 94 – 103.